THE BEHAVIOUR OF REINFORCED

CONCRETE SINGLE LAYER PANELS AND SANDWICH PANELS

A THESIS

PRESENTED TO

THE FACULTY OF GRADUATE STUDIES

THE UNIVERSITY OF MANITOBA

AS A REQUISITE TO OBTAINING

THE DEGREE OF

MASTER OF SCIENCE IN ENGINEERING

BY

YØUNG YOONKOL KANG

1968

S Y N O P S I S

This thesis gives the result of an investigation of reinforced concrete single layer panels and sandwich panels subject to axial compression and lateral loads.

Panel proportions, reinforcing and ultimate concrete strength in the panels were investigated. Approximate relationships of load-deflection and load-strain were also investigated. The various failure patterns for both single layer panels and sandwich panels were observed.

It is hoped that the results which have been obtained will be helpful in practical application.

ACKNOWLEDGEMENTS

The author hereby expresses his sense of deep gratitute to Professor R. Lazar, Department of Civil Engineering, University of Manitoba, for his helpful guidance throughout the duration of the laboratory experimental work and the preparation of this thesis. Appreciation is expressed for helpful suggestions received from Drs. H. C. Cohen and B. Thadani, Department of Civil Engineering, University of Manitoba.

The author is highly obliged to Professor A. J. Carlson, Assistant Dean, Faculty of Engineering, and Dr. A. Lansdown, Head, Department of Civil Engineering, University of Manitoba, without whose kindness, guidance, and encouragement this study could not have been completed. He is also obliged to the Canadian Prestressed Concretc Institute who supported this investigation.

The author is indebted to C. S. Juvet, Ottawa, and Y. S. Kang, Korea, for helping his studies.

TABLE OF CONTENTS

PART ONE

GENERAL INTRODUCTION

This thesis is based upon an investigation regarding the behaviour of precast reinforced concrete single layer and sandwich panels.

In recent years precast reinforced concrete sandwich panels are usually favored for one-story industrial buildings.

A few years ago the sandwich wall panels which consisted of two concrete face plates and four side plates reinforced with wire fabric, and a layer of insulation between were used by the Metropolitan Winnipeg Sewage Treatment Plant project, Winnipeg, Manitoba. After the construction of the precast concrete building, many cracks appeared on the sandwich panels as shown in Plate no. 1. When the author visited the plant, he observed the cracks and got interested in doing some research on sandwich panels. That was the beginning of this research project.

The precast reinforced concrete sandwich panel consists of two reinforced concrete face plates and four narrow concrete side plates reinforced with plain steel bars around a layer of Styrofoam insulation core between the plates as shown in Figure 2.

The function of the insulation core is to stabilize the surrounding thin plates, as a wood form during the pouring of the concrete into the casting frame.

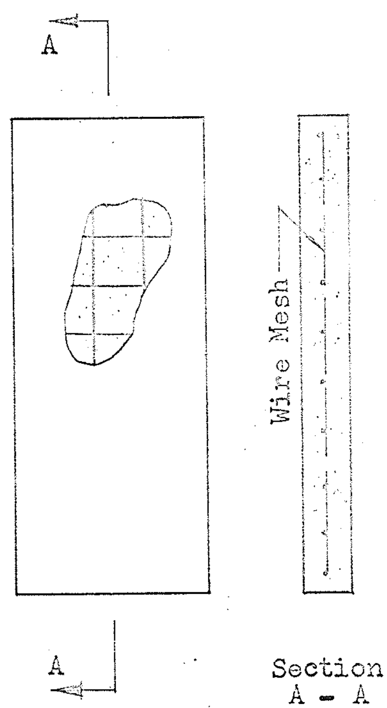

Fig. 1. SINGLE LAYER PANEL

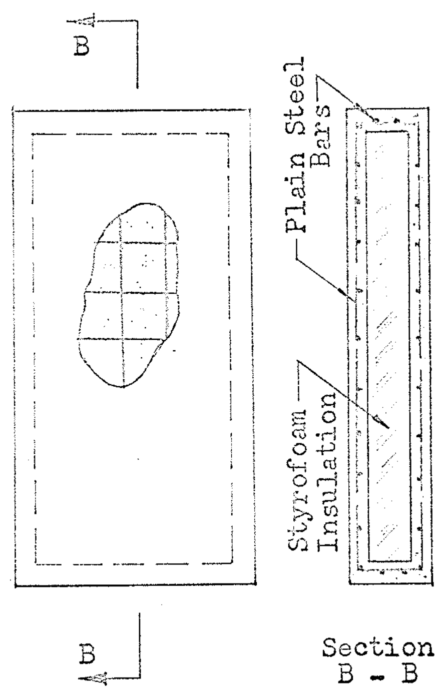

Fig. 2. SANDWICH PANEL

Precast reinforced concrete sandwich panels have a high stiffness factor at the edges of panels. These stiffer panels are relatively new, but have become an important feature of the construction industry.

The ordinary reinforced concrete construction involves concreting on site and requires money, time and labour to form, pour, cure, and strip. It crowds valuable space, and involves delay to other work which may have to be held up until site concreting operations are completed. There is always the possibilty of unforeseen delay due to unexpected inclement weather, which can completely defeat the scheduled plans of construction.

Relatively lighter, stronger, and good insulated sandwich panels can be mass-cast under good plant conditions. It is also easy to erect and maintain such units made of sandwich panels. Attractive surfaces may be obtained by the manufacturer, such as exposed aggregate or three dimensional patterns. Therefore the newly developed precast concrete sandwich panels are becoming more popular in the building industry.

The shortage of housing at present and the potential at the same time of increased production through prefablication are likely to lead to some rapid reconsideration of structural sandwich panel design.

The application of this new and untried method of construction to housing raises many questions related directly to design, material selection, fablication methods, strength, and durability.

5

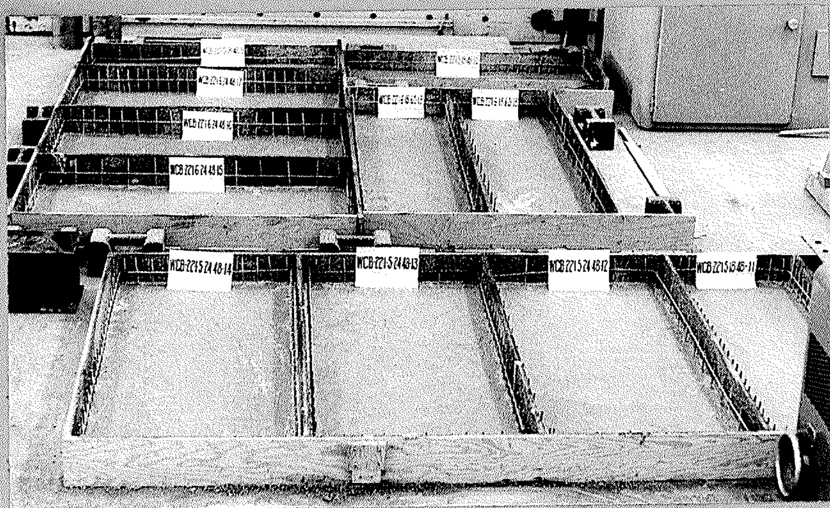

PLATE No. 3. Face Plate after Casting.

PLATE No. 1. Cracked Sandwich Panel of Metropolitan Winnipeg Sewage Treatment Plant.

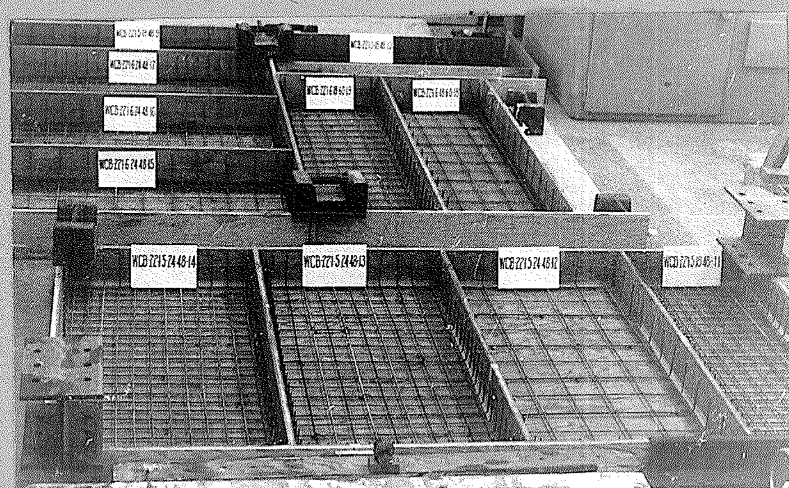

PLATE No. 2. Face Plate Reinforcement in Position.

The object of this thesis is to investigate certain problems concerned with the application of this new method in the concrete sandwich panels, namely, relationships between the axial compressive load carrying abilities, panel proportions, reinforcing, and strength of the sandwich panels compared with those of the single layer panels.

PART TWO

DEVELOPMENTS OF REINFORCED CONCRETE SANDWICH PANEL

Concrete sandwich panels have a great future for the reasons mentioned in the general introduction to this thesis. It has a history more than a hundred years old, though the interest shown in its use has not been very consistent.[1]

The concrete sandwich principle was applied, perhaps for the first time, in 1849 by William Fairbairn in experimenting with bridge design. The materials used were laminated wood for decking and concrete as a composite beam.

In 1906 the engineers in the United States examined the possibilities of constructing sandwich concrete walls.

In 1933 in Sweden a sandwich panel of light weight concrete five in. thick and bonded to dense in situ concrete was made. A 5/8 in. thick lime cement mortar was then plastered on the outside of the lightweight concrete block as shown in Figure 3. The experiment was a success. In the United States, on the other hand, in cold storage work the cement plastering was one inch thick on the inside face or the cold face as shown in Figure 4.

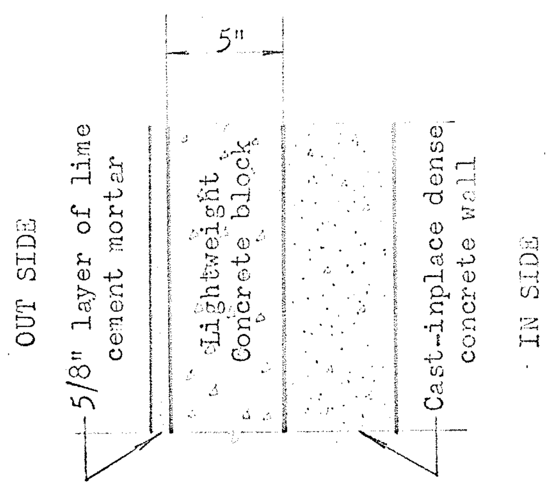

Fig. 3. Swedish Sandwich Wall.

In 1946 in the United States E.I. du Pont de Nemours Co. constructed for industrial buildings with sandwich walls which used cored gypsum filler block as the insulation material.

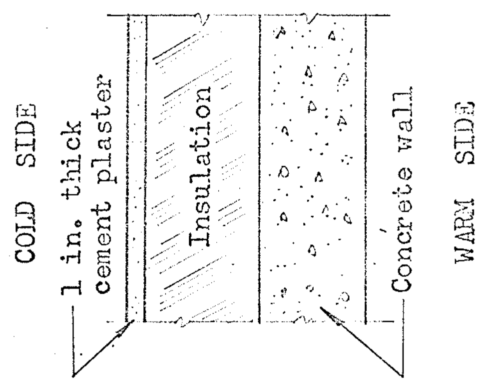

Fig. 4. American Insulated Sandwich Wall.

Some four decades ago, an efficient sandwich panel[2] composed of metal facings and a plywood core was produced commercially. After that honeycomb cored plywood sandwich panels have been developed by the Forest Prducts Laboratory, Department of Agriculture, in the United States.

There had been some metal faced sandwich constructions[3] but it was only after World War II that this type of construction aroused great interest. Most of the metal faced sandwich constructions are applied to aircraft and missiles. The metals used in this construction are aluminum alloys, titanum, steels, etc.

In 1951 S. B. Roberts[4] reported the construction of a sandwich panel of 6 x 10 ft . It consisted of a 2-in. layer of cellular glass insulation and two wire mesh reinforced slabs.

In the same year the archtectural firm of Shaw, Metz, and Dorio, of Chicago, designed an outstanding sandwich panel as shown in Fig. 5.

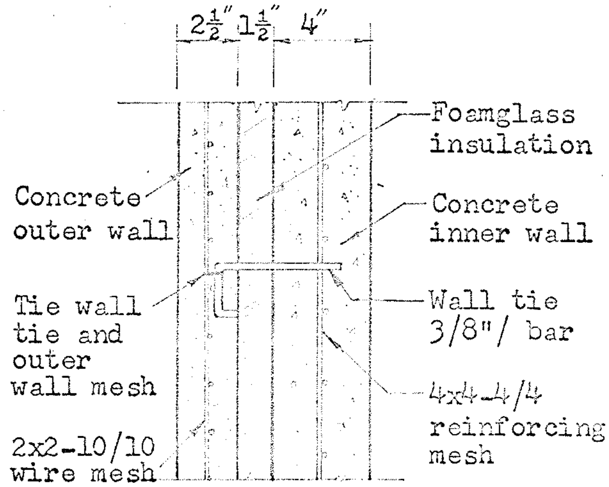

Fig. 5. Sandwich-type precast wall panel.

In 1952 P. M. Grennan[5] reported the development of the mineralized wood chip sandwich panel in the United States. Each panel was 8 x 8 ft and composed of two outer walls of regular concrete 1¼" thick reinforced with 4 x 4 -10/10 wire mesh. Lightweight precast insulation was 1½ in. thick using chemical mineralized wood chips as aggregate as shown in Fig. 6. Edges of the panel were tongue-and-groove joints. Panels were assembled with a one inch wide impervious rubber strip inserted at the center of all joints.

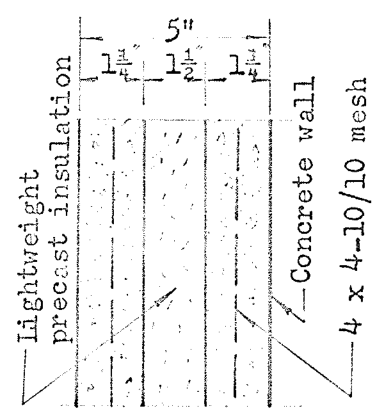

Fig. 6. Sandwich Panel

In 1953 Arshan Amirikian[6] reported the 22'-5½" x 23'-7½" precast concrete sandwich panel which was obtained by placing a layer of foam glass block insulation between two slabs concrete to form a laminated element as shown in Figure 7.

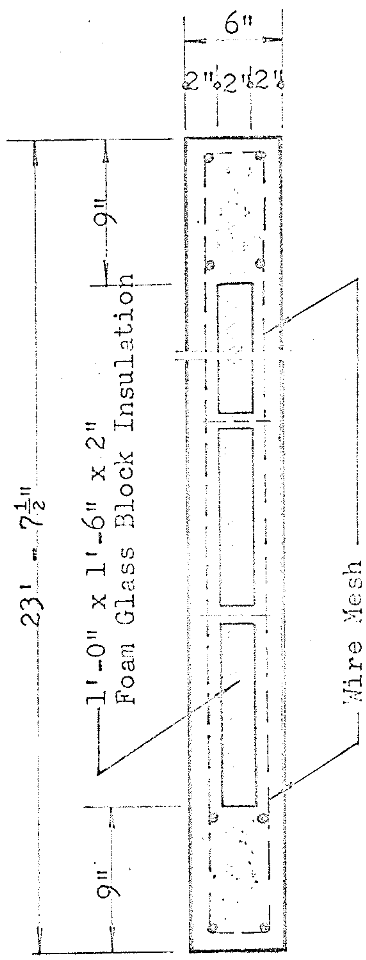

Fig. 7. Foam Glass Sandwich Panel.

Early studies in the concrete sandwich slab construction and sandwich walls were made by F. T. Collins in 1954. Vermiculite sandwich panels were tested for several years by him. The vermiculite was placed in a plastic state on the fresh lower layer of regular concrete, and a two inches top layer of regular concrete placed on the vermiculite layer as soon as it has set sufficiently to carry the top layer. The concrete shells are attached by ¼ in. sinusoidal shear reinforcing spaced vertically with a maximum 4 ft. center to center spacing. This panel design is shown in Figure 8. In

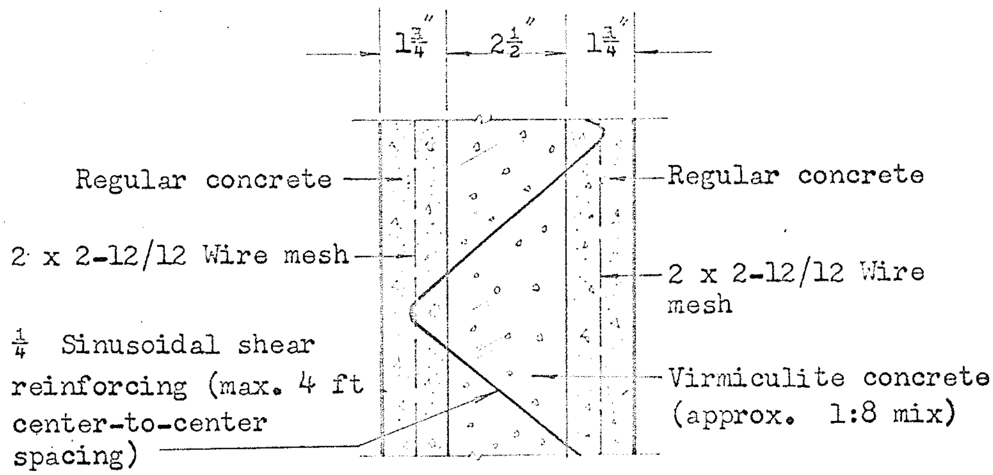

Fig. 8. Virmiculite Sandwich Panel

his opinion the ideal design for precast sandwich panel is one which consists of prestressed outer shells. This design is not economical for smaller panels but suitable for large two and three storey buildings. The design is shown in Fig. 9. The two examples of open-face sandwich

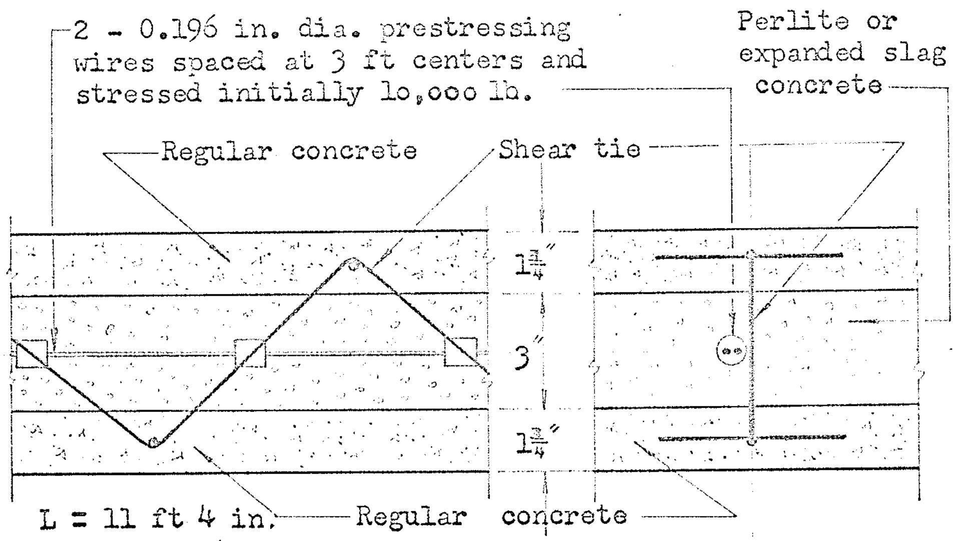

Fig. 9. Prestressed Sandwich Panel

construction and one of the true tilt-up sandwich wall panels were also reported by him. In the open-face type, the wall consists of just two layers of material, a hard outer layer and the second a soft insulation layer. Design of the open -face wall panels is shown in Figs. 10 and 11. The recently

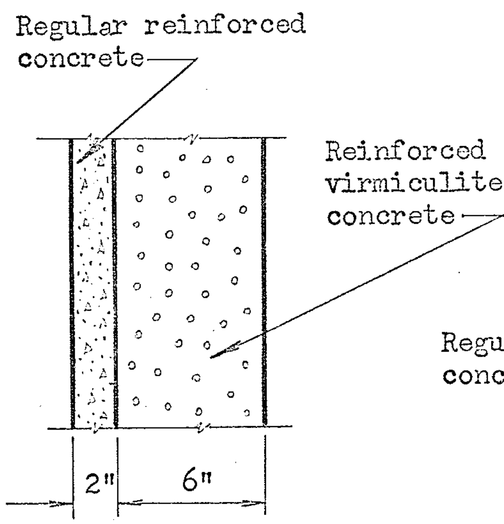

Fig. 10. Open-face Sandwich Panel.

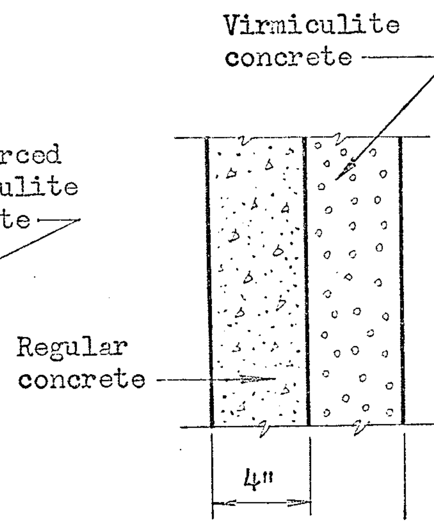

Fig. 11. Open-face Sandwich Panel.

developed true tilt-up sandwich wall panel in Sweden is composed of two inches outer shells of regular dense concrete with four inches of expanded shale concrete between as shown in Fig. 12. and metal ties between the outer shells were also used.

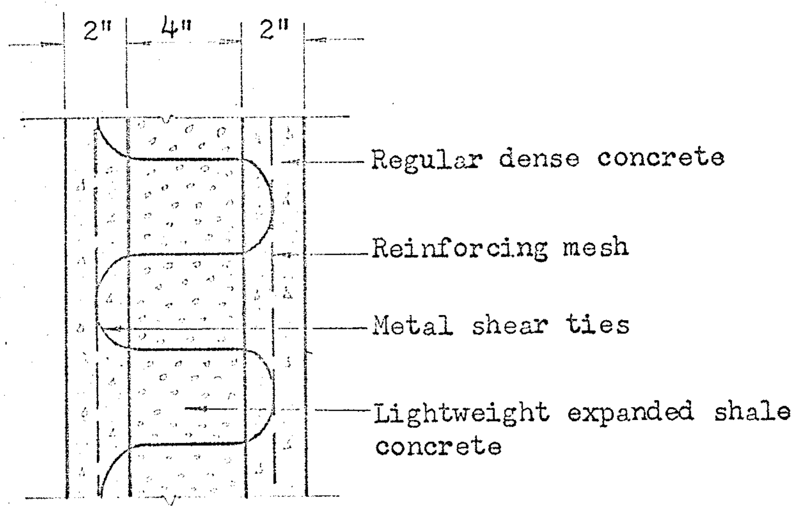

Fig. 12. Expanded Shale Sandwich Panel

In 1959 V. F. Leabu[7] tested insulated sandwich panels and measured variation in color, inefficient heat transmission factor, and bulging of panels. The temperature gradient through four different types of precast concrete panels measured for a temperature range of 10° F outside to 70° F inside are shown in Fig. 13. The sandwich panel with its highly efficient insulation shows the greatest temperature differential and regular concrete panel the least.

		SANDWICH PANEL	FOAM CONCRETE	LIGHTWEIGHT CONCRETE	REGULAR CONCRETE
Heat transmission Btu/Hr/sf/°F		0.15	0.19	0.49	0.84
Thermal conductivity Btu/Hr/sf/°F/in	Concrete	12.0	1.1	4.0	12.0
	Insulation	0.24	-	-	-
Weight of panel psf		45.0	21.0	42.0	63.0
Weight of concrete pcf		150.	50.	100.	150.
Weight of insulation pcf		11.	-	-	-

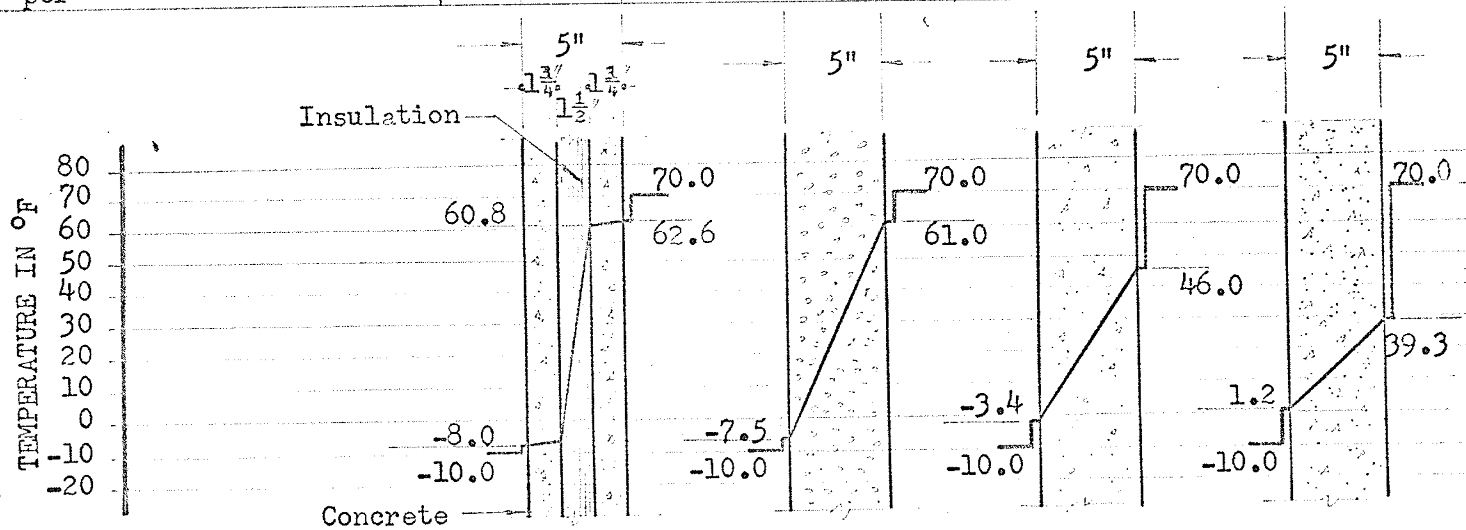

Fig. 13. Temperature Gradient.

In 1965 D. W. Pfeifer and J. A. Hanson tested 31 concrete sandwich panels[8] under uniform flexural loading. A specimen size of 3 x 5-ft was chosen and the over all thickness of the panels varied from $2\frac{1}{4}$ to 6 in. The shells of most panels contained a single layer of 2 x 2 - 14/14 welded wire fabric. Only two panels were reinforced 6 x 6 - 8/8 welded wire fabric. The majority of the sandwich panels contained three types of metal shear connectors between the concrete shells as shown in Fig. 14. The insulating materials used between the

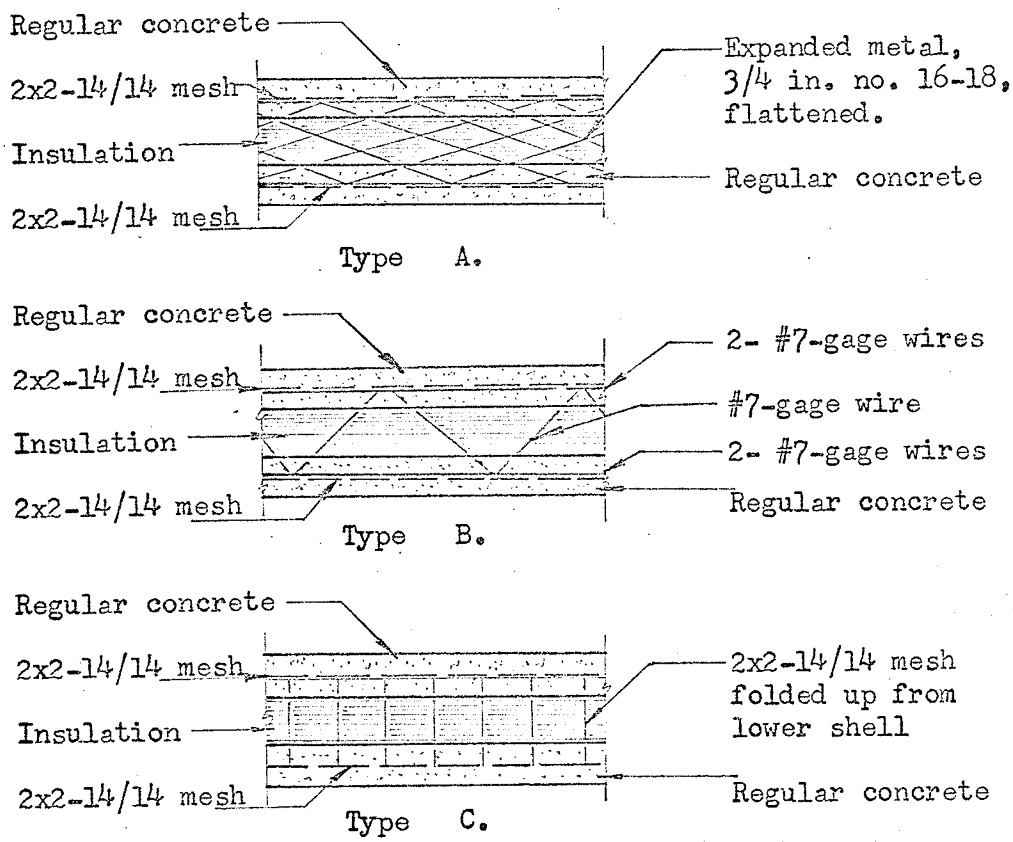

Fig. 14. Shear Tied Sandwich Panels.

concrete shells were a foamed polyurethane plastic, foamed polystyrene plastic, glass fiber, foamed glass, and autoclaved cellular concrete. Two inches thick insulation has been used for the greater number of sandwich panels. The panels with foamed glass insulation combined with metal shear connectors performed as well as, or better than, those with plastic or glass fiber cores. Panels containing autoclaved cellular concrete cores, even though fabricated without shear connectors, exhibited moment resistance and deflection stiffness generally superior to all other types of panels. This improved behaviour was ascribed to the higher modulus of elasticity of the cellular concrete. It was recognized that the insulation values of these different core materials would vary, depending on their unit weight and moisture content. Closer mesh spacing of the welded wire reinforcement in the shells was effective in reducing deflection under the applied flexural loads.

In 1966 Preco Division of BACM Limited, Winnipeg, Manitoba, made precast sandwich panels for Stoney Mountain Penitentiary. The typical panel was 7 x 15 ft. and was composed of two outer shells with $1\frac{1}{2}$ in. of rigid insulation between. One shell was 5 in. thick and made of regular dense concrete reinforced with 4 x 4 -4/4 welded wire fabric, and the other shell was $1\frac{1}{2}$ in. thick with 4 x 4 -10/10 fabric. The panel had #10-gauge galvanized wire shear connectors with a 2 ft. 8 in. center-to-center spacing vertically between two shells.

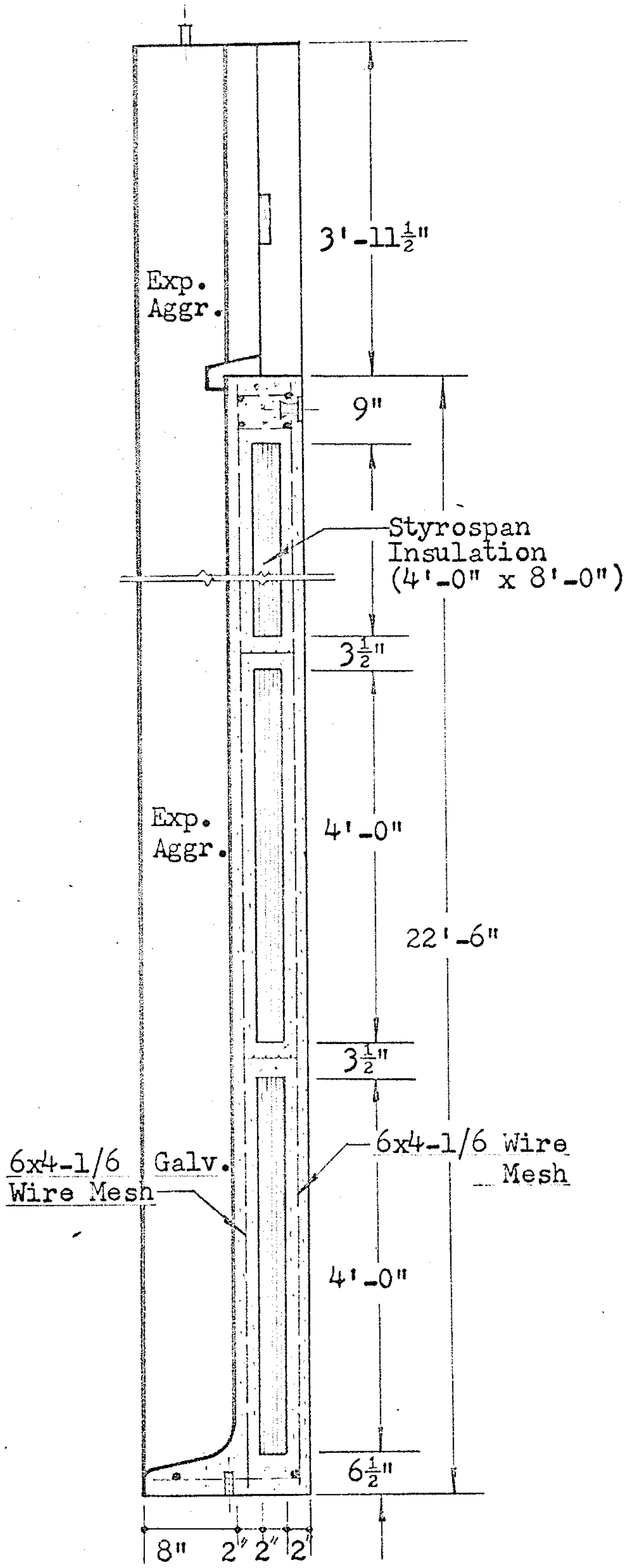

Fig. 14a. Section View of Exposed Aggregate Sandwich Panel.

In 1967 Schell Industries Limited, Woodstock, Ontario, constructed exposed aggregate sandwich panels for a warehouse project at London, Ontario. This exposed aggregate panel was 22'-6" x 10' -0" x 6 in. thick, and composed of two outer shells of regular dense concrete with two in. of Styrospan insulation between, as shown in Figure 14a.

P A R T   T H R E E

EXPERIMENTAL PROGRAM AND PROCEDURE

3.1. DESCRIPTION OF TEST PANELS

The specimens of the experimental panels were of two general types - single layer and sandwich panels.

A. Single Layer Panels

The single layer panels were eight in number. The thickness of the panels varied from one to two inches, the width from twelve to eighteen, and the length from twenty four to sixty. The ratio of reinforcement area to effective section area of concrete in the panels ranged from 0.32 to 0.53 % with 6 x 6 - 10/10 welded wire fabric. The concrete compressive strength varied from 5100 psi. to 5980 psi. at age of 28 days.

B. Sandwich Panels

The sandwich panels tested were eleven in number. The over-all thickness of the sandwich panels varied from five to six inches, the width from eighteen to twenty four, and the length from forty eight to sixty. One inch thick face shells were employed for all specimens of the panels. All panels had insulating cores the thickness of which varied from three to four inches. The ratio of reinforcement area to effective section area of concrete in the panels ranged from 0.5 to 1.5 % with steel bars 3/16 and 1/8 in. in diameter.

The concrete compressive strength varied from 4900 to 5970 psi at age of 28 days.

Both single layer and sandwich panels were generally tested about fifty days after concrete was poured into the forms. Electric strain gages, SR-4 type A-3-S6, were mounted on all panels to measure strains on the concrete surface and to observe mode of failure of concrete. The arrangement of the SR-4 strain gages on the concrete faces of the panels varied in the tests (see Section 4.2.).

3.2. MATERIALS

CONCRETE

High early strength portland cement Class III was used in the concrete mix with a small amount of "neutralized vinsol resin" to improve workability and plasticity. The maximum size of aggregate was 3/4 in. The mix proportions were chosen by the weigh-scale method for batching as shown in Table (1). Paraffin paper molds, six inches in diameter by twelve inches long, with base plates, were used for casting concrete cylinders. Four cylinders were made for each batch. Typical compression stress-strain curve from direct compression tests on six inches by twelve inches cylinders are shown in Fig. 15.

REINFORCEMENT

A. Single layer Panels

The single layer panels were reinforced with 6 x 6 - 10/10 welded wire fabric conforming to ASTM A185. The welded wire had an average ultimate strength of approximately 76 ksi and an average minimum yield strength of approximately 62 ksi.

B. Sandwich Panels

The concrete outer shells of sandwich panels were reinforced with steel bars 3/16 and 1/8 in. in diameter. The steel wires had an average ultimate strength of approximately 70 and

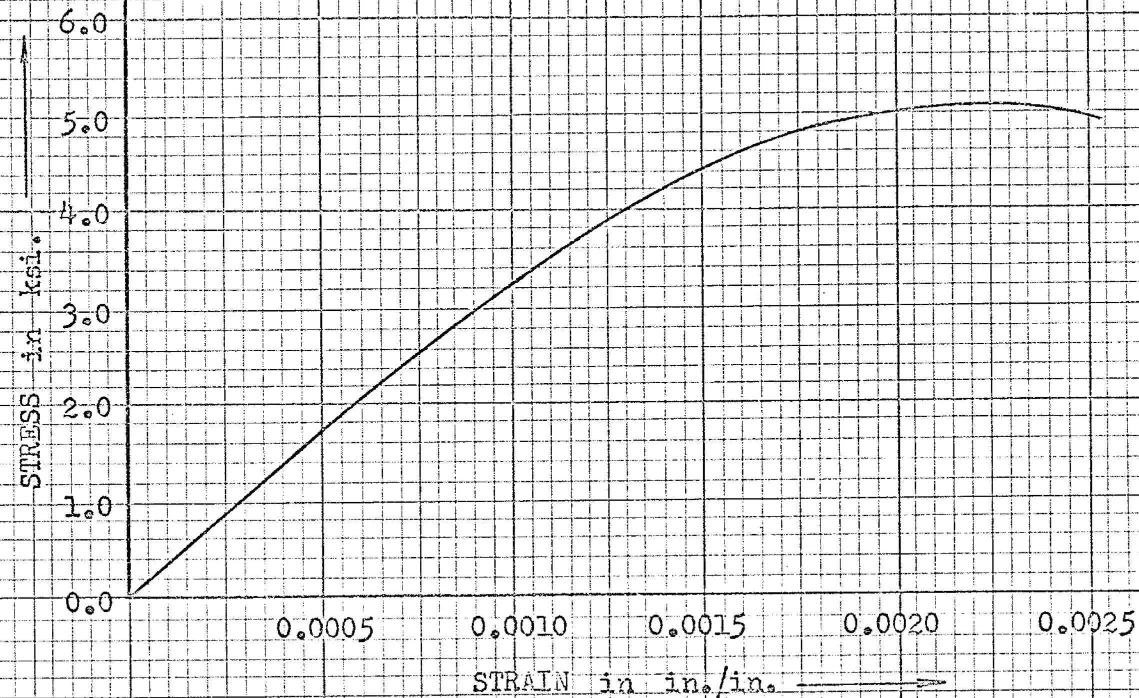

Fig. 15. TYPICAL CONCRETE STRESS-STRAIN CURVES FROM COMPRESSION CYLINDERS AT AGE OF 28 DAYS.

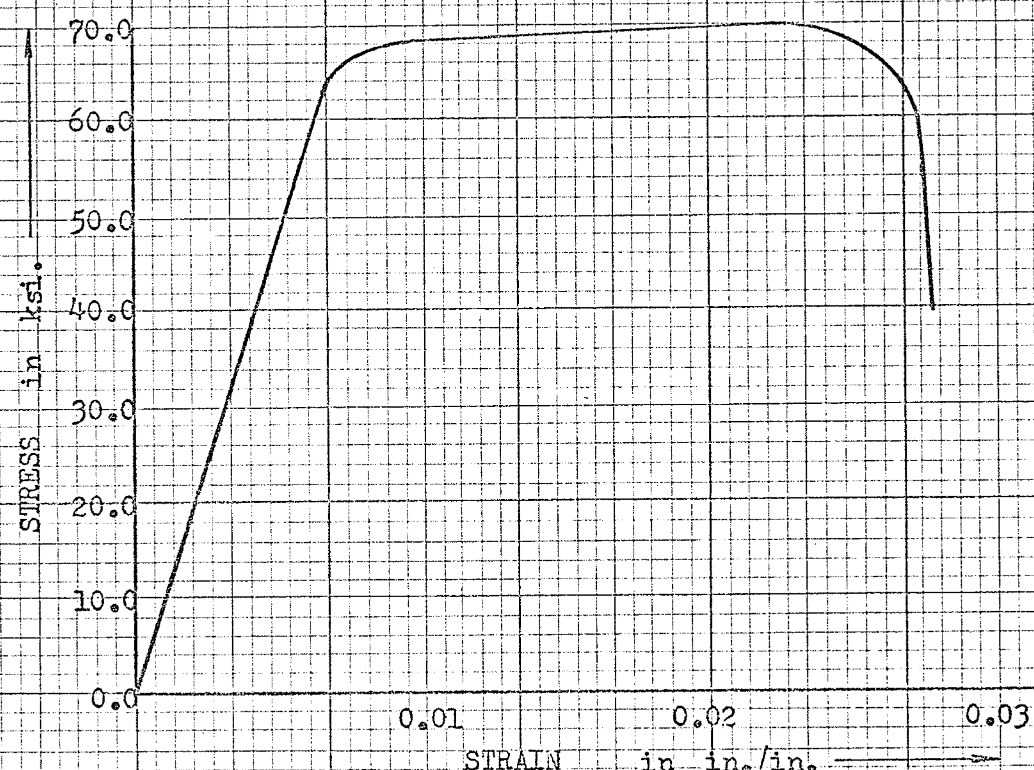

Fig. 16. TYPICAL STEEL STRESS-STRAIN CURVES FROM TENSION BARS (3/16"ϕ)

TABLE (1) Mix design for 3 cu ft Batch

		Mix A	Mix B	Mix C	Mix D
Cement		58.0 lbs	63.0 lbs	67.0 lbs	72.0 lbs
water		32.7 lbs	34.0 lbs	37.0 lbs	37.2 lbs
Coarse Aggregate	3/4"	53.6 lbs	234.0 lbs	-	-
	1/2"	176.0 lbs	-	150.0 lbs	160.0 lbs
Fine Aggregate		120.0 lbs	138.0 lbs	150.0 lbs	142.0 lbs
A. E. A.		0.59 oz	0.67 oz	0.60 oz	0.62 oz
Average Compression Strength from Direct Compression Tests on 6 by 12 in. Cylinder at age of 28 days		5100 psi	5980 psi	4900 psi	5970 psi
Specimen		#1, #2, #3, and #7	#4, #5, #6, and #8	#12, #13, #14, #15, #16, and #17	#9, #10, #11 #18, and #19

TABLE (2) Heat Transmission

Construction Features	Thermal Conductivity Btu/SF/hr/in/°F	Total Thickness In.	Heat Transmission Btu/SF/hr/°F
Reinforced Concrete	12.0	2.0	24.0
Styrofoam Insulation at 40 °F mean temperature	.24	3.0	.72
		4.0	.96

79 ksi, and an average minimum yield strength of approximately 67 and 71 ksi. Typical stress-strain curve for 3/16 in. in diameter tension steel wires are as shown in Fig. 16.

INSULATION

Sandwich Panels

The rigid boards of Syrofoam insulation were used as a core of sandwich panels throughout the test. The sandwich panel specimens of over-all thickness of five and six inches used three and four inches thick insulation rigid boards. The maximum operating temperature of Styrofoam insulation for continuous use was 165° F average and thermal conductivity of the insulation was 0.24 Btu per Hr per sq ft per deg F per in. at mean temperature of 40° F. The over-all coefficient of heat transmission is given in Table (2). Average density of insulation boads was 2.5 pcf and water absorption was less than 0.25 % by volume. Typical compression stress -strain curve from direct compression tests on 2 x 2 in. squmre - 4 in. long are shown in Fig. 17. The tensile strength of the Styrofoam insulation was tested by 2 tests on concrete-Styrofoam -concrete sandwich specimens in direct tension. Average tensile strength-strain curve from direct tension tests is shown in Figure 17a.

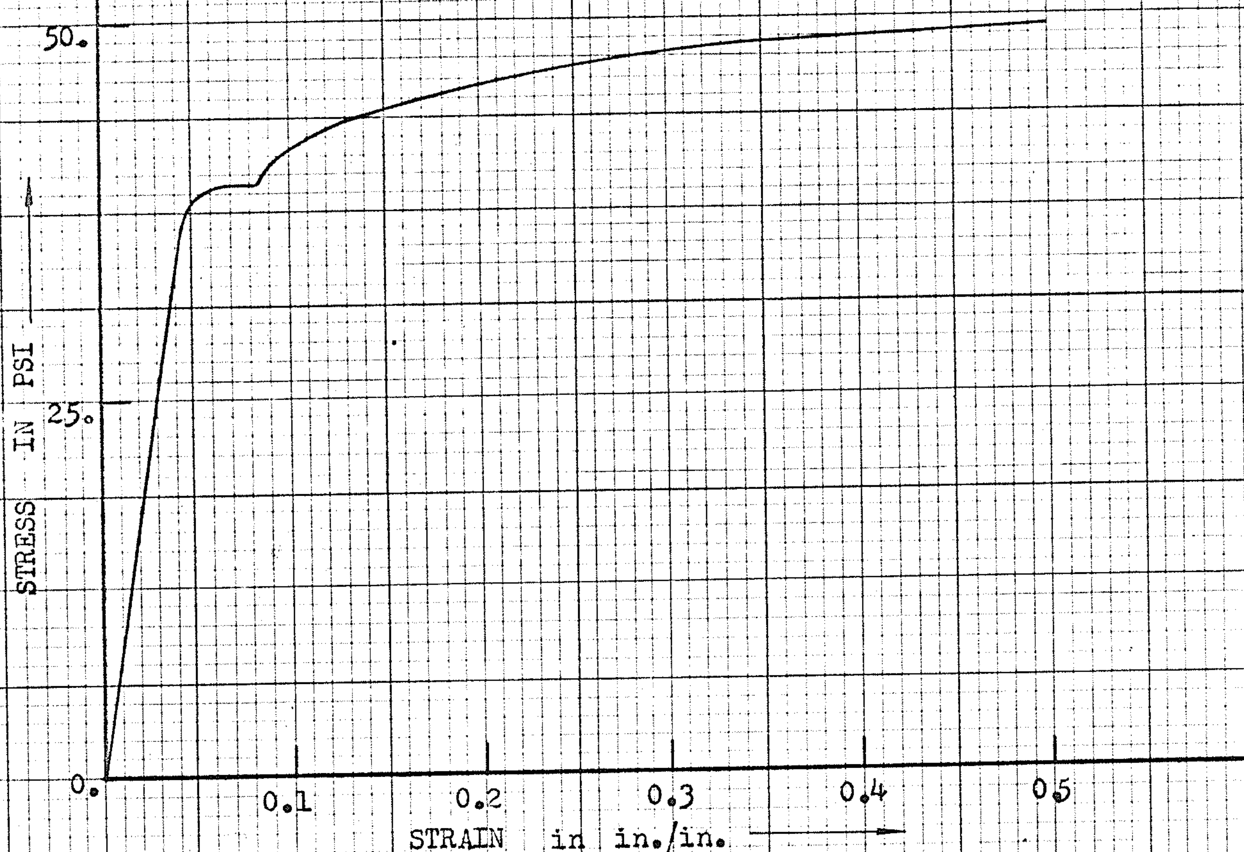

Fig. 17. Typical Styrofoam Insulation Stress-Strain Curve from Compression Cubes.

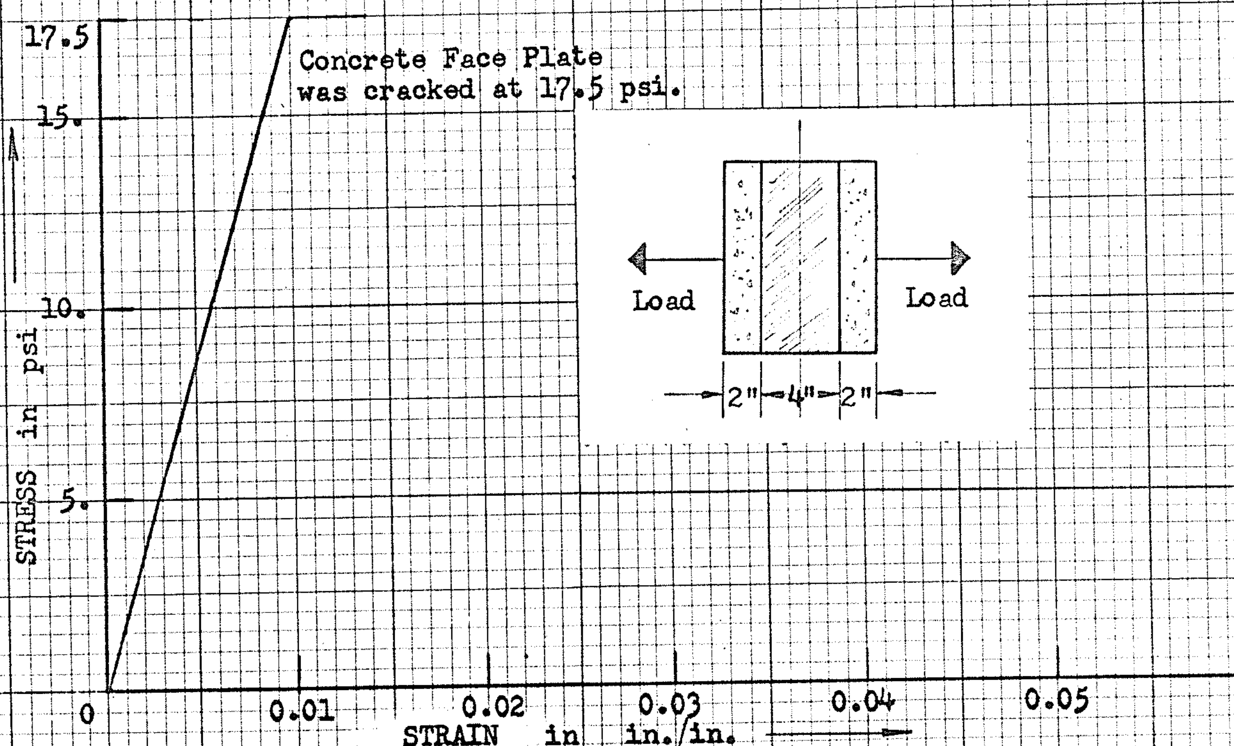

Fig. 17a. Typical Styrofoam Insulation Tensile Stress-Strain Curve.

3.3. FABRICATION OF SPECIMENS

A. Single layer Panels

The reinforcement of 6 x 6 - 10/10 welded wire fabric was cut properly before it was placed in the oiled forms for casting. The panels were cast in horizontal position. Horizontal casting may cause in practice a differential in strength across the cross section of the panels but it was not possible to cast vertically relatively very narrow panels. The panels were cast in forms built from plywood nailed together. Spacers were used to keep the wire meshes centered in the forms. A predetermined weight of concrete was mixed in a three cubic foot mixer, poured, and vibrated internally for proper panel thickness.

B. Sandwich Panels

The sandwich panels were cast in oiled plywood forms. Reinforcing wires were connected with steel wire #16-gage for shell reinforcement of the panels. Then the reinforcement of the bottom shell were positioned with spacers in the forms as shown in Plate 2. The procedure of preparing concrete mixture, pouring, and vibrating was the same as the one described above in the case of single layer panels. After the bottom concrete shell had reached its initial set (Plate 3.), the insulation was placed as shown in Plate 4. The reinforcement of the upper shell was then positioned on the insulation. The reinforcement for the top shell was tied to the reinforcement for the bottom shell as shown in Plate 5, and the concrete was then poured and vibrated.

Both panels were moist-cured under cotton cloth for seven days at the room temperature and the forms were then stripped. The panels were left to air dry in the room until tests were held.

PLATE No. 4. Styrofoam Insulation in Position after Face Plate was Cast.

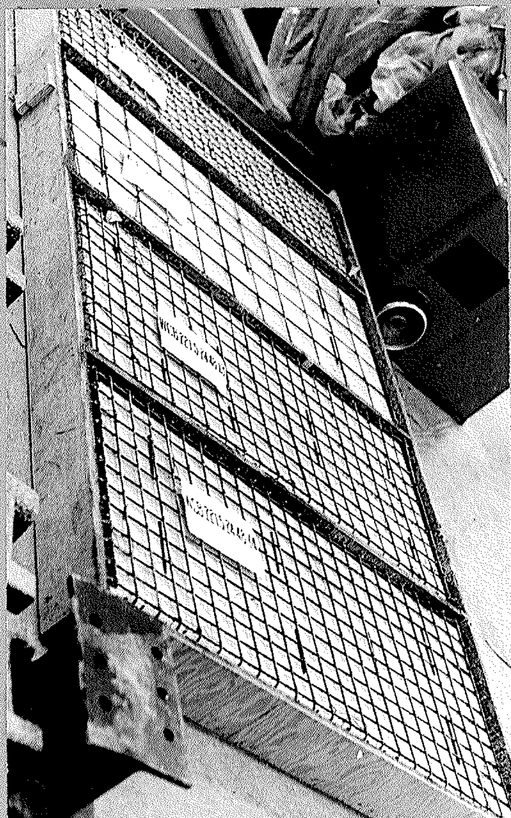

PLATE No. 5. Rear Plate Reinforcement on Styrofoam Insulation in Position.

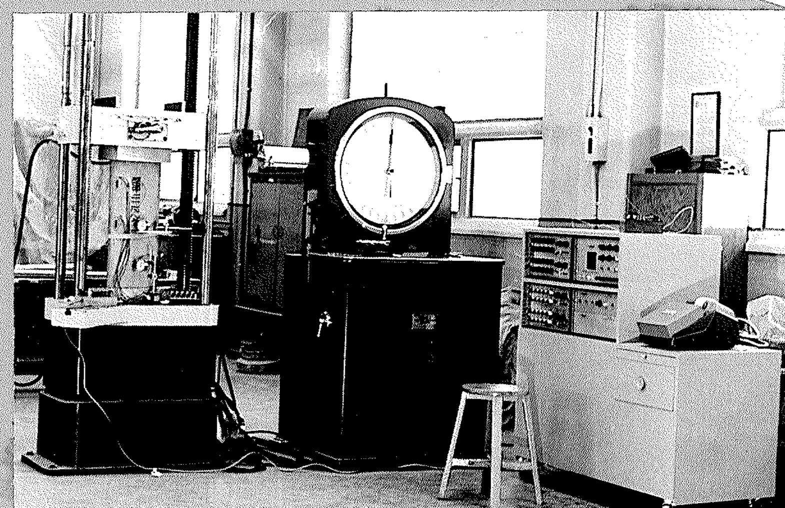

PLATE No. 6. Single Layer Panel in Riehle Hydraulic Testing Machine of Sixty kips.

3.4. TESTING PROCEDURE

A. Single Layer Panels

Three single layer panels were tested in a 60,000 lbs capacity Riehle hydraulic testing machine. A view of the machine during the test of a panel is shown in Plate 6. The load was applied through plywood at the top and bottom of the panels and it was applied in increments of 2,000 lbs. The other panels were tested in a 200,000 lbs capacity testing frame. The loads were applied by hydraulic jack with gage as shown in Plate 7. The smallest graduation represented approximately 4,000 lbs of axial load (the gage was graduated 200 psi). Before the testing, 200,000 lbs loading jack with gage was calibrated in the Reihle strength testing machine as shown in Figure 18. During the loading, thin plywoods were provided at the ends of the specimens for the uniaxial loading (Fig. 19).

B. Sandwich Panels

All sandwich panels were subjected to uniaxial loads in a 200,000 lbs capacity testing frame as described above in the case of single layer panels. Some panels were loaded with combined axial and lateral loads. For lateral loading, testing frame was fabricated with 3" x $2^3/8$" I 5.7 lbs/lf I beams and steel bars $\frac{1}{2}$ in. in diameter. This lateral load was applied by a

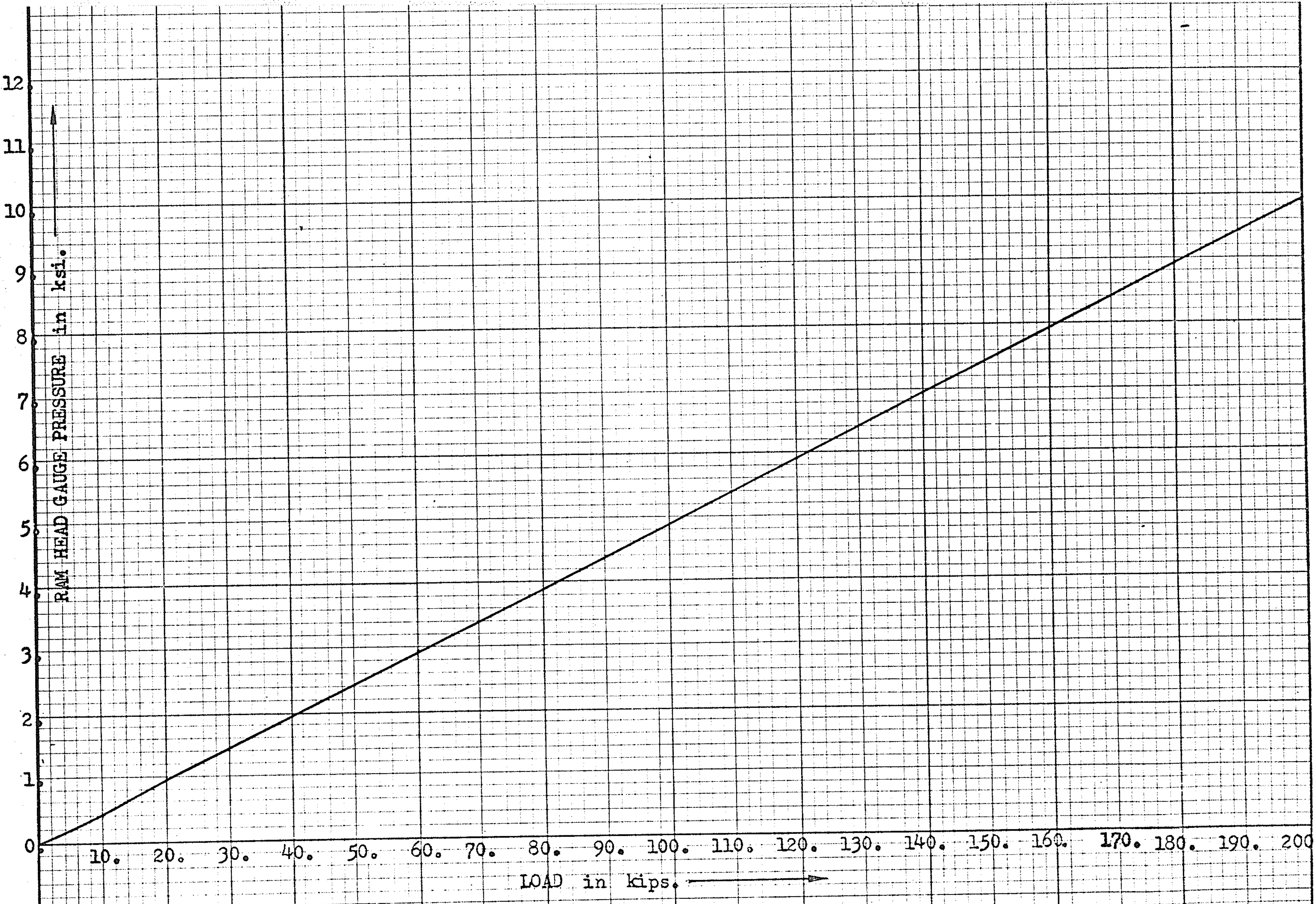

FIG. 18. CALIBRATION OF LOADING FRAME HYDRAULIC JACK.

20,000 lbs capacity hydraulic jack with Budd portable strain indicator model P-350 as shown in Plates 8 and 9. A sketch of the testing in a 200,000 lbs capacity testing frame for the uniaxial load is given in Figure 19.

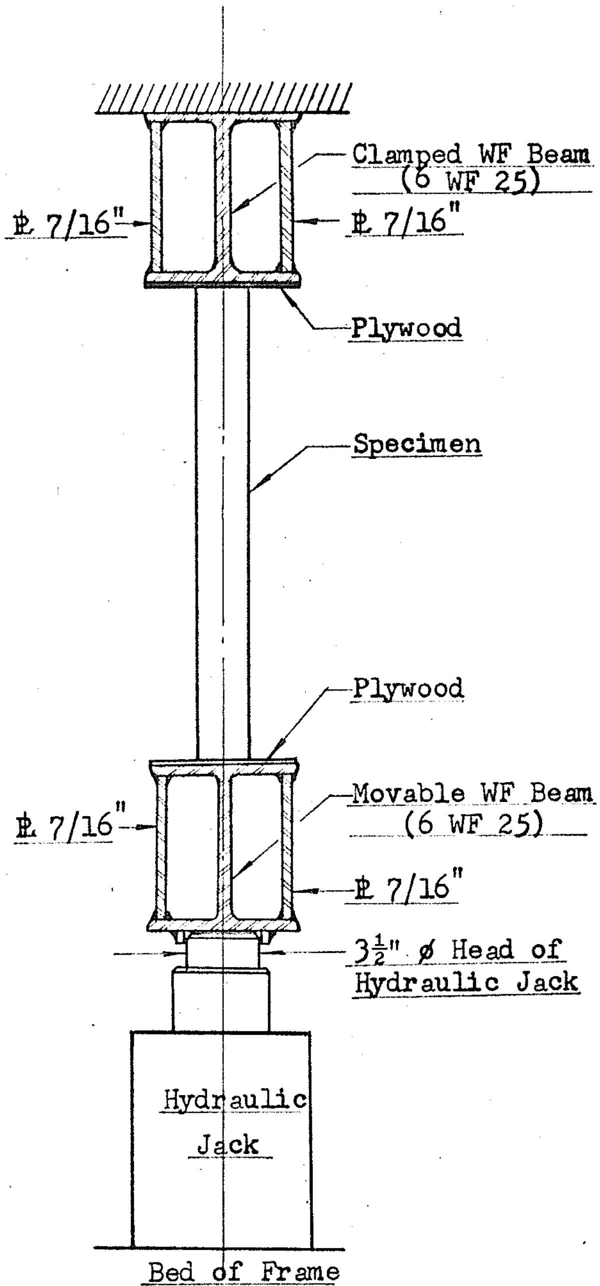

Fig. 19. Testing Arrangement in 200,000 lbs Testing Frame.

The concrete strains of both the panels were measured with SR-4 type A-3-S6 strain gages and the dial gages were also provided for deflections and lateral movements of the panels. The locations of the gages are shown in the detailed drawing for each panel (Section 4.2.).

For strain measuring Budd

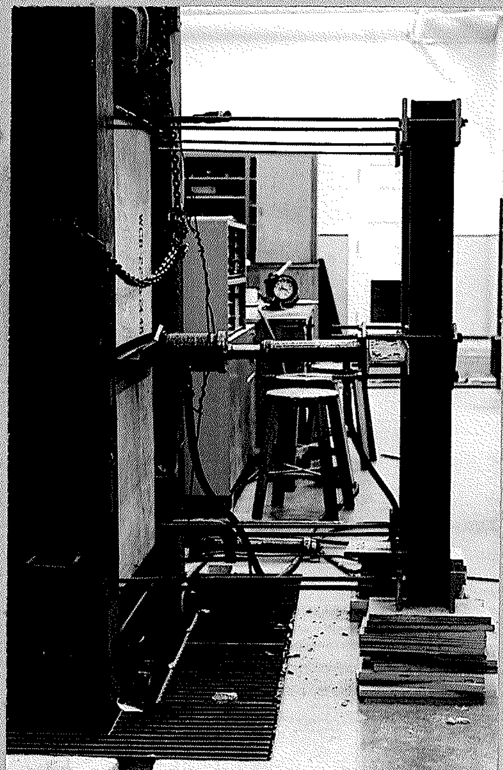

PLATE No. 9. Front View of 20 kips Lateral Loading Frame with Hydraulic Jack.

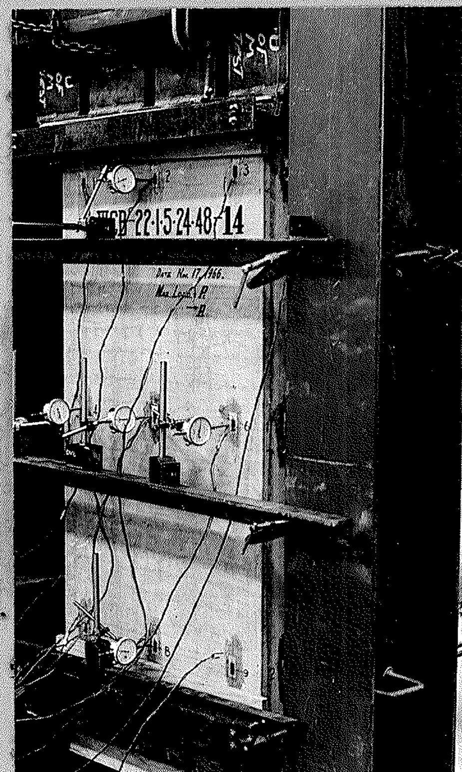

PLATE No. 8. Rear View of Testing Frame of 20 kips for Lateral Load.

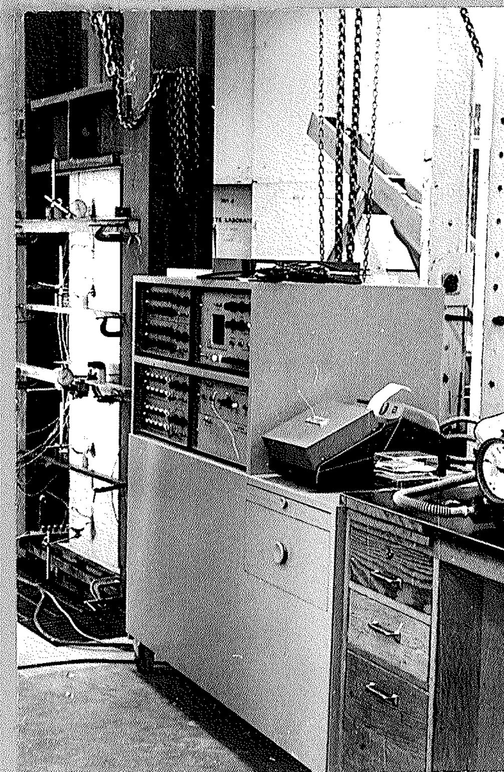

PLATE No. 7. Panel in Testing Frame of 200 kips with A-110 Digital Strain Indicator.

model A-110 digital strain indicator was used as shown in Plates 6 and 7. All dial gages were removed when a strain reached approximately 0.002 in/in. The relationships of the load to deflection and the load to strain to failure were measured is shown in Appendices A and B. Each increment of loads was maintained for a period sufficient to read the strains and deflections. After failure, the crack patterns of each panel were observed. The panel was removed from the loading machine or frame and was then photographed.

P A R T F O U R

DISCUSSION OF OBSERVATIONS

4.1. GENERAL BEHAVIOUR

Table (3) shows a summary of the test results for eight single layer panels and six sandwich panels based on the axial load tests, and for five sandwich panels based on the tests of axial and lateral loads combined.

The author's original intention in this research work was to apply axial loads only on the panels. The available equipment had an axial load capacity of 200 kips which was insufficient to produce failure in some sandwich panels. Therefore lateral load was applied in addition to the axial load to observe the failure patterns of those panels.

All panels were loaded to ultimate failure except specimen WCB 22.1.5.24.48- 12 which was cracked by being dropped through mishandling.

The strain distribution on the panels was measured until ultimate load was attained as shown in Appendix A.

The lateral deflections of the center of the panels due to axial loads were recorded and are shown in Appendix B.

A. Single layer Panels

The variations of the ultimate load capacity of the single layer panels were due to differences in concrete compression strength and slenderness ratio. The panel proportions, length,

TABLE (3) SUMMARY OF TEST RESULTS

SPECIMEN NUMBER	GROSS DIMENSION t x b x L (in)	L/r L/(I/A_g)	A_g (sq-in)	A_s (sq-in)	p (100/A_s/A_g)	f_y (ksi)	f'_c (psi)	f_{cu} (psi)	f_{cu}/f'_c	$\bar{P}_o$ (kips)	$\bar{P}_u$ actual (kips)	$\bar{P}_L$ actual (kips)	$\bar{P}_u$ actual / $\bar{P}_o$	REMARK
WCB 11.1.12.24- 1	1 x 12 x 24	84.5	12	0.055	0.460	62.0	5100	3850	0.76	55.2	46.2	-	0.836	
WCB 11.1.12.30- 2	1 x 12 x 30	105.6	12	0.055	0.460	62.0	5100	2950	0.58	55.2	35.4	-	0.642	
WCB 11.1.12.36- 3	1 x 12 x 36	126.8	12	0.055	0.460	62.0	5100	2920	0.57	55.2	35.0	-	0.633	
WCB 11.1.13.48- 4	2 x 13 x 48	83.3	26	0.083	0.320	62.0	5980	4080	0.68	136.9	106.0	-	0.774	
WCB 12.2.13.42- 5	2 x 13 x 42	72.8	26	0.138	0.530	62.0	5980	3820	0.64	140.0	99.2	-	0.708	
WCB 12.2.13.48- 6	2 x 13 x 48	83.3	26	0.138	0.530	62.0	5980	4060	0.68	140.0	105.4	-	0.753	
WCB 12.2.18.60- 7	2 x 18 x 60	104.0	36	0.165	0.460	62.0	5100	3430	0.67	165.5	123.6	-	0.746	
WCB 12.2.18.60- 8	2 x 18 x 60	104.0	36	0.165	0.460	62.0	5980	4090	0.68	192.2	147.4	-	0.767	
WCB 22.1.5.18.48- 9	5 x 18 x 48	25.26	42	0.210	0.500	69.5	5970	4190	0.70	226.7	176.0	-	0.776	
WCB 22.1.5.18.48-10	5 x 18 x 48	25.26	42	0.420	1.000	69.5	5970	4400	0.74	240.2	184.8	-	0.768	
WCB 22.1.5.18.48-11	5 x 18 x 48	25.26	42	0.630	1.500	67.0	5970	3480	0.58	252.1	146.0	-	0.580	
WCB 22.1.5.24.48-12	5 x 24 x 48	25.44	57	0.285	0.500	69.5	4900	3510	0.72	256.0	200.4	-	0.782	
WCB 22.1.5.24.48-13	5 x 24 x 48	25.44	57	0.570	1.000	69.5	4900	2460	0.50	274.6	140.0	0.25	0.511	
WCB 22.1.5.24.48-14	5 x 24 x 48	25.44	57	0.855	1.500	67.0	4900	3510	0.72	291.1	200.0	5.00	0.687	
WCB 22.1.6.24.48-15	6 x 24 x 48	20.80	60	0.300	0.500	69.5	4900	3340	0.68	269.5	200.0	16.00	0.742	
WCB 22.1.6.24.48-16	6 x 24 x 48	20.80	60	0.600	1.000	67.0	4900	3340	0.68	287.6	200.0	20.00	0.696	
WCB 22.1.6.24.48-17	6 x 24 x 48	20.42	56	0.340	1.500	67.0	4900	3070	0.63	286.0	172.0	0.050	0.602	
WCB 22.1.6.18.60-18	6 x 18 x 60	25.74	44	0.220	0.500	69.5	5970	4130	0.70	237.4	184.0	-	0.776	
WCB 22.1.6.18.60-19	6 x 18 x 60	25.74	44	0.440	1.000	67.0	5970	3710	0.62	250.5	163.0	-	0.652	

width, and thickness, influenced the lateral deflection and the average ultimate concrete stress due to the axial load. Thin panels showed a greater lateral deflection than thicker panels as shown in Fig. 20.

Raising of the slenderness ratio brought about a corresponding decrease in the average ultimate concrete stress in the specimen and an increase of the width of the specimen caused a corresponding increase of this stress (Table 3).

The first visible crack of panels appeared at around nine -tenths of the ultimate load.

The panels had two different modes of failure. The first possible mode of failure is characterized by a panel buckling failure as shown in Plates 10, 11, 12, and 13. Due to the buckling of the panels a brittle failure suddenly resulted in the concrete compression block and this brittle failure occurred as soon as the first visible cracking was observed. These cracks rapidly spread along the horizontal lines of the middle part of the panels. The maximum deflection due to axial load occurred in the plane of symmetry near the center of the panel. This is so because the thin ends of a panel could be easily rotated which caused buckling of the panel, as shown in Fig. 21. In the discussion of the bending at the center of a slender panel

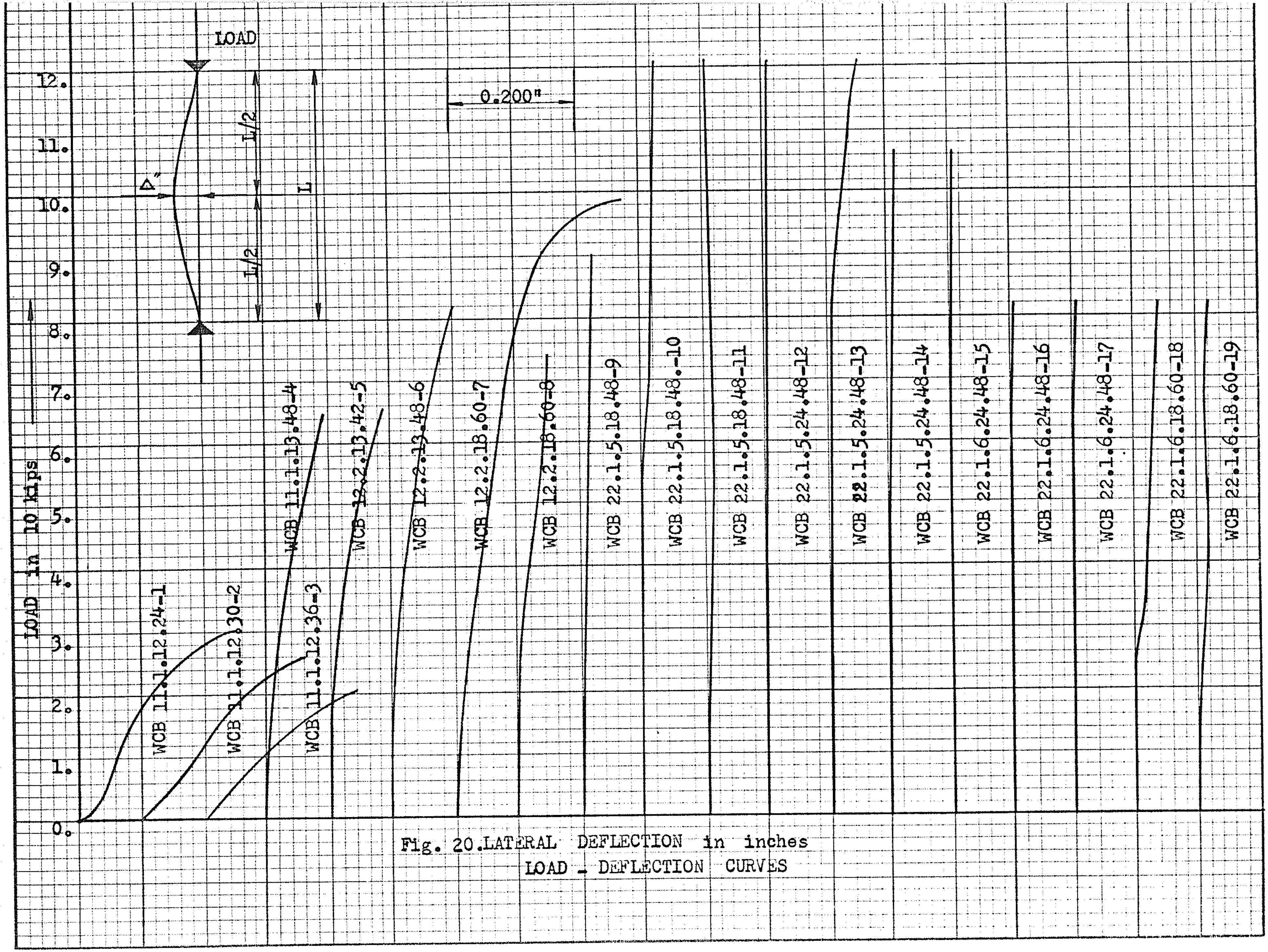

Fig. 20.LATERAL DEFLECTION in inches

LOAD - DEFLECTION CURVES

under the action of an eccentric load due to deflection, the tension may be neglected at the ultimate load because it is very small in comparison with the compression in the panel as the panel was previously compressed by axial load. Therefore, the panel failed by crushing of the concrete of the compression edge due to combined bending and axial compression at the center.

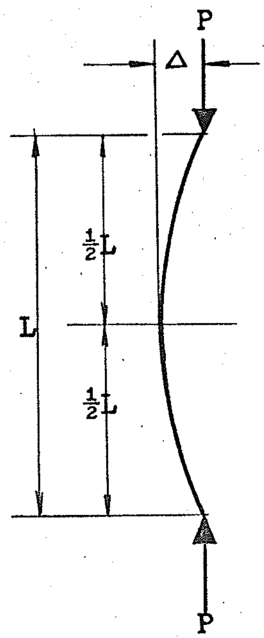

Fig. 21. Single Layer Panel under Axial Load.

The second possible mode of failure involves the panels cracking diagonally under the shearing stress. Immediately after the ultimate load is reached, panels fail with a diagonal shearing of the concrete at the top of the panel. This failure is like a cone-shaped failure of standard compression concrete cylinders as shown in Plates 14, 15, 16, and 17. The reason for the second possible mode of failure seems to be due to these specimens being thicker and wider than the specimens in the first possible mode of failure. When single layer panels started to buckle due to uniformly applied axial load, the edges of the upper and lower ends of the panel resisted rotation of the ends. At the upper end of the panel, the clamped WF beam in the loading frame (Fig. 19) remained fixed. But the head of the loading frame hydraulic jack at the

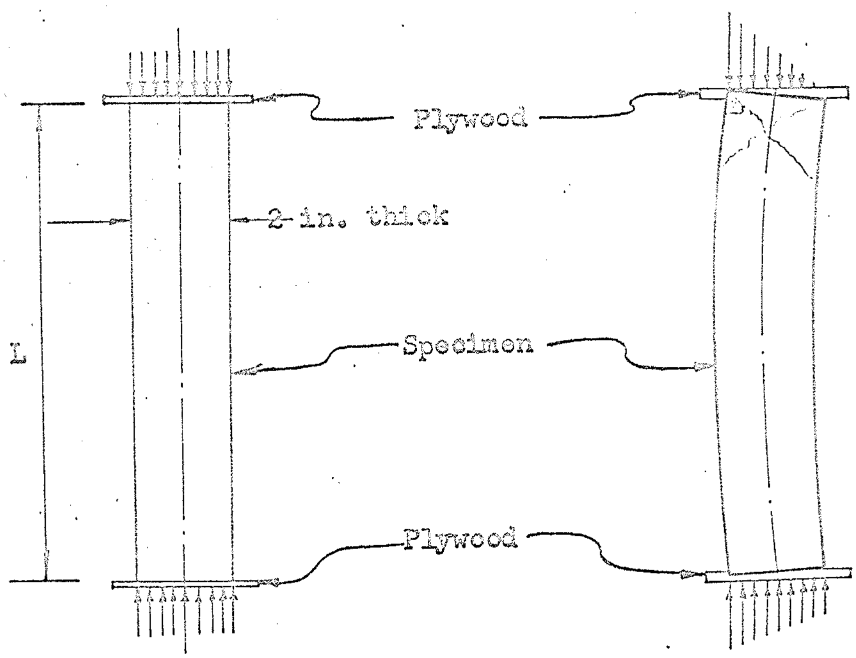

Fig. 22. Single Layer Panel under Uniaxial Compression.

Fig. 23. Single Layer Panel under edgewise compression.

lower end of the panel allowed a very small angle of rotation of the movable WF beam in the loading frame during the buckling of the panel. Therefore, at the same time, very small amount of lateral movement of the hydraulic jack occurred due to transverse component of rotational force at the lower end of the panel. Then the load distribution on the panel changed from the loads as shown in Fig. 22. to the loads as shown in Fig. 23. and the intensity of the compressive edge load at the top of the panel increased until the edge started to collapse.

B. Sandwich Panels

The tests show that compression sandwich panel failure is a function of concrete strength and panel proportions. Steel area is not an important function as long as the steel bars are appropriately placed in the panel. As shown in Appendix B, we can see that the lateral deflections at the center of sandwich panels due to axial loads are much smaller than of single layer panels. Very slender one inch thick individual face plates of the panels showed very high average ultimate concrete compressive stress in comparison with the one inch thick single layer panels. The first visible crack in the sandwich panels appeared at around one-quater to one-half of the ultimate load.

The sandwich panels also had two different modes of failure. The first possible mode of failure in the sandwich panels is similar to the second mode of failure in the single layer panels which has been described above with the longitudinal splitting of the concrete on the weak plane along the vertical lines at the side plates of the panels (Plates 18, 19, 20, 27, and 28).

The other mode of failure is associated with cracking, splitting, and bending due to combined axial and lateral loads. The higher combined stresses due to axial and lateral loads on the sandwich panel are in effect longitudinal compressive and shearing stresses acting on the section between the insulation core and the concrete face plate. The friction resistance between the faces of the core and plate is negligible. Also, compressive and shearing stresses of the Styrofoam insulation core between concrete face plates are very small in comparison with the stresses of concrete face plates and almost do not affect the strength of the sandwich panels. In this case the longitudinal shear strength due to combined loads is wholly dependent on the shear resistance of horizontal bars and concrete thickness of the narrow side plates in the sandwich panel, but these bars in the side plates are not well enough embedded in the concrete to develop bond against over a considerable length of steel. Hence the longitudinal splitting of the concrete on the weak plane along the vertical lines of the edges of the insulation core faces can be closely associated with diagonal tension and flexural cracks.

4.2. INDIVIDUAL INVESTIGATION

1. SPECIMEN WCB 11.1.12.24- 1

As shown in Plate 10, compression falure by buckling resulted in the panel. As the compressive strain was raised on the compression face (back side of the panel), a corresponding increase in the axial load occurred. Near the ultimate load, the strain at the center of the panel (Figure 24, gage no. 9) increased sharply to the value of 0.002448 in/in, as is shown in Figure 26. The compressive strain on the face side increased continuously under increasing load until the load reached 30,000 lbs. and in the range from 30,000 lbs to 40,000 lbs no apparent strain change was observed. Beyond the 40 kips load value, the compressive strain decreased, and at the load of 40,200 lbs, tensile strain of 0.0004 in/in was measured at the center of the panel (Figure 24, gage no. 5). Because this tensile strain is very small in comparison with the compressive strain, the steel could not have developed any tensile stress as it was located at the center of the concrete section. . The ratio of an average concrete stress in the panel to its standard concrete cylinder strength is 3850 to 5100 psi, or 76 % (Table 3). The center deflection of the panel increased under increasing axial load and measured to be 0.23 in. at the load of 30 kips (Figure 20), so that a moment of 6.9 in-kips was developed at the center due to the load of 30 kips.

2. SPECIMEN WCB 11.1.12.30- 2

This panel failed in compression by buckling as shown in Figure

27 and Plate 11.

The compressive strains on the rear compression face of the panel increased continuously under increasing axial load. At the center the strain increased very rapidly near the ultimate load. The final failure was caused by this rapid increase of the concrete compression at the center. On the face plate of the panel the compressive strains increased continuously near the top of the panel under increasing load until it reached 30 kips. Beyond a load of 30 kips, the strains decreased a little (Fig. 27, gage nos. 1, 2, and 3). The tensile strains increased near the bottom of the panel under increasing load up to about 15 kips, and in the range from 15 kips to near the ultimate load, no apparent strain changes were observed (Fig. 27, gage nos. 7, 8, and 9). At the center of the panel no apparent strains were observed below the load of 30 kips, but small amounts of rapid increases of tensile strains were observed in the load range from 30 kips to the ultimate load (Fig. 27, gage nos. 4, 5, and 6).

An average concrete stress of 2950 psi was found at the ultimate load of 35,200 lbs in the panel. The ratio of an average concrete stress of the panel to its standard concrete cylinder strength is 58 % (Table 3).

The center deflection of the panel increased sharply under increasing axial load and was 0.25 in. for a load of 25 kips (Fig. 20), so that a moment of 6.25 in-kips was developed at the center due to the axial load of 25 kips.

3. SPECIMEN WCB 11.1.12.36-3

As shown in Plate 12, compression failure by buckling resulted

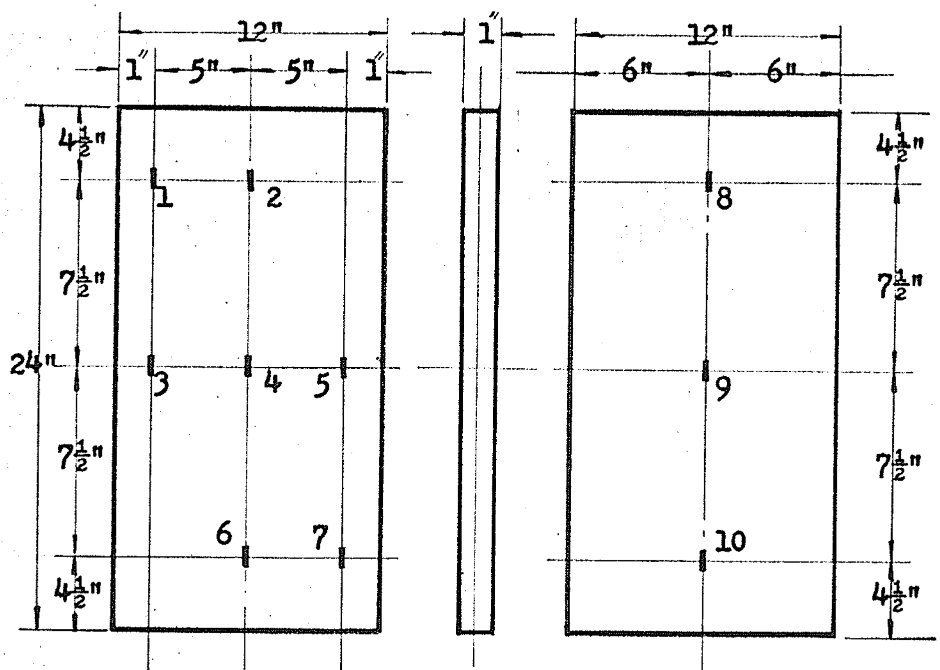

Fig. 24. STRAIN GAUGE LOCATIONS OF WCB 11.1.12.24- 1.

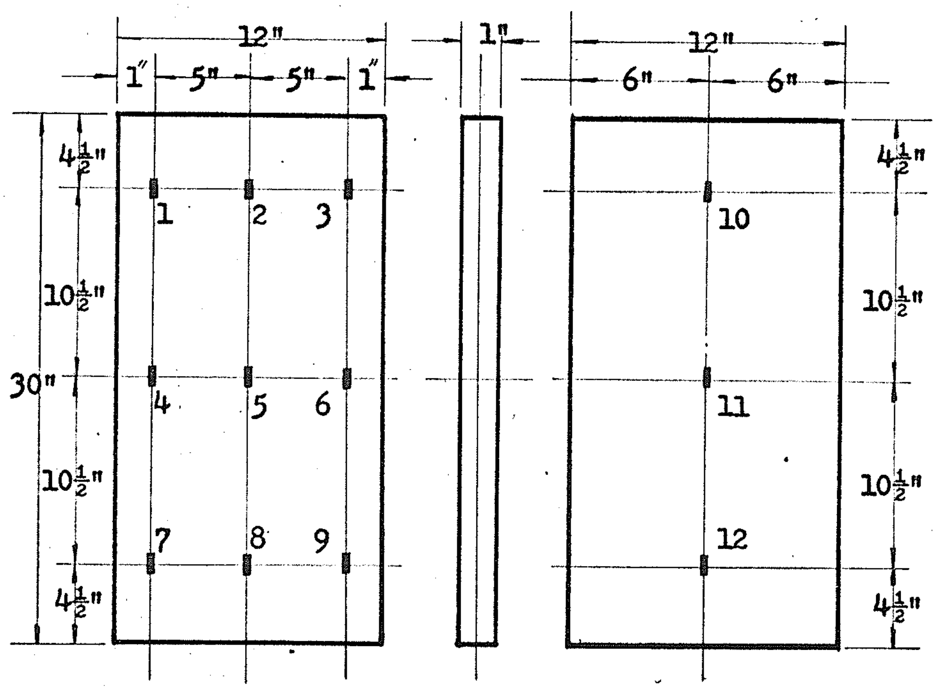

Fig. 25. STRAIN GAUGE LOCATIONS OF WCB 11.1.12.30- 2.

FIG. 26. WCB 11.1.12.24- 1 LOAD — STRAIN CURVES

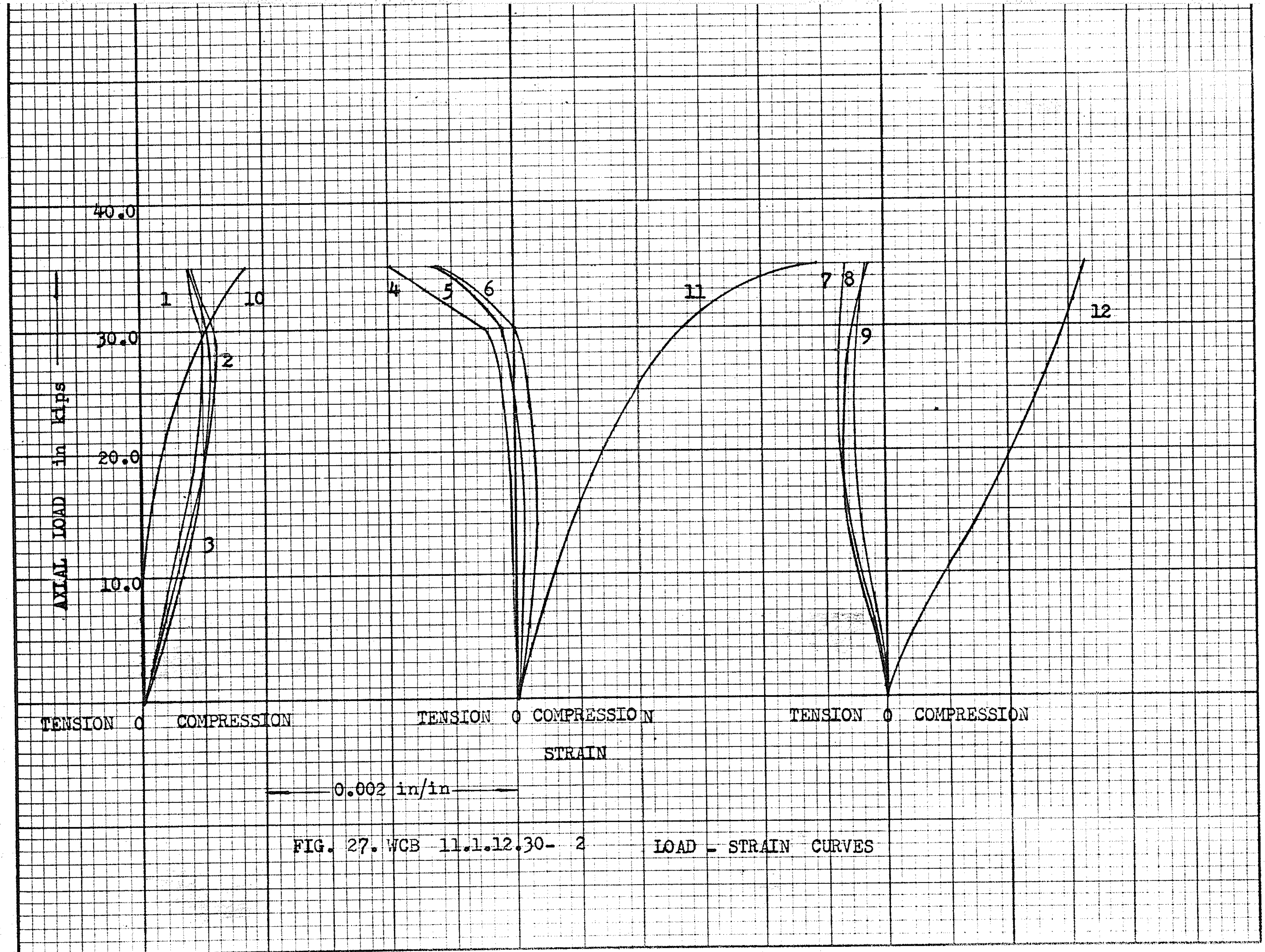

FIG. 27. WCB 11.1.12.30- 2 LOAD - STRAIN CURVES

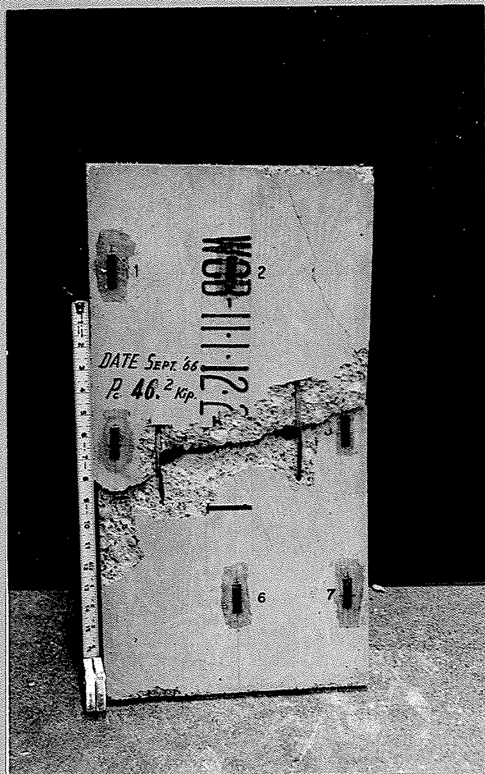

PLATE No. 10. View of Panel WCB 11.1.12.24- 1 after Failure.

PLATE No. 10a. Enlarged View of Failure of WCB 11.1.12.24- 1.

PLATE No. 11. View of Panel WCB 11.1.12.30- 2 after Failure.

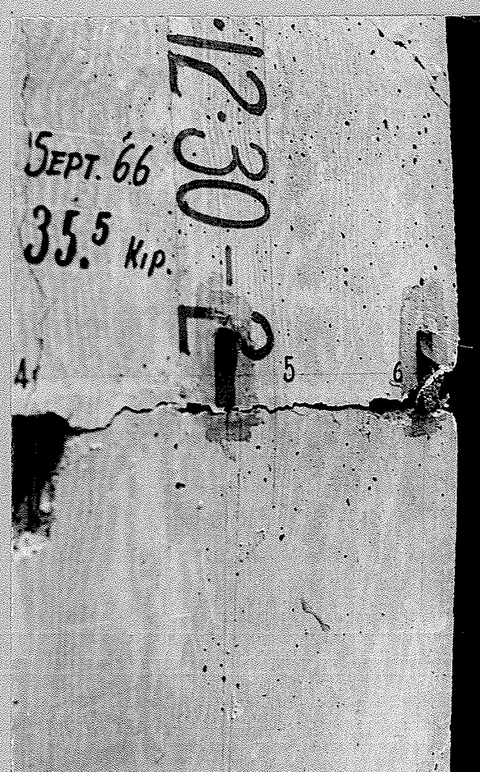

PLATE No. 11a. Enlarged View of Failure of WCB 11.1.12.30- 2.

in the panel.

On the compression face, near face of the panel, the compressive strains increased under increasing axial load and near the center of the panel (Figure 30, gage no. 12), a very rapid increase of the strain was measured (0.001624 at the load of 35,000 lbs) before the concrete failed. This rapid increase of the concrete compression in the panel near the ultimate load brought on the final failure, as shown in Fig. 30.

On the front face of the panel in Plate 12, the compressive strains increased under increasing load, and in the load range from 20,000 lbs to 30,000 lbs, no apparent strain changes were observed in the upper and central regions of the panel. Beyond a load of 40,000 lbs these compressive strains, except at both end parts of the panel, decreased under increasing load. Near the ultimate load, a tensile strain of .000286 was measured at the center (gage no. 4).

An average concrete stress of 2920 psi was found at the ultimate load of 35,000 lbs in the panel. The ratio of an average concrete stress of the panel to its standard concrete cylinder strength is 57% (Table 3).

The center deflection of the panel increased more sharply than the others under increasing axial load and was measured at 0.24 in. for a load of 20,000 lbs (Figure 20), so that a moment of 4.8 in-kips was developed at the center due to axial load of 20 kips.

4. SPECIMEN WCB 11.2.13.48-4

The mode of failure for this panel was a typical compression failure by buckling, as shown in Plate 13. Observed strains on the compression and tension concrete faces at the center of the panel are presented in Figure 31. As the strain on the compression face of the panel was raised, a corresponding increase in the axial load occurred. Near failure the compressive strain increased rapidly to the value of 0.002280, and concrete crushing was evident, spreading horizontally near the middle of the panel. Then final failure was caused by crushing of the concrete at the compression face of the specimen. The strain on the tension face of the panel increased gradually under increasing axial load and was measured at the value of 0.000454 for a load of 97,610 lbs. The steel could not have developed any tensile stress as it was located at the center of the concrete section. This measured tensile strain is very small in comparison with the compressive strain near the ultimate load.

An average concrete stress in the panel was computed as 4080 psi for an ultimate load of 106 kips, and the ratio of an average concrete stress of the panel to its standard concrete cylinder strength was 68 % (Table 3).

The center deflection of the panel increased gradually under increasing axial load having a value of 0.102 in. at the load of 64,690 lbs (Figure 20), so that a moment of 6.6 in-kips was developed at the center due to an axial load of 64,690 lbs.

5. SPECIMEN WCB 12.2.13.42-5

As shown in Plate 14 and Figure 34, the concrete panel failure resulted from compression. On the face side of the panel, the

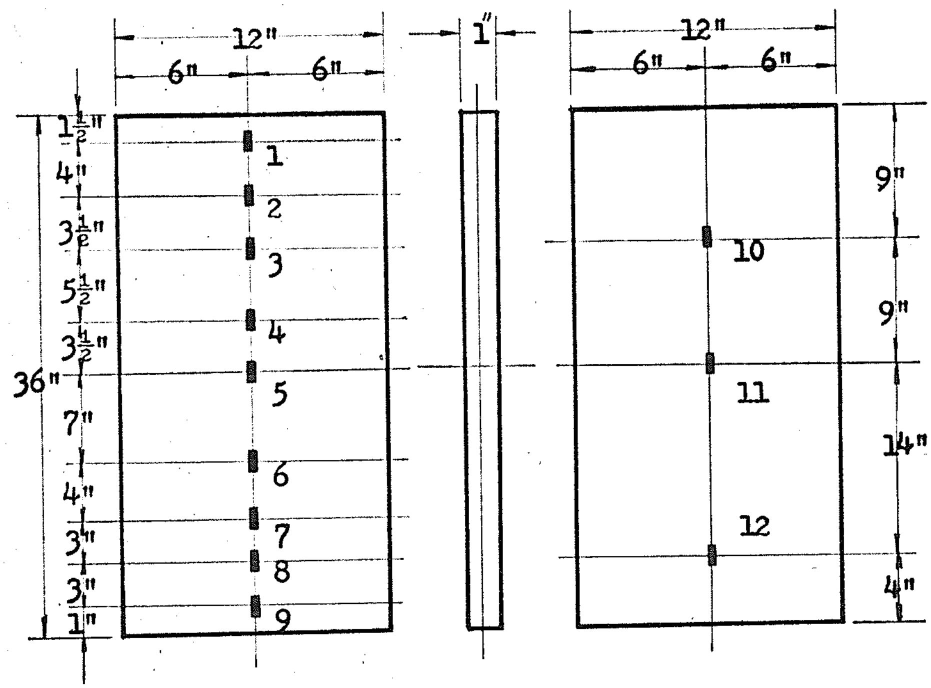

Fig. 28. STRAIN GAUGE LOCATIONS OF WCB 11.1.12.36- 3.

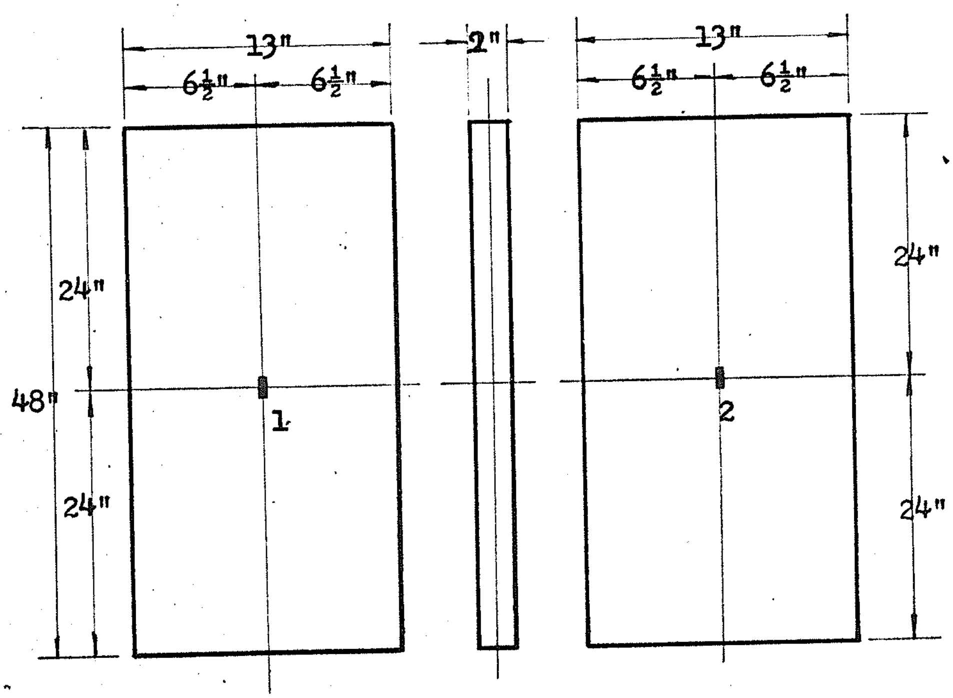

Fig. 29. STRAIN GAUGE LOCATIONS OF WCB 11.2.13.48- 4.

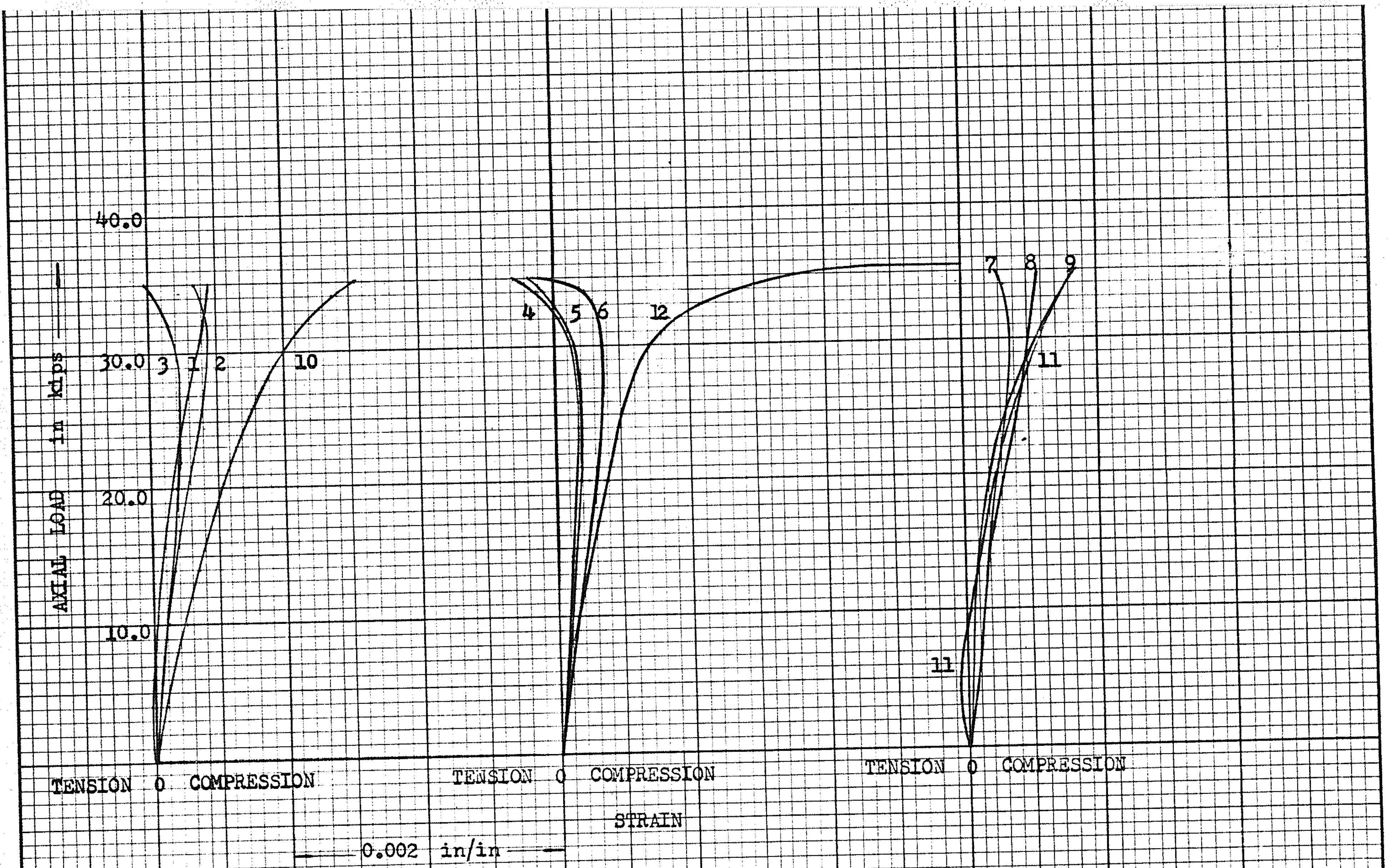

FIG. 30. WCB 11.1.12.36- 3 LOAD - STRAIN CURVES

Fig. 31. WCB 12.2.13.48- 4 LOAD - STRAIN CURVES

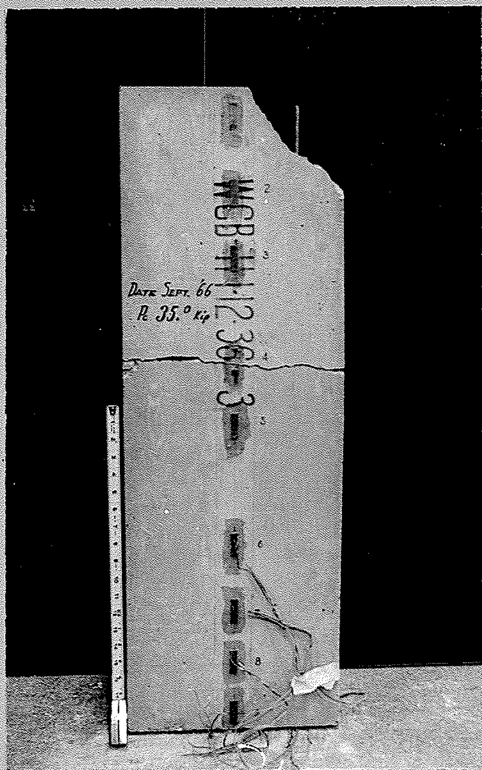

PLATE No. 12. View of Panel WCB 11.1.12.36- 3 after Failure.

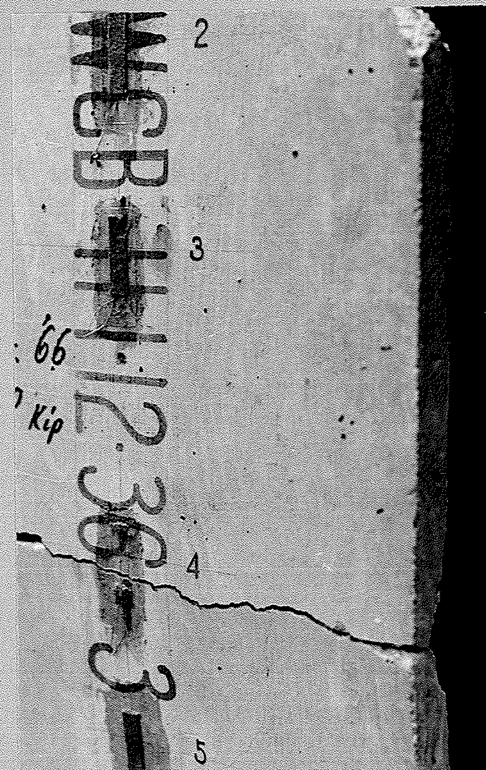

PLATE No. 12a. Enlarged View of Failure of WCB 11.1.12.36 - 3.

PLATE No. 13. View of Panel WCB 11.1.13.48- 4 after Failure.

PLATE No. 13a. Enlarged View of Failure of WCB 11.1.13.48 - 4.

compressive strain increased gradually under increasing load until a load of about 80 kips was reached, and beyond this, the strain increased very rapidly. The compressive strain of 0.00292 was measured at a load of 97,610 lbs. The concrete compression failure in the panel was caused by crushing of the corner region at the upper end of the panel. This in turn was due to some rotational movement at the end towards the compression edge before the concrete reached its ultimate compressive strain. In other words, this final failure was caused by a very rapid increase of the compressive strain in the concrete under gradually increased axial load. On the rear face of the panel in Plate 14, no significant compressive strain was measured as shown in Figure 34.

An average concrete stress of 3,820 psi at the ultimate load of 99,200 lbs was determined, and the ratio of an average concrete stress of the panel to its standard concrete cylinder strength was 64 % (Table 3).

The center deflection of the panel increased gradually under increasing axial load and was measured at 0.094 in. for a load of 64,690 lbs (Fig. 20). So that a moment of 6.07 in-kips was developed at the center of the panel due to the load of 64,690 lbs.

6. SPECIMEN WCB 12.2.13.48-6

Panel WCB 12.2.13.48-6 is an example of compression failure as shown in Plate 15 and Figure 35.

On the face side of the panel in Plate 15, the compressive strain increased gradually under increasing load until a load of about 80 kips was reached and beyond this, the strain increased very rapidly as shown in Figure 35. Near failure, compression cracks were developed, spreading diagonally near the upper part on the face side of the panel. These were caused by the rapid increase of the concrete strain, and final failure caused by crushing of the concrete. The concrete compressive strain at the face side was measured at 0.002183 for a load of 97,610 lbs.

On the back side of the panel, no significant compressive strain was observed. An average concrete stress in the panel was computed as 4060 psi for an ultimate load of 105,400 lbs and the ratio of an average concrete stress of the panel to its standard concrete cylinder strength was 68 %. This neglects the stress due to moment.

The center deflection of the panel increased gradually under increasing axial load. Near failure, very large deformation took place practically without any increase in load until the concrete failed, and the compression steel buckled. The center deflection of the panel measured 0.102 in. at the load of 81,630 lbs (Figure 20), so that a moment of 8.33 in-kips at the center was developed due to an axial load of 81,630 lbs.

7. SPECIMEN WCB 12.2.18.60-7

As shown in Plate 16, the panel failed in compression at the upper end. This panel was tested with a large number of SR-4 gages attached to the face of the panel. The distribution of strains on the panel faces is given in Figure 38. A general trend of increasing strains exists from both ends towards the center near the ultimate load. As shown in Figure 38, the attachment of SR-4 strain gage no. 14 was

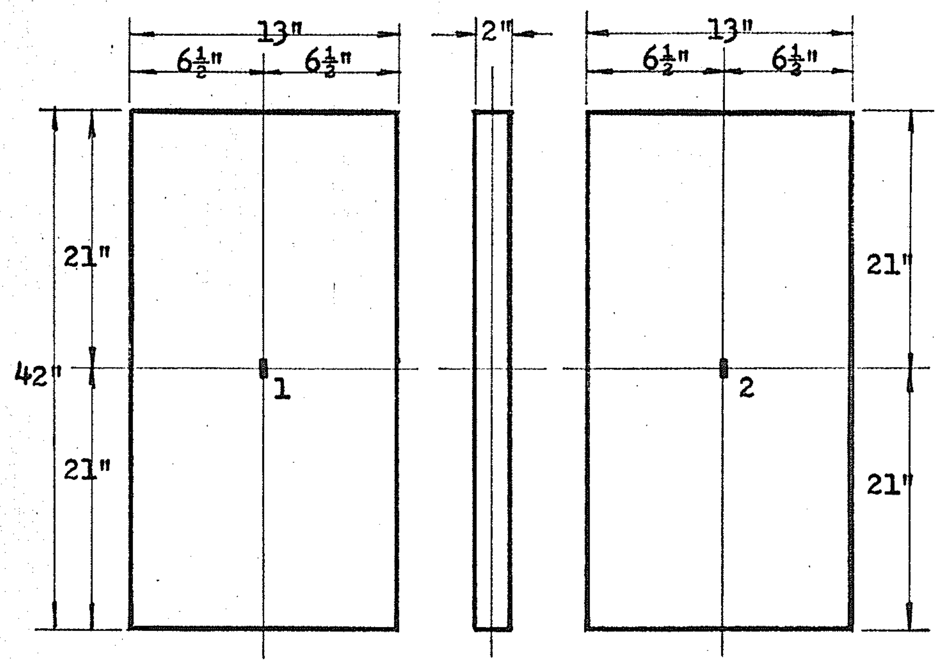

Fig. 32. STRAIN GAUGE LOCATIONS OF WCB 12.2.13.42- 5.

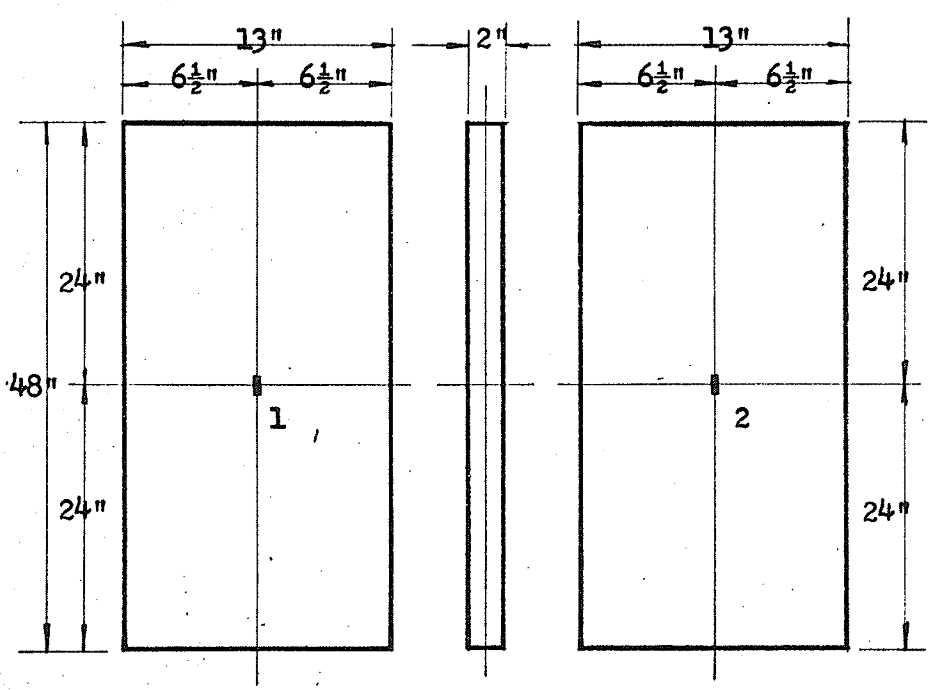

Fig. 33. STRAIN GAUGE LOCATIONS OF WCB 12.2.13.48- 6.

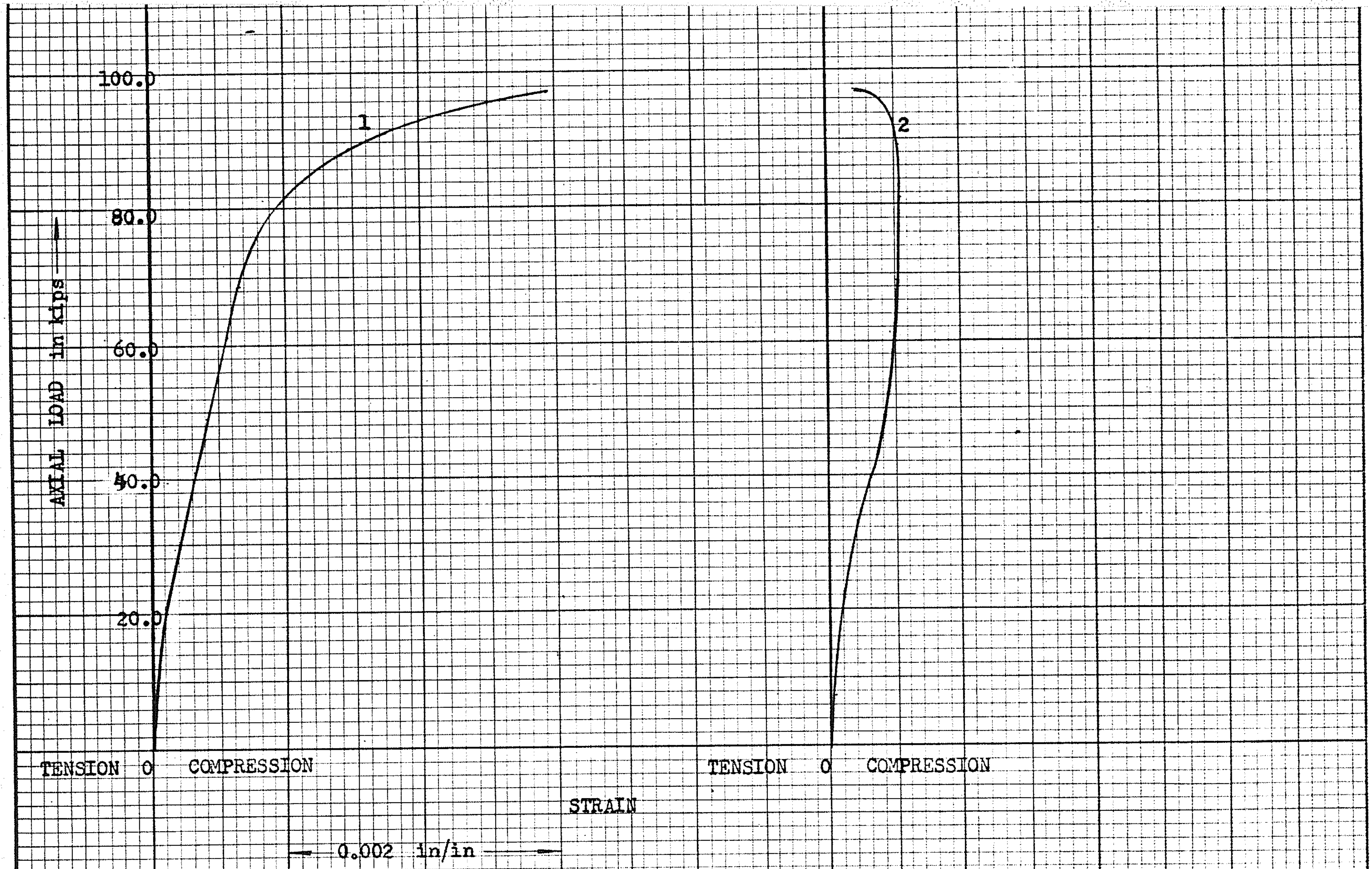

Fig. 34. WCB 12.2.13.48- 5 LOAD - STRAIN CURVES

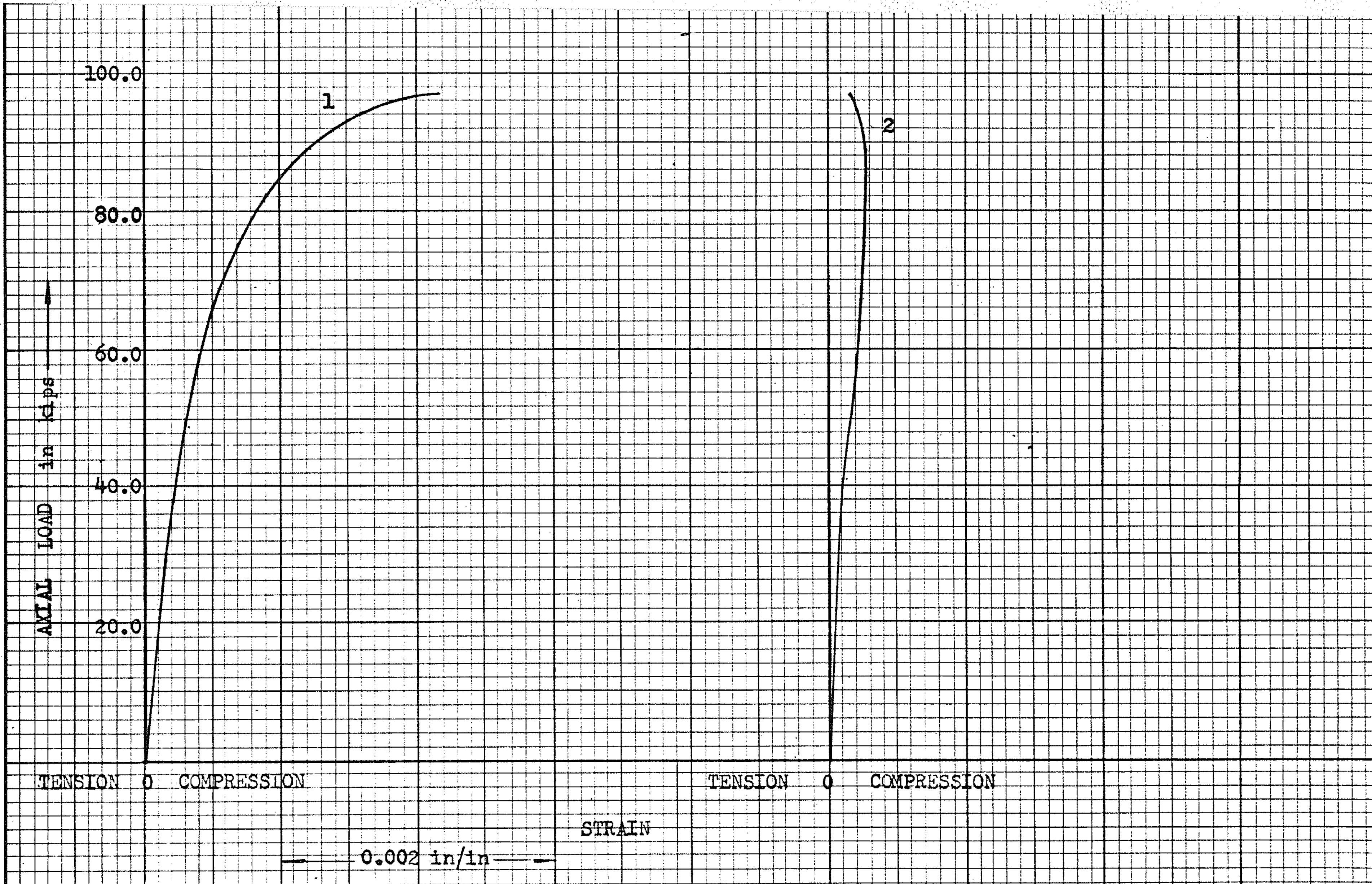

Fig. 35. WCB 11.2.13.48- 6 LOAD - STRAIN CURVES

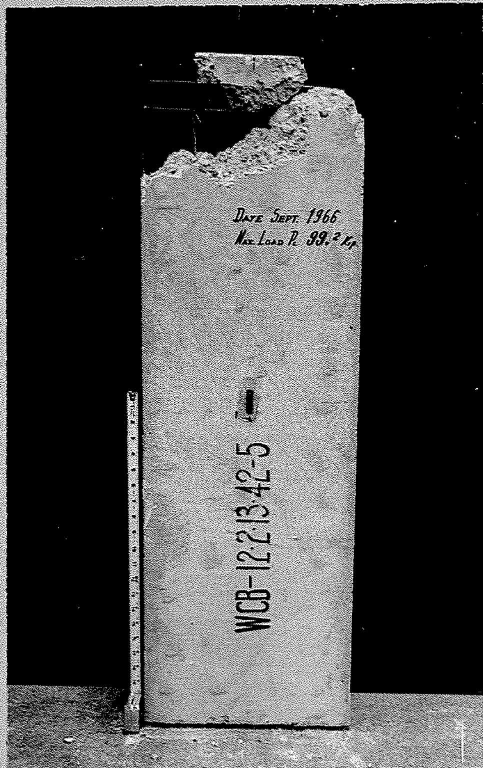

PLATE NO. 14. View of Panel WCB 12.2.13.42- 5 after Failure.

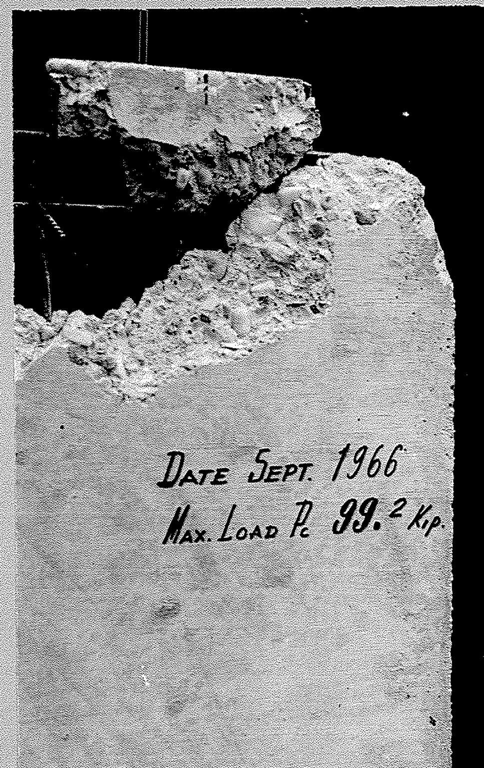

PLATE No. 14a. Enlarged View of Failure of WCB 12.2.13.42 - 5.

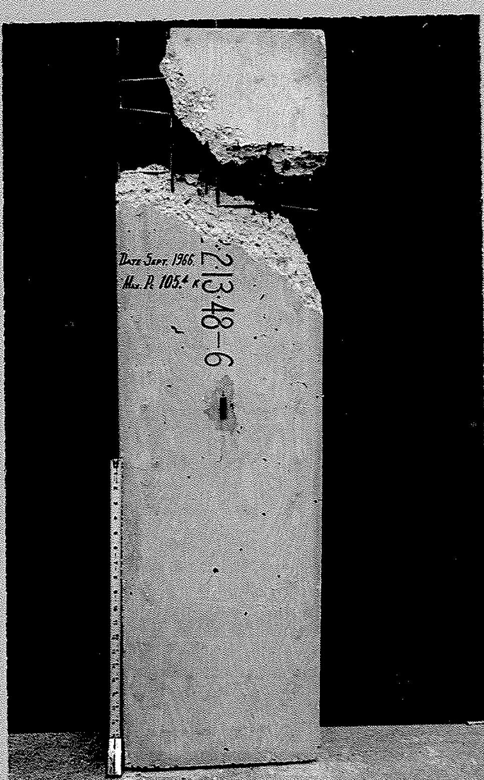

PLATE No. 15. View of Panel WCB 12.2.13.48- 6 after Failure.

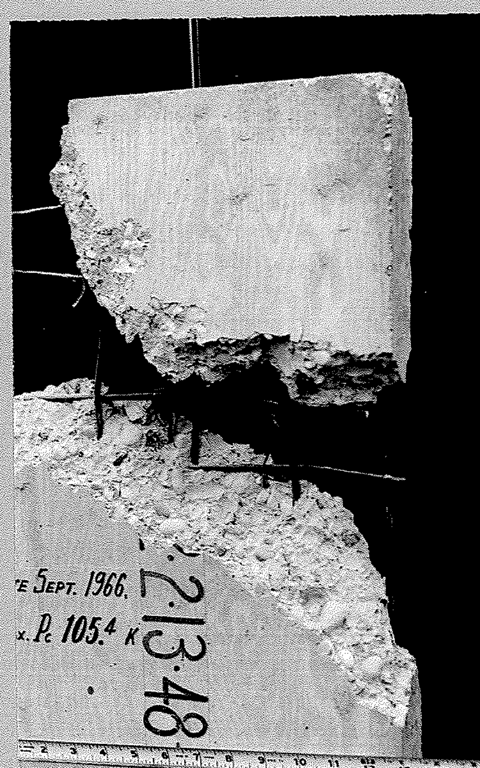

PLATE No. 15a. Enlarged View of Failure of WCB 12.2.13.48 - 6.

quite imperfect as indicated by the erratic strain record. As the strain on the compression face of the panel was raised, a corresponding increase in the axial load occured. Near the ultimate load, the compressive strain was measured at the value of 0.00214 at the center. Near failure, due to buckling at the center and lateral movement at the lower end of the panel, edgewise compression occured at the upper end (Figure 23) by the reason mentioned above in Part 4.1. Then compression cracks spreading horizontally across the top part of the panel were developed and the final failure was caused by crushing of the concrete at the top of the panel. However, no significant strain on the rear face of the panel in Plate 16 was observed. An average concrete stress of 3430 psi was found at the ultimate load of 123.6 kips. The ratio of an average concrete stress to its standard concrete cylinder strength is 67% (Table 3).

The deflection at the center of the panel increased gradually under increasing axial load and near failure, very large deformation took place before the concrete failed as shown in Figure 20. The center deflection of 0.266 in. was measured at a load of 97,610 lbs, so that a moment of 25.96 in-kips was developed at the center of the panel due to an axial load of 97,610 lbs.

8. SPECIMEN WCB 12.2.18.60-8

Compression failure resulted in the panel, as shown in Plate 17. This panel was tested with ten SR-4 gages attached to the face side and three to the back side of the panel. All strains increased in compression under increasing load and the distribution of strains is

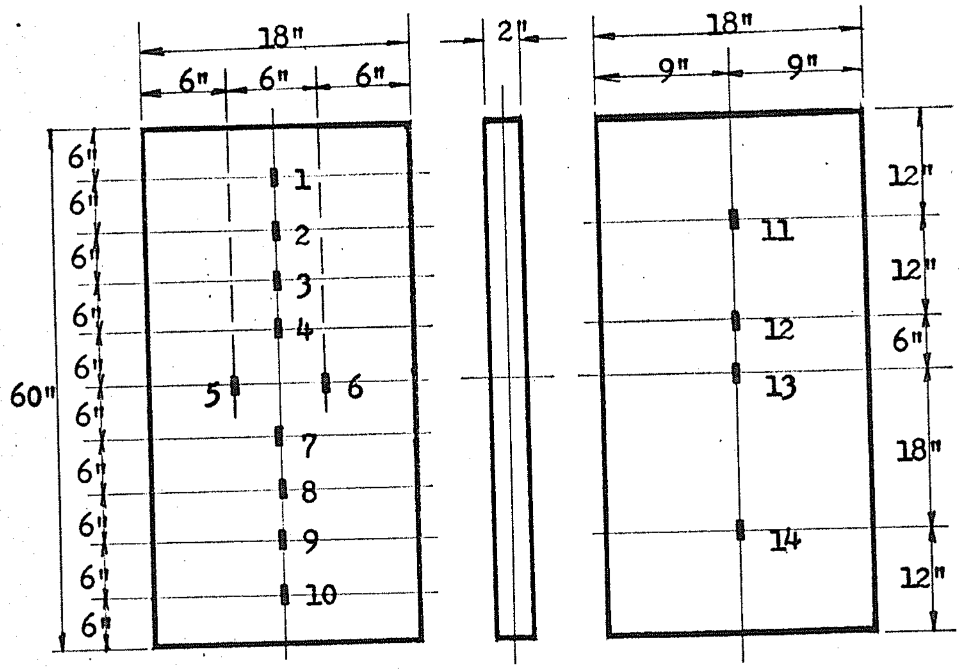

Fig. 36. STRAIN GAUGE LOCATIONS OF WCB 12.2.18.60- 7.

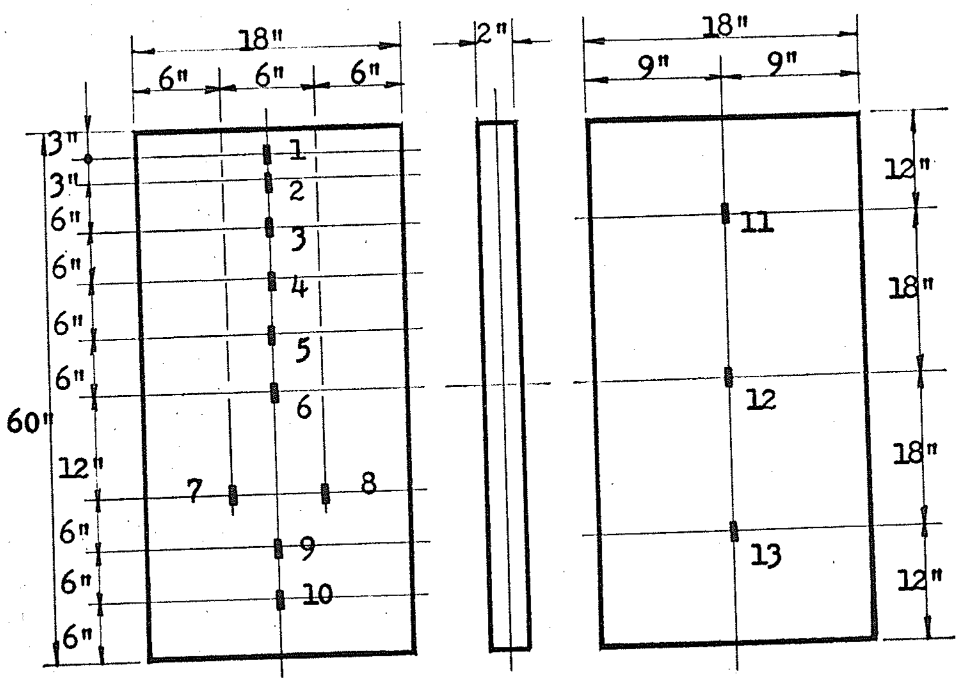

Fig. 37. STRAIN GAUGE LOCATIONS OF WCB 12.2.18.60- 8.

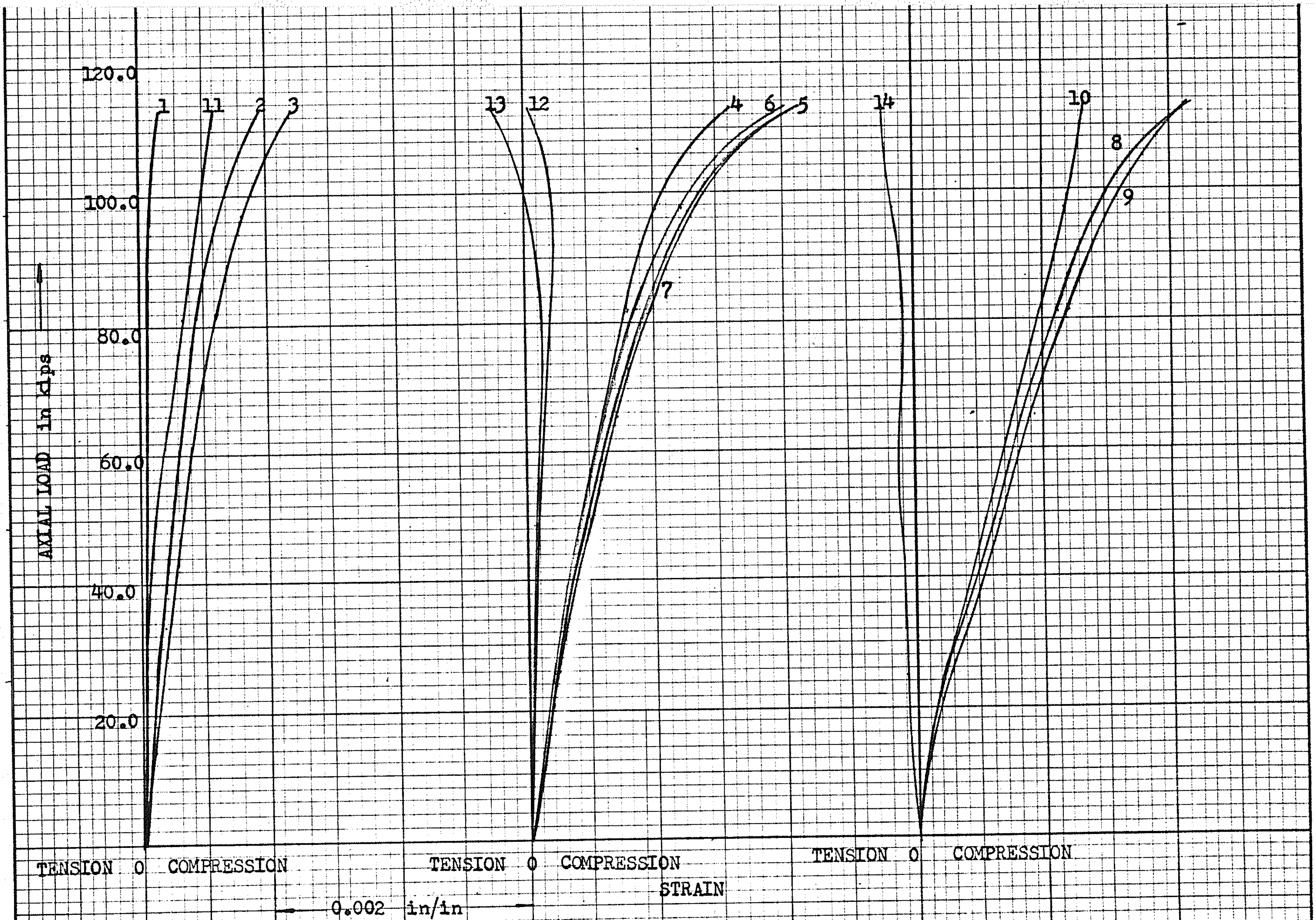

Fig. 38. WCB 12.2.18.60- 7 LOAD - STRAIN CURVES

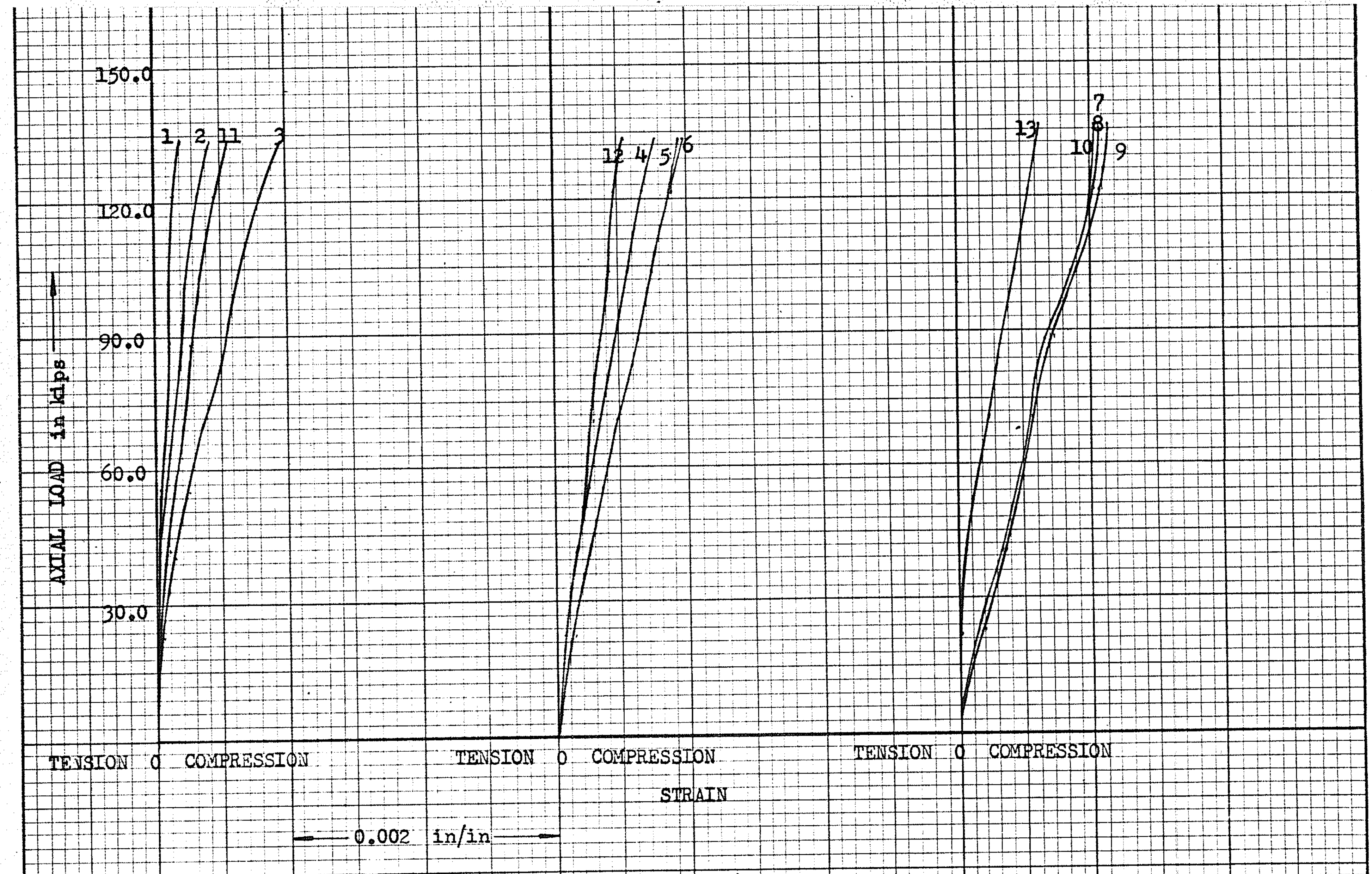

Fig. 39. WCB 12.2.18.60 - 8 LOAD - STRAIN CURVES

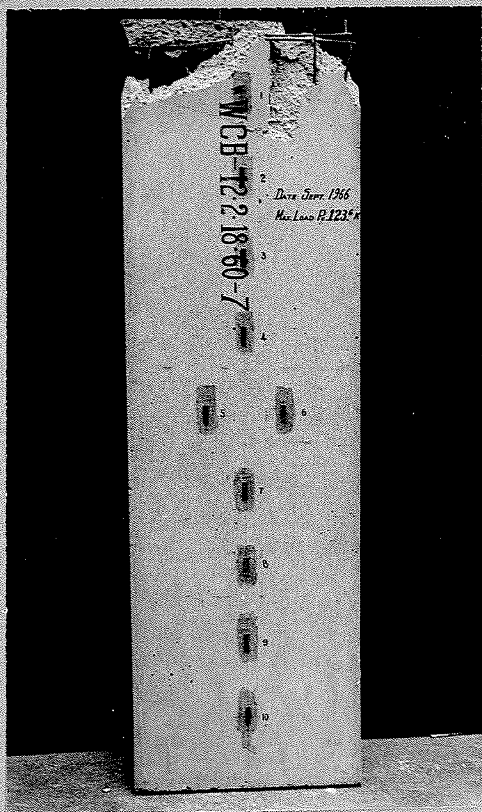

PLATE No. 16. View of Panel WCB 12.2.18.60- 7 after Failure.

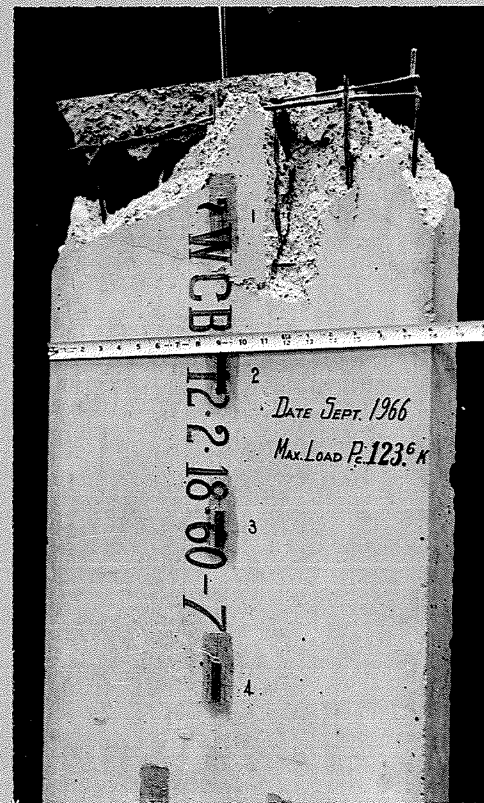

PLATE No. 16a. Enlarged View of Failure of WCB 12.2.18.60 - 7.

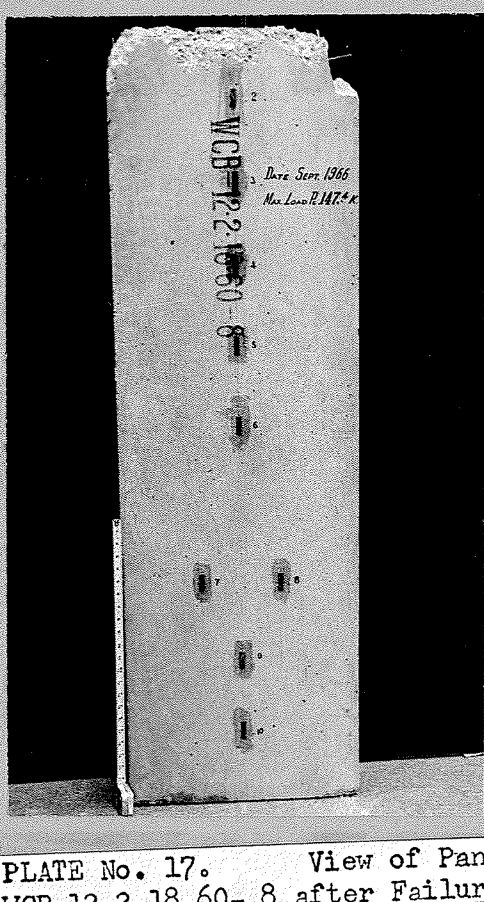

PLATE No. 17. View of Panel WCB 12.2.18.60- 8 after Failure.

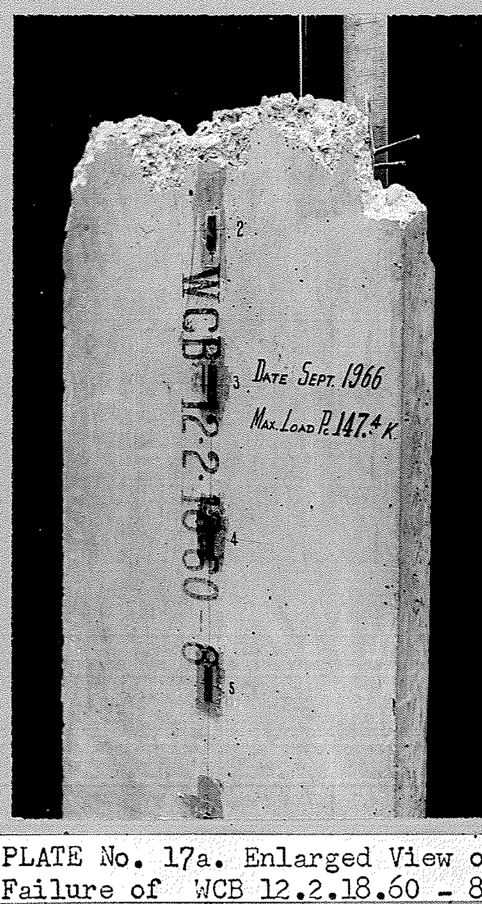

PLATE No. 17a. Enlarged View of Failure of WCB 12.2.18.60 - 8.

given in Figure 39. It is noticed that a general trend of increasing strains exists from the top towards the bottom of the face side plate. On the back side of the panel, the compressive strains increased similarly from the top to the bottom of the panel under increasing load. At the load of 133,200 lbs the maximum compressive strains were measured to be of 0.001148 at the face side and 0.000620 at the back side of the panel. The final failure was caused by crushing of the edge of the concrete at the top of the face side due to the reason that was described above in the investigation of the specimen WCB-12.2.18.60-7.

An average concrete stress of 4090 psi was found at the ultimate load of 147.4 kips in the panel. The ratio of an average concrete stress of the panel to its standard concrete cylinder strength is 68% (Table 3).

The center deflection of the panel due to axial load increased gradually under increasing load and was measured at the value of 0.05 in. at a load of 72,940 lbs (Figure 20), so that a moment of 3.65 in-kips occured at the center due to an axial load of 72,940 lbs.

9. SPECIMEN WCB 22.1.5.13.48-9

This panel is an example of tension failure of horizontal reinforcement due to splitting of the side plate as shown in Plate 18. This panel was tested with sixteen SR-4 gages attached to the four faces of the panel, i.e., eight gages horizontally and eight gages vertically as shown in Figure 40. All horizontal strain gages indicated tensile strains and all the vertical ones compression. The distribution of strains on the faces of the panel is given in

Figure 42. At the center of the panel, no apparent horizontal tensile strains were observed before the panel reached the final failure. The vertical compressive strains increased continuously under increasing load except gage no. 2 on the back face plate of the panel in Plate 18. Near failure, the concentrated compressive strain at the center of the face plate was released rapidly due to a rapid increase of horizontal elongations at the top (gage no. 1) and at the bottom (gage no. 16). Then all compressive strains at the center of the panel approached the similar values near the ultimate load. But these strains were not important factors in panel failure because these measured values at the failure were very small in comparison with the concrete ultimate strain. At the top of the panel, there was no significant increase in the vertical compressive strains under increasing load. On the right side of the panel, horizontal tensile strain (gage no. 16) also increased gradually until a load of about 120 kips was reached. Beyond the load of 120 kips, the tensile strain on the side plate rapidly increased until the load was of about 150 kips when longitudinal splitting of the concrete appeared along the vertical edge line of the insulation core. At the same time, very high compressive strain of 0.0021 in/in (gage no. 13) at the load of 160,970 lbs on the same side of the panel affected the split concrete. Then the final failure was caused by the crushing of the concrete at the side of the panel after the concrete split, and the steel in the side concrete reached yielding. An average concrete compressive stress of 4190 psi was found in the panel at the ultimate load of 176,000 lbs. The ratio of an average concrete compressive stress of the panel to its standard concrete cylinder strength is 70 % (Table 3). The deflection at the center of

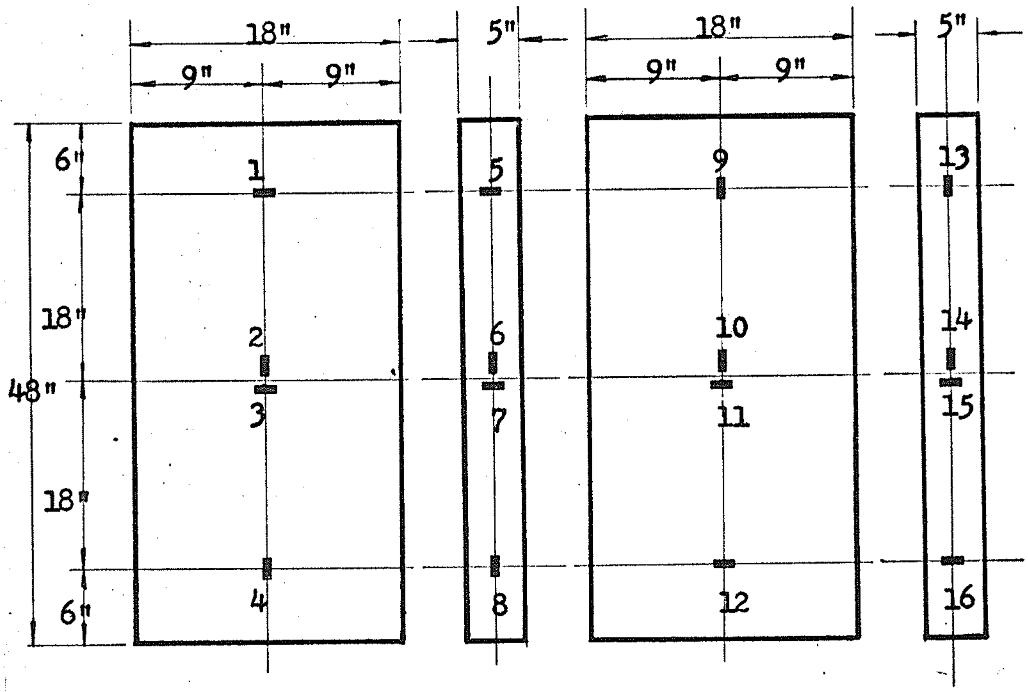

Fig. 40. STRAIN GAUGE LOCATIONS OF WCB 22.1.5.18.48- 9.

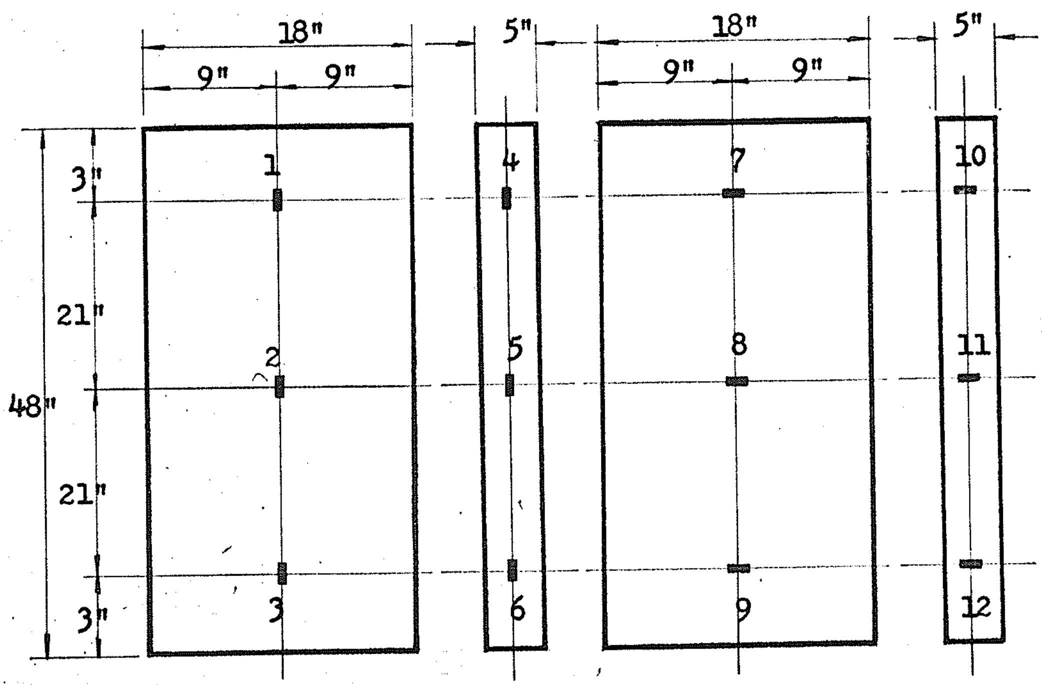

Fig. 41. STRAIN GAUGE LOCATIONS OF WCB 22.1.5.18.48- 10.

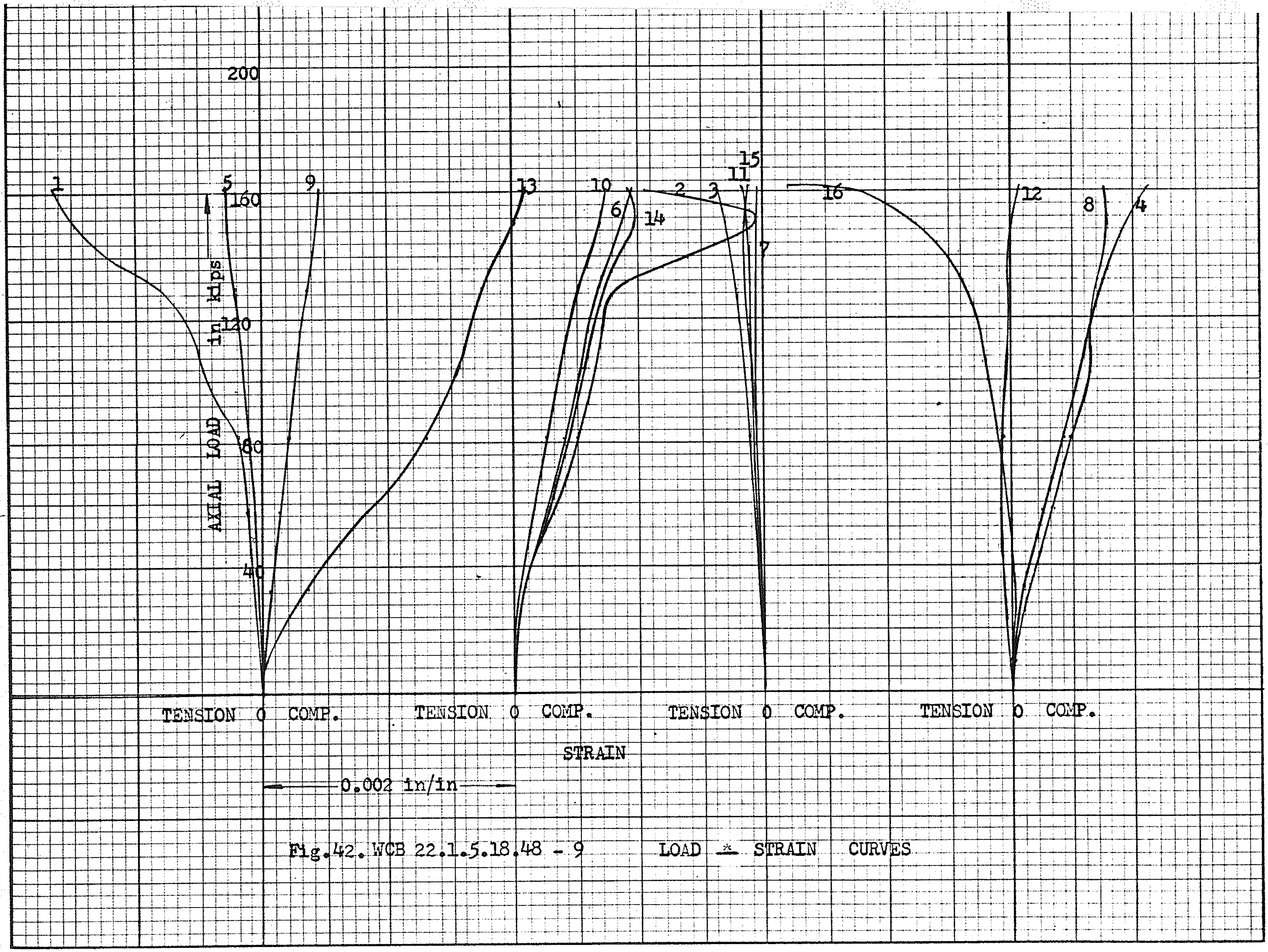

Fig. 42. WCB 22.1.5.18.48 - 9 LOAD - STRAIN CURVES

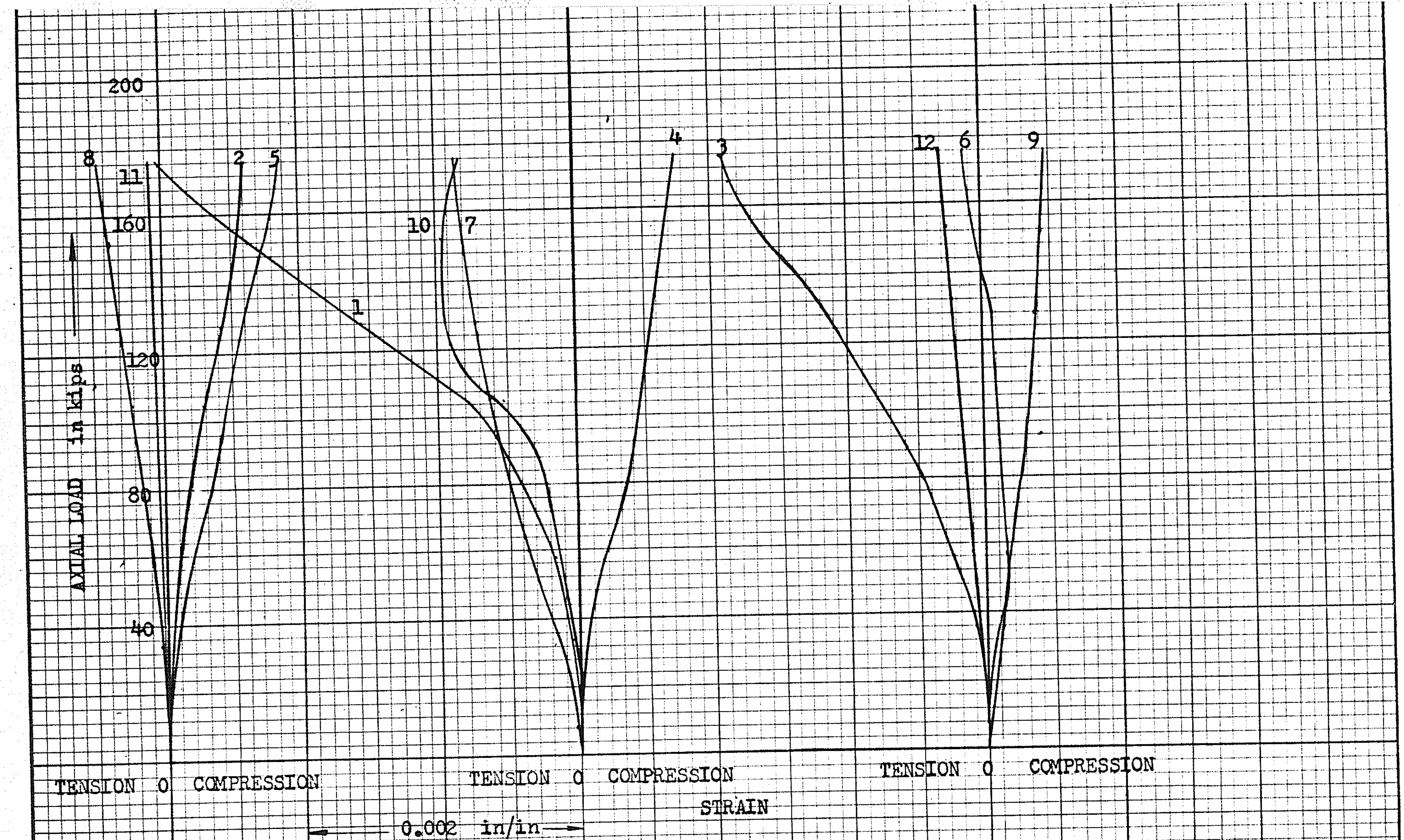

Fig. 43. WCB 22.1.5.18.48- 10 LOAD - STRAIN CURVES

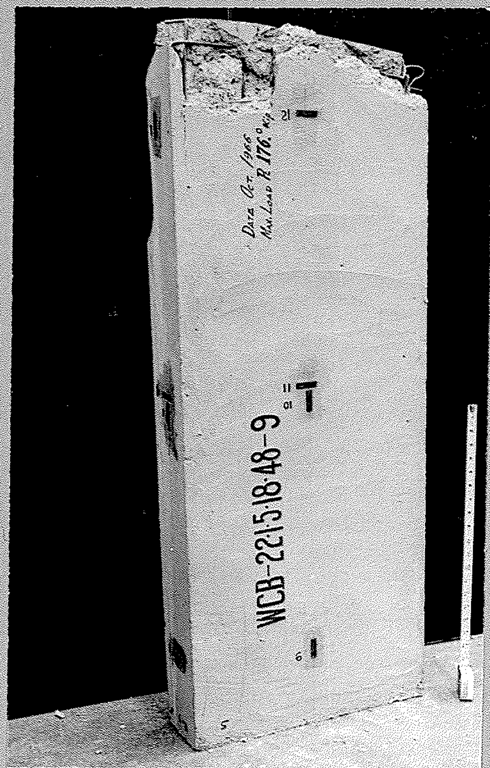

PLATE No. 18. View of Panel WCB 22.1.5.18.48-9 after Failure

PLATE No. 18a. Enlarged View of Failure of WCB 22.1.5.18.48- 9.

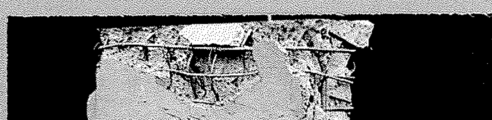

PLATE No. 19. View of Panel WCB 22.1.5.18.48-10 after Failure.

PLATE No. 19a. Enlarged View of Failure of WCB 22.1.5.18.48-10.

the back face plate of the panel in Plate 18 was not observed until the load of 14,000 lbs was applied. Beyond this load, the center deflection increased gradually under increasing load. The center deflection of 0.022 in. was measured at the load of 89,610 lbs (Figure 20).

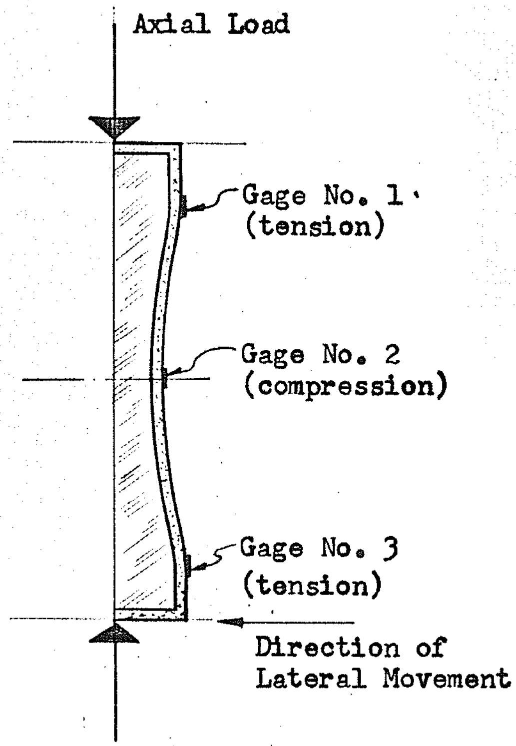

Fig. 44. Center Section of Specimen WCB 22.1.5.18.48- 10 after Loading.

10. SPECIMEN WCB 22.1.5.18.48-10

This panel is an example of tension failure of horizontal reinforcement as shown in Plate 19 and was tested with twelve SR-4 strain gages attached to the four faces of the panel, i.e., six gages horizontally and six gages vertically as shown in Figure 41. On the front face plate of the panel in Plate 19, the tensile strain (gage no. 1) increased gradually under increasing load until a load of 100,000 lbs was reached, and beyond that load, the tensile strain increased rapidly until the load reached near the ultimate load as shown in Figure 43. The final failure was caused by the yielding of the steel at the top of the front face plate due to increasing concave deformation at the center of the panel, from the face side towards the insulation core, and due to the increasing of the lateral movement at the lower end of the panel, under increasing load as shown in Figure 44. Near the ultimate load, the tensile strains of 0.00301 in/in at the upper part (gage no. 1), and of 0.00193 in/in at the lower part (gage no. 3), on the front face were measured. The compressive strain at the center of the panel (gage no. 2) was only of the value of 0.0006 in/in. Most horizontal strains showed considerable increase in tension under increasing load, and the bottom strain gage no. 9 on the rear face plate indicated the compressive strain, i.e., 0.000472 in/in at the ultimate load of 176,500 lbs. The center deflection at the rear face plate in Plate 19 increased very gradually under increasing load and the deflection measured was 0.029 in. at the load of 121,200 lbs. An average concrete stress of 4400 psi was found in the panel at the ultimate load of 184,800 lbs. The ratio of an average concrete compressive stress of the panel to its standard concrete cylinder strength is 74% (Table 3).

11. SPECIMEN WCB 22.1.5.18.48-11

This panel failed in tension as shown in Plate 20, and was tested with twelve SR-4 strain gages attached to the four faces of the panel, i.e., six horizontally and six vertically as shown in Figure 45. At the upper part of the panel in Plate 20, no apparent vertical changes were observed but the horizontal tensile strains on the face plate and the side plate (gage nos. 3 and 6) increased very rapidly under increasing load. Near the ultimate load, longitudinal splitting of the concrete appeared along the vertical edge line of the insulation core after the steel in the side plate at the upper part of the panel reached yielding. The final failure was caused by sudden crushing of the concrete horizontally across the upper part of the panel. Then the vertical compression steel reached yielding and buckled. At the middle part of the panel, no apparent horizontal tensile strains were observed, and the vertical compressive strains increased continuously under increasing load (gage nos. 8 and 11). At the lower part of the panel, the vertical tensile strains (gage nos. 1 and 7) and the horizontal compressive strain (gage no. 10) increased under increasing load, but these strains were not important factors. Concave deformation at the center of the right side plate in Plate 20 occurred towards the insulation core due to axial load. The deflection at the center increased under increasing load until the load of 49,070 lbs was reached, and beyond that load it decreased as shown in Figure 20. Near failure, a very small degree of the concave deformation was observed, and no convex deformation at the center of the side plate was observed until the concrete failed. An average concrete compressive stress of 3,480 psi was found in the panel at the ultimate load of 146,000 lbs. The ratio of an average concrete stress to its standard concrete cylinder strength is 58 % (Table 9).

12. SPECIMEN WCB 22.1.5.24.48-12

This panel was tested with twelve SR-4 strain gages attached to the four faces of the panel, i.e., six horizontally and six vertically as shown in Figure 46. At the upper part of the panel in Plate 21, no apparent vertical and horizontal strains were observed except on gage no. 10 at the side plate of the panel. This strain on the side plate increased very rapidly beyond the applied load of 40,000 lbs. Visible

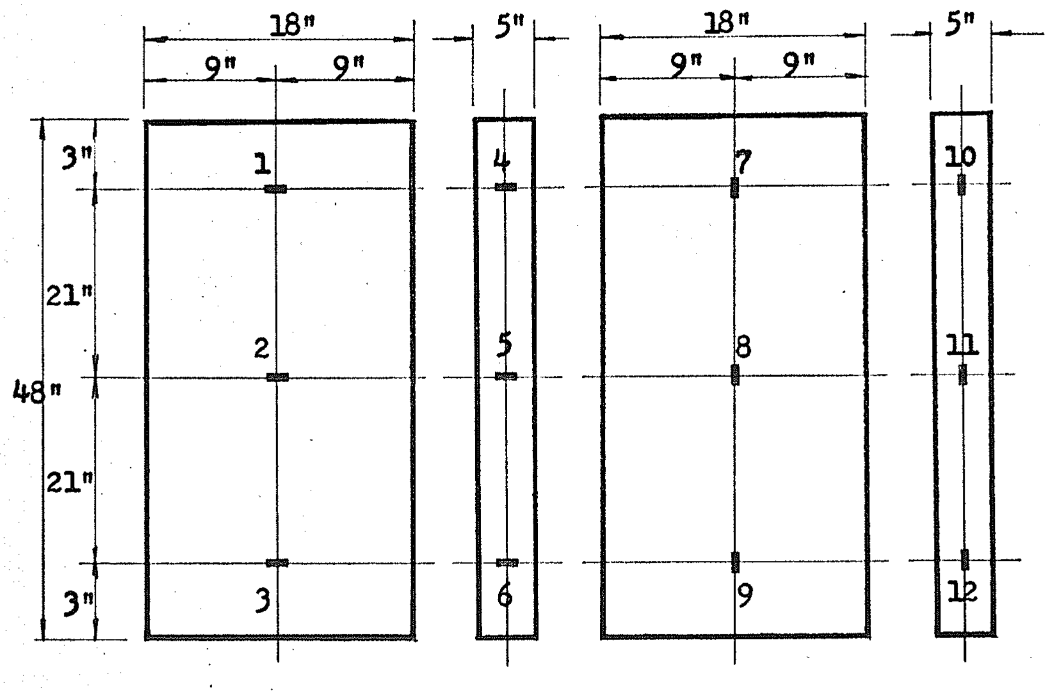

Fig. 45. STRAIN GAUGE LOCATIONS OF WCB 22.1.5.18.48- 11.

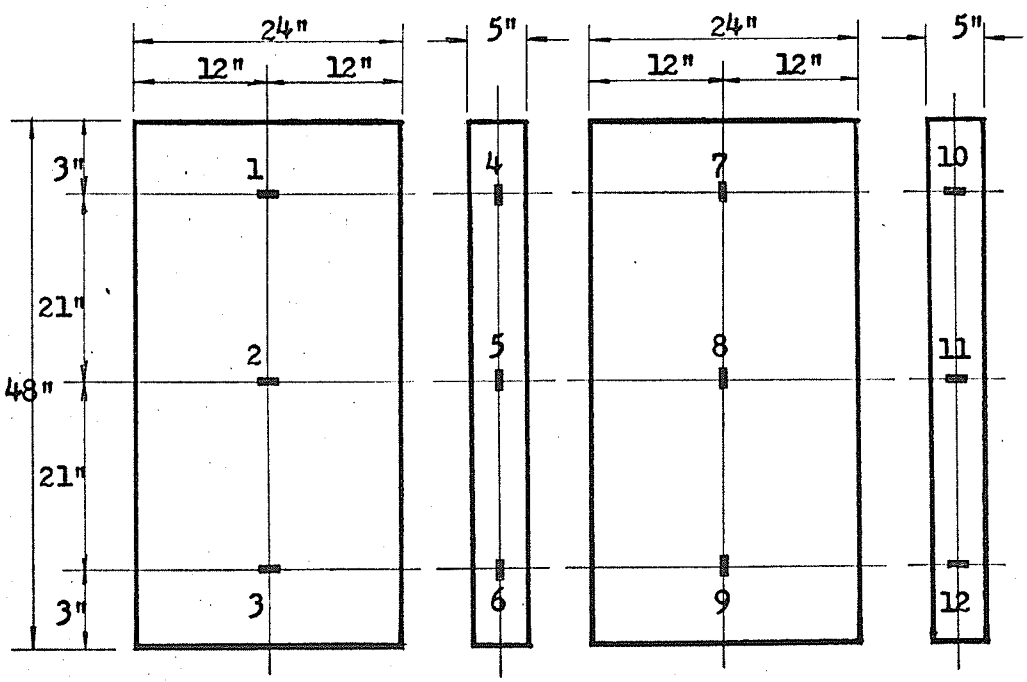

Fig. 46. STRAIN GAUGE LOCATIONS OF WCB 22.1.5.24.48- 12.

Fig. 47. WCB 22.1.5.18.48 - 11 LOAD - STRAIN CURVES

Fig. 48. WCB 22.1.5.24.48-12 LOAD - STRAIN CURVES

PLATE No. 20. View of Panel WCB 22.1.5.18.48-11 after Failure.

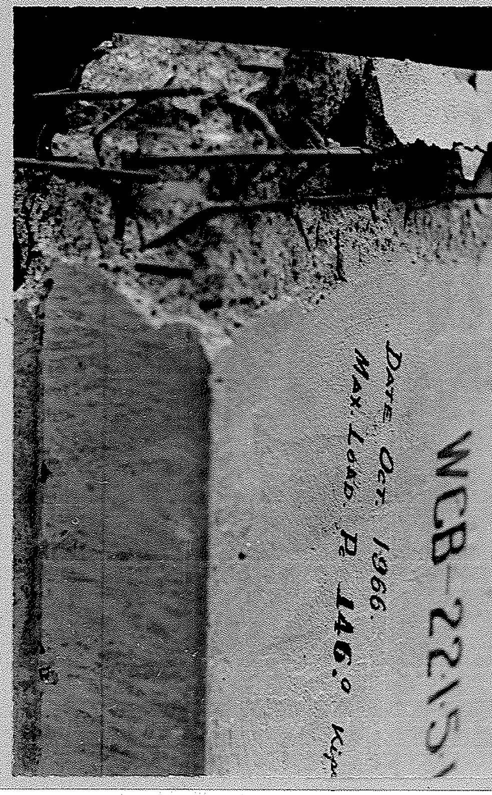

PLATE No. 20a. Enlarged View of Failure of WCB 22.1.5.18 48-11.

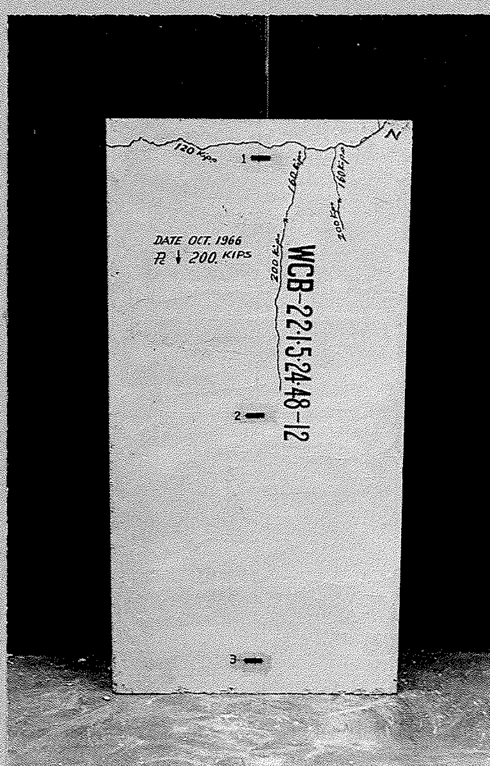

PLATE No. 21. View of Panel WCB 22.1.5.24.48-12 after Failure.

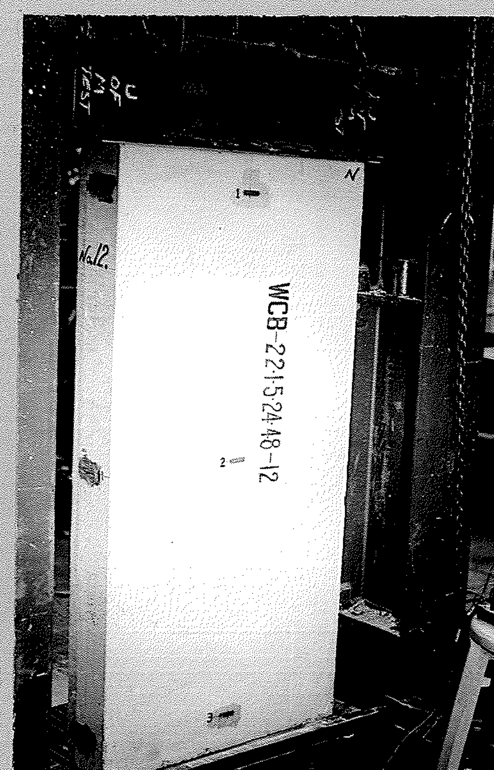

PLATE No. 21a. Panel WCB 22.1.5.24.48 - 12 in Testing Frame before Loading.

longitudinal cracks appeared on the side plate near the load of 100,000 lbs, and at the same time, horizontal tensile reinforcement in the side plate was yielding. Near the load of 120,000 lbs, major cracks extending horizontally across the upper part of the panel developed as shown in Plate 21. Near the load of 200 kips, longitudinal splitting of the concrete appeared along the vertical edge line of the insulation core after the steel in the side plate of the panel yielded. The tensile strain of 0.00557 in/in was indicated at the upper side plate due to splitting of the concrete at a load of 193,960 lbs. As mentioned above in Section 4.1., the available equipment had an axial load capacity of 200 kips only which was insufficient to produce the final failure in this panel. Before the lateral load could be applied to observe the final failure, the panel broke due to mishandling. At the center of the panel vertical compressive strain increased continuously under increasing load but the compressive strain of 0.00083 in/in at a load of 193,960 lbs (gage no. 8) may be considered negligible in comparison with the tensile strain on the side plate (gage no.10). The center deflection at the rear face plate increased very gradually under increasing load due to axial load, and the deflection measured was 0.007 in. at a load of 121,200 lbs. An average concrete compressive stress of 3,510 psi was found in the panel at a load of 200 kips. The ratio of an average concrete stress of the panel to its standard concrete cylinder strength is 72 % (Table 3).

13. SPECIMEN WCB 22.1.5.24.48-13

This panel is an example of tension failure at the top of the side plate as shown in Plate 22. The panel was tested with fourteen SR-4 strain gages attached to two faces, i.e., nine gages vertically on the face plate and five gages (2 horizontally and 3 vertically) on the side plate as shown in Figure 50. This panel was provided with lateral loading frame and hydraulic jack to apply lateral load in addition to an axial load of 200 kips as shown in Plates 8 and 9. The distribution of strains on the concrete faces of the panel is given in Figure 52. No apparent compressive strain and tensile strain were observed except, in the upper region of the side plate (gage nos. 10 and 11). Until an axial load of about 50,000 lbs was reached, no lateral movement at the lower end of the panel were observed. Beyond this load, the hydraulic jack in the lateral loading frame indicated lateral load without pumping of this jack, due to a deflection of the face plate and a lateral movement at the lower end of the panel. As soon as the lateral load was found, the hydraulic jack pressure was released, and the lateral load became zero. The vertical tensile strain (gage no. 11) and horizontal compressive strain

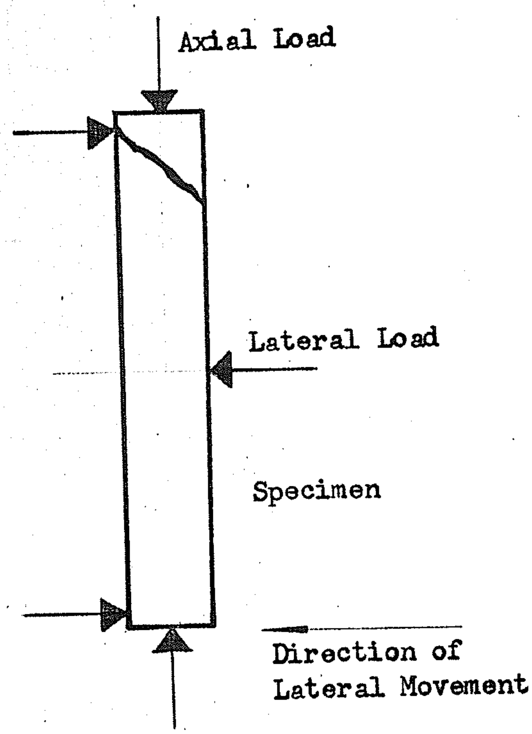

Figure 49. Development of a Diagonal Tension Crack.

(gage no. 10) increased continuously under increasing axial load at the top of the side plate until it reached near the ultimate load due to the reason mentioned above (Figure 49). Near failure, a sudden decrease of the compressive strain and a rapid increase of the tensile strain under increasing axial load were observed. The lateral load of 0.25 kips was measured when the panel failed. The final failure caused by the tension cracks diagonally, splitting of the side concrete plate longitudinally, and crushing of the concrete horizontally at the top of the panel (Plate 22). An average concrete compressive stress in the panel was computed as 2460 psi for an axial load of 140 kips, and the ratio of an average concrete compressive stress of the panel to its standard concrete cylinder strength was 50% (Table 3). The low ratio of 50% was due to the lateral movement at the lower end of the panel and the lateral load on the lower precompressed specimen. No apparent deflection at the center of the face plate was observed until an axial load of about 80,000 lbs was reached, and beyond it, a rapid increase of the center deflection was observed due to combined axial and lateral load (Figure 20).

14. SPECIMEN WCB 22.1.5.24.48-14

The mode of failure for this panel was a typical second mode of failure in the sandwich panel which has been described above in Part 4.1. The panel was tested with eleven SR-4 strain gages attached to two faces vertically, i.e., nine gages on the face plate and two gages on the side plate, as shown in Figure 51. The distribution of strains on the concrete faces of the panel is shown in Figure 53. It should

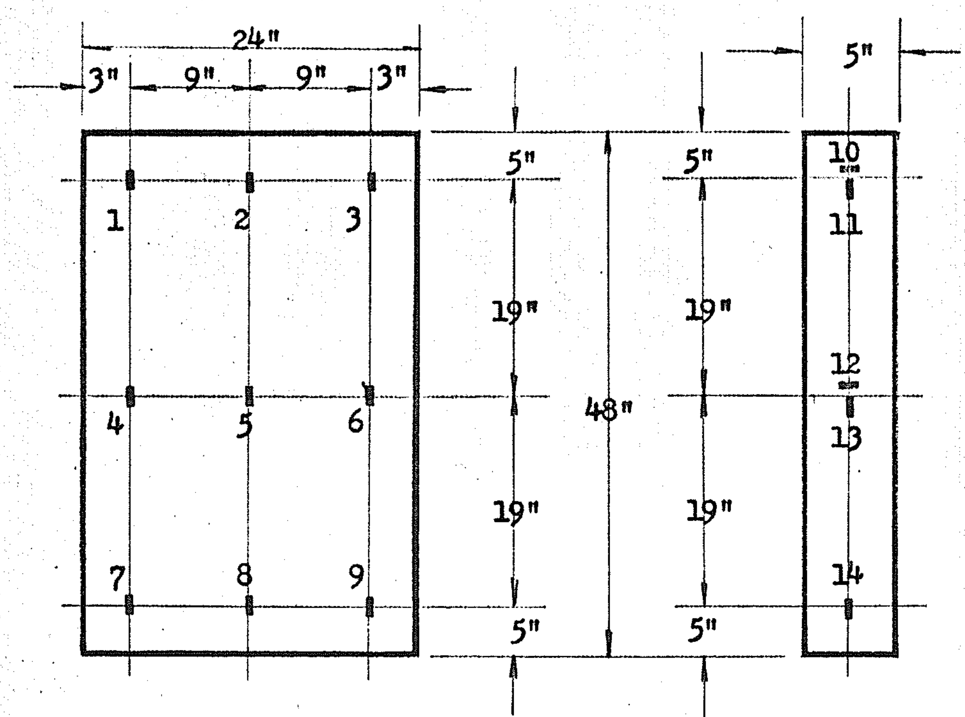

Fig. 50. STRAIN GAUGE LOCATIONS OF WCB 22.1.5.24.48- 13.

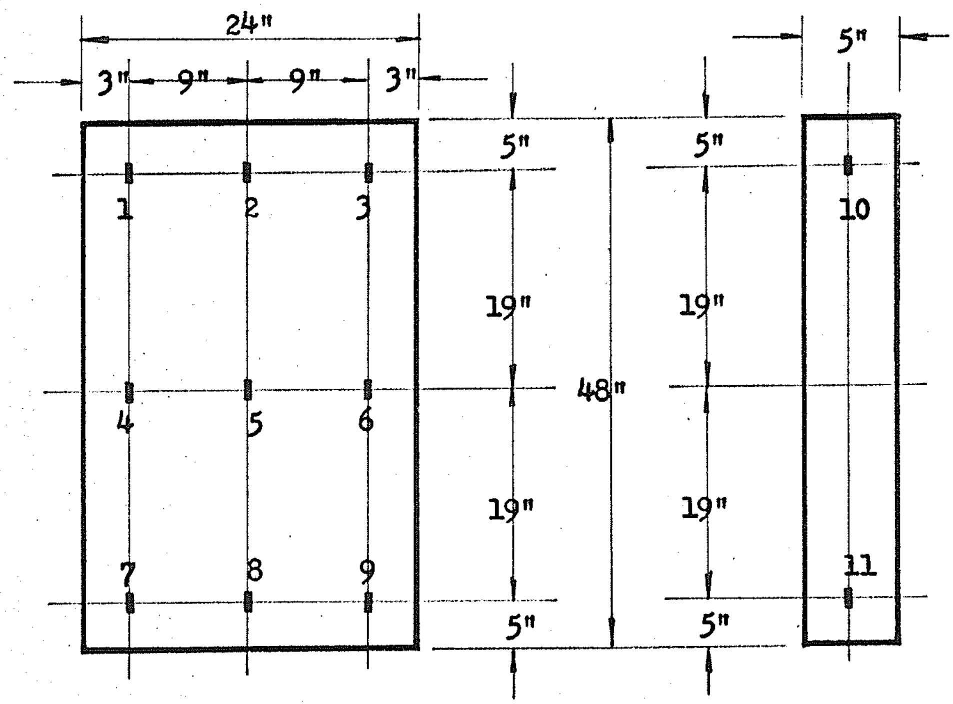

Fig. 51. STRAIN GAUGE LOCATIONS OF WCB 22.1.5.24.48- 14.

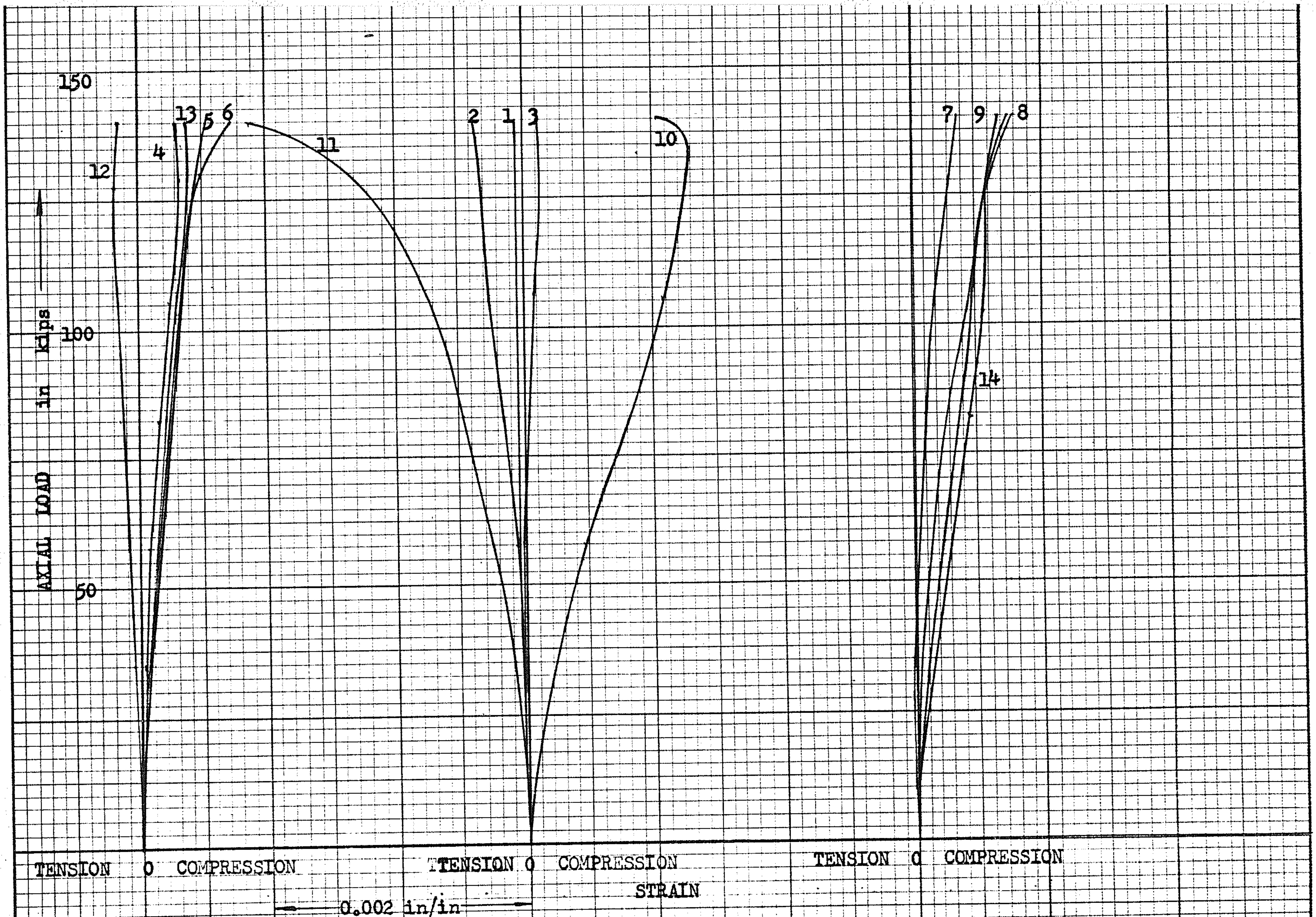

Fig. 52. WCB 22.1.5.24.48 - 13 LOAD - STRAIN CURCES

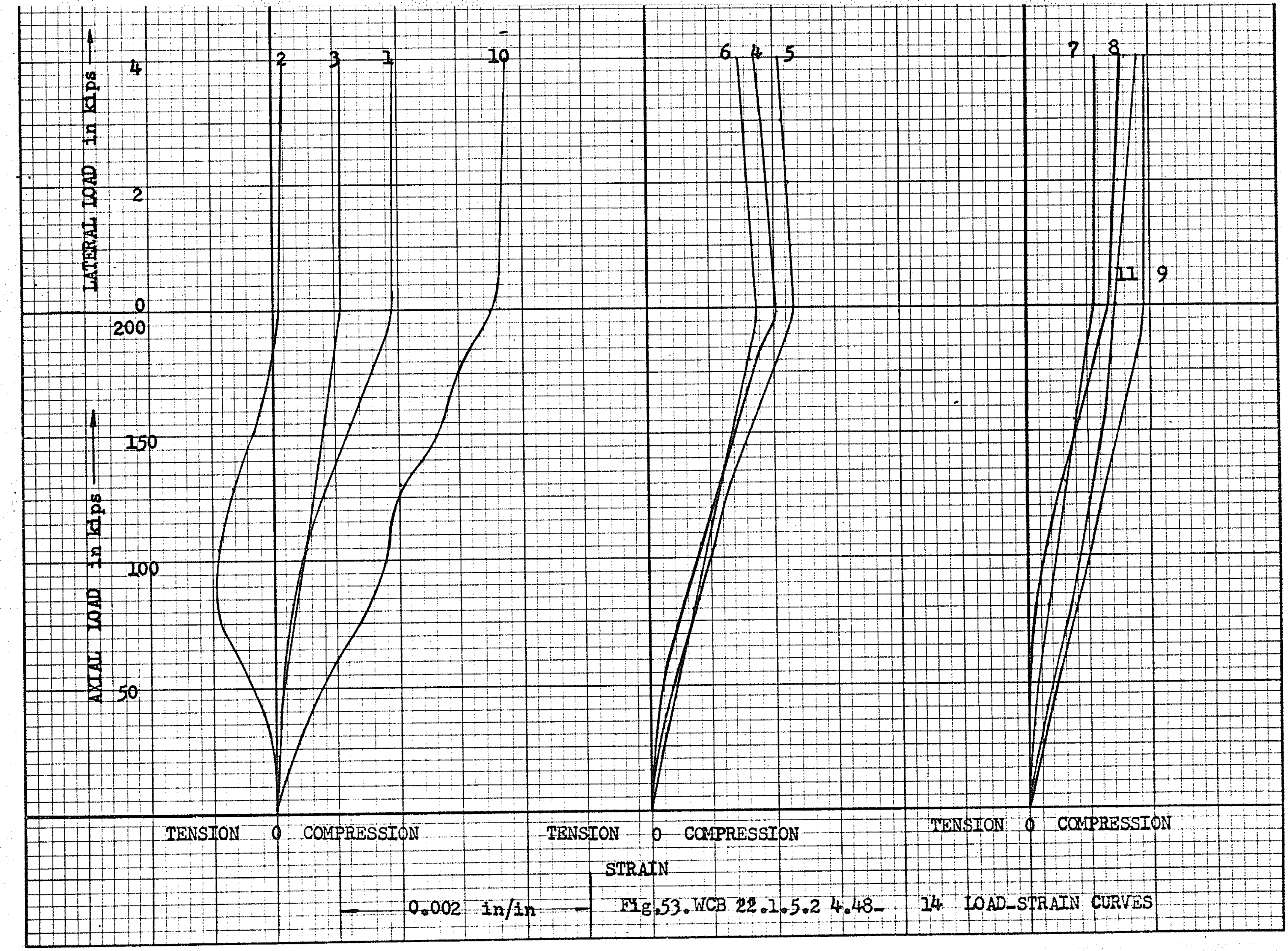

Fig.53. WCB 22.1.5.2 4.48- 14 LOAD-STRAIN CURVES

PLATE NO. 22. View of Panel WCB 22.1.5.24.48-13 after Failure.

PLATE No. 22a. Enlarged View of Failure of WCB 22.1.5.24.48-13.

PLATE No. 23. View of Panel WCB 22.1.5.24.48-14 after Failure.

PLATE No. 23a. Enlarged View of Failure of WCB 22.1.5.24.48-14.

be noticed that all strain gages showed the tensile strain except gage no. 2 at the center in the upper region of the face plate under axial load. Most compressive strain at the upper side of the panel (gage no. 10) was observed to increase significantly until an axial load of 200 kips was reached. Under combined axial and lateral loads, no tensile strain appeared on the gage and no apparent strain changes were observed until a lateral load of 4,000 lbs was applied in addition to the axial load of 200,000 lbs. The final failure was caused by the crushing of the highly precompressed concrete at the top of the side plate due to the combined load and the lateral movement at the lower end. This failure is associated with longitudinal splitting, diagonal tension cracks, and flexural cracks due to combined axial and lateral loads. The deflection at the center of the face plate increased very gradually under increasing axial load until an axial load of 97,610 lbs was reached. For this load the deflection was of 0.012 in. (Figure 20). For an axial load of 200 kips, the average concrete compressive stress in the panel was found to be 3510 psi, and for combined axial and lateral loads of 200 and 5 kips respectively, the average maximum extreme fiber compressive stress was computed as 4180 psi. The ratios of these compressive stresses of the panel to the standard concrete cylinder strength are 72 and 85 % respectively.

15. SPECIMEN WCB 22.1.6.24.48-15

This panel is an example of the second mode of failure in the sandwich panel which has been mentioned in Section 4.1. and as shown in Plate 24. For this panel test, ten SR-4 strain gages were attached vertically to two faces of the panel as shown in Figure 54. Figure 56 shows graphically the amount of strain observed in the panel during the loading. In the central regions of the panel, these compressive strains generally increased continuously under increasing axial load until an axial load of 200 kips was reached, and when the lateral load was applied in addition to the axial load of 200 kips, these compressive strains decreased. Especially at the side plate of the panel, the tensile strain (gage no. 9) appeared, and near failure, this strain increased very rapidly under increasing lateral load in addition to the axial load of 200 kips. In the upper regions of the panel, a small degree of tensile strain appeared on the face plate when first loaded, and the compressive strain on the side plate increased under increasing axial load. Near an axial load of 200 kips, these strains at the upper part of the panel became compressive strains. During the lateral loading in addition to the axial load of 200 kips, no apparent strain changes were observed. In the lower regions of the panel, as the compressive strains were raised, a corresponding increase in the axial load occured. When lateral load was applied, no apparent strain changes were observed at the face plate but near failure, a rapid increase of the tensile strain was observed at the side plate (gage no. 10). This rapid increase of the tensile strain at the side plate of the panel brought about a great deformation of the panel, and the final failure was associated with the concrete crushing, bond splitting, diagonal tension cracks, and flexural cracks due to combined axial and lateral loads. No apparent center deflection at the face plate was observed

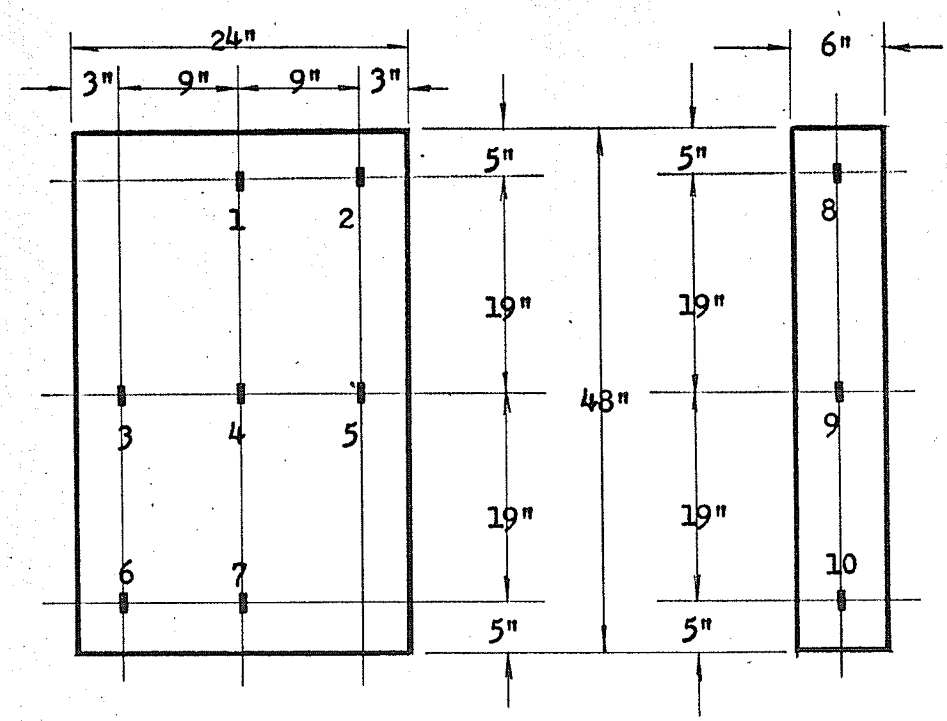

Fig. 54. STRAIN GAUGE LOCATIONS OF WCB 22.1.6.24.48- 15.

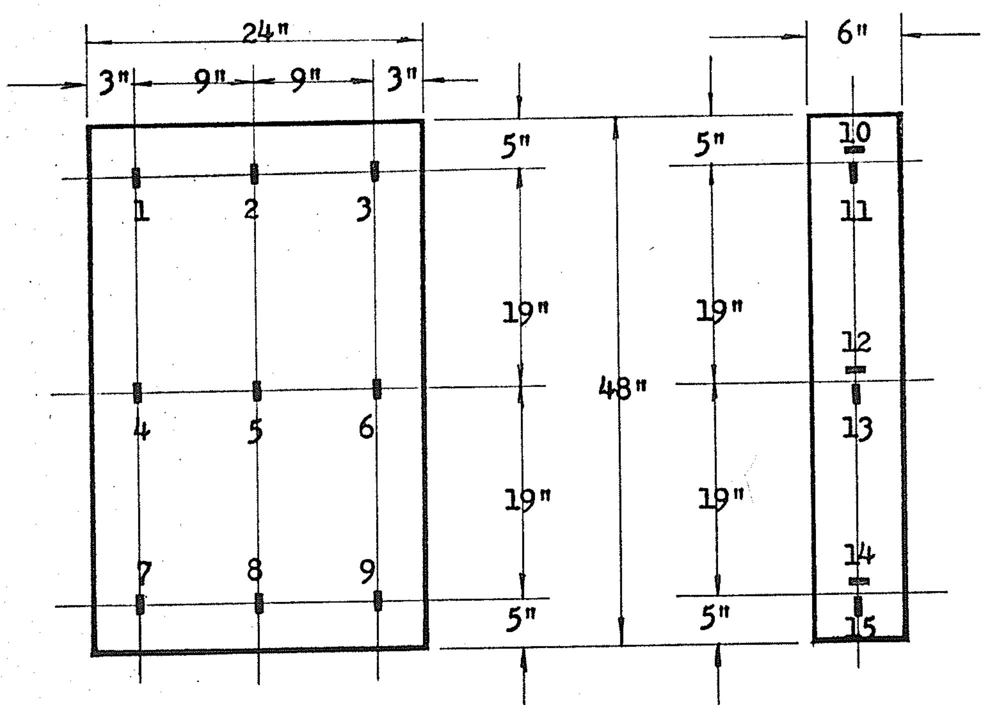

Fig. 55. STRAIN GAUGE LOCATIONS OF WCB 22.1.6.24.48- 16.

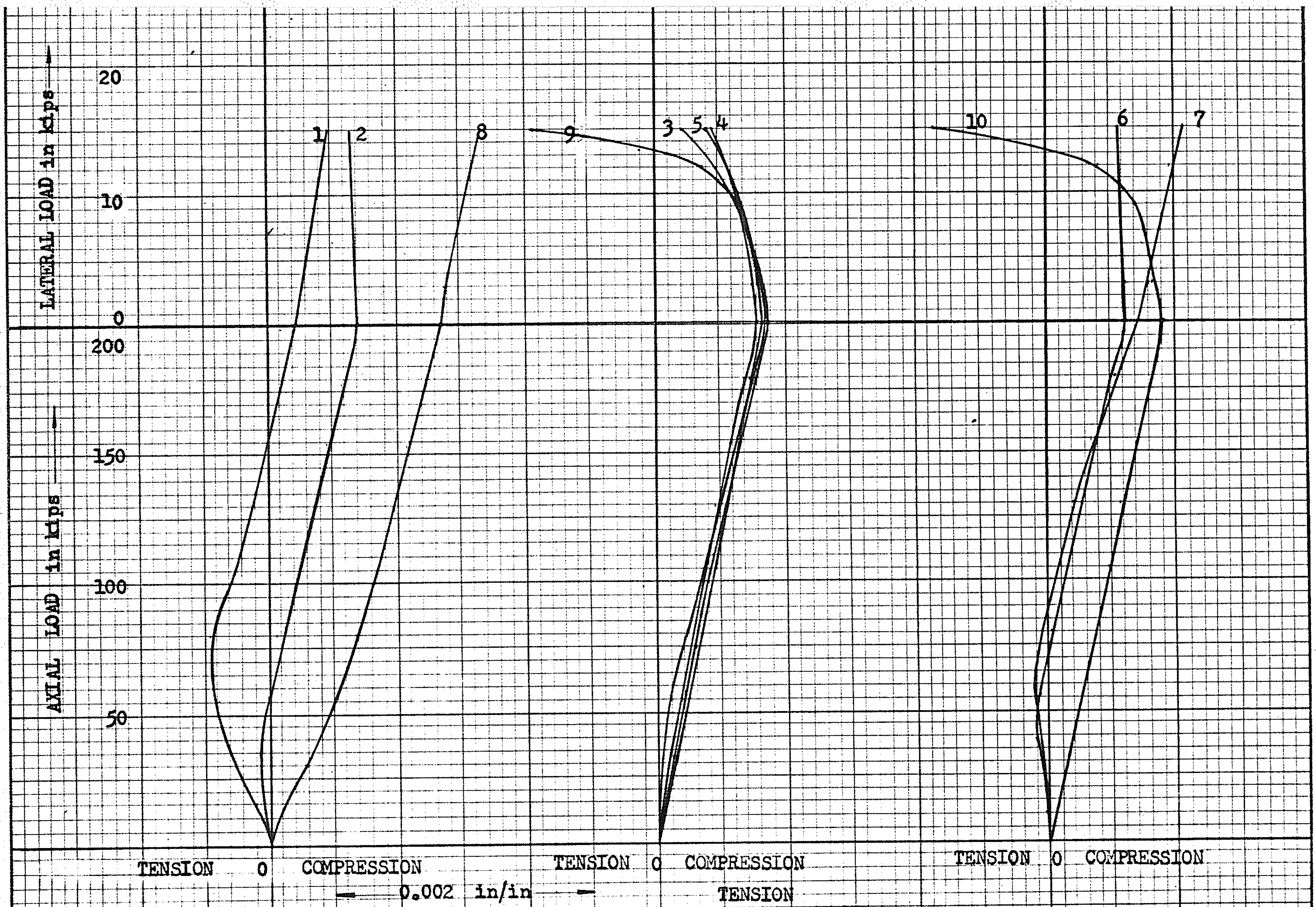

Fig. 56. WCB 22.1.6.24.48 - 15 LOAD — STRAIN CURVES

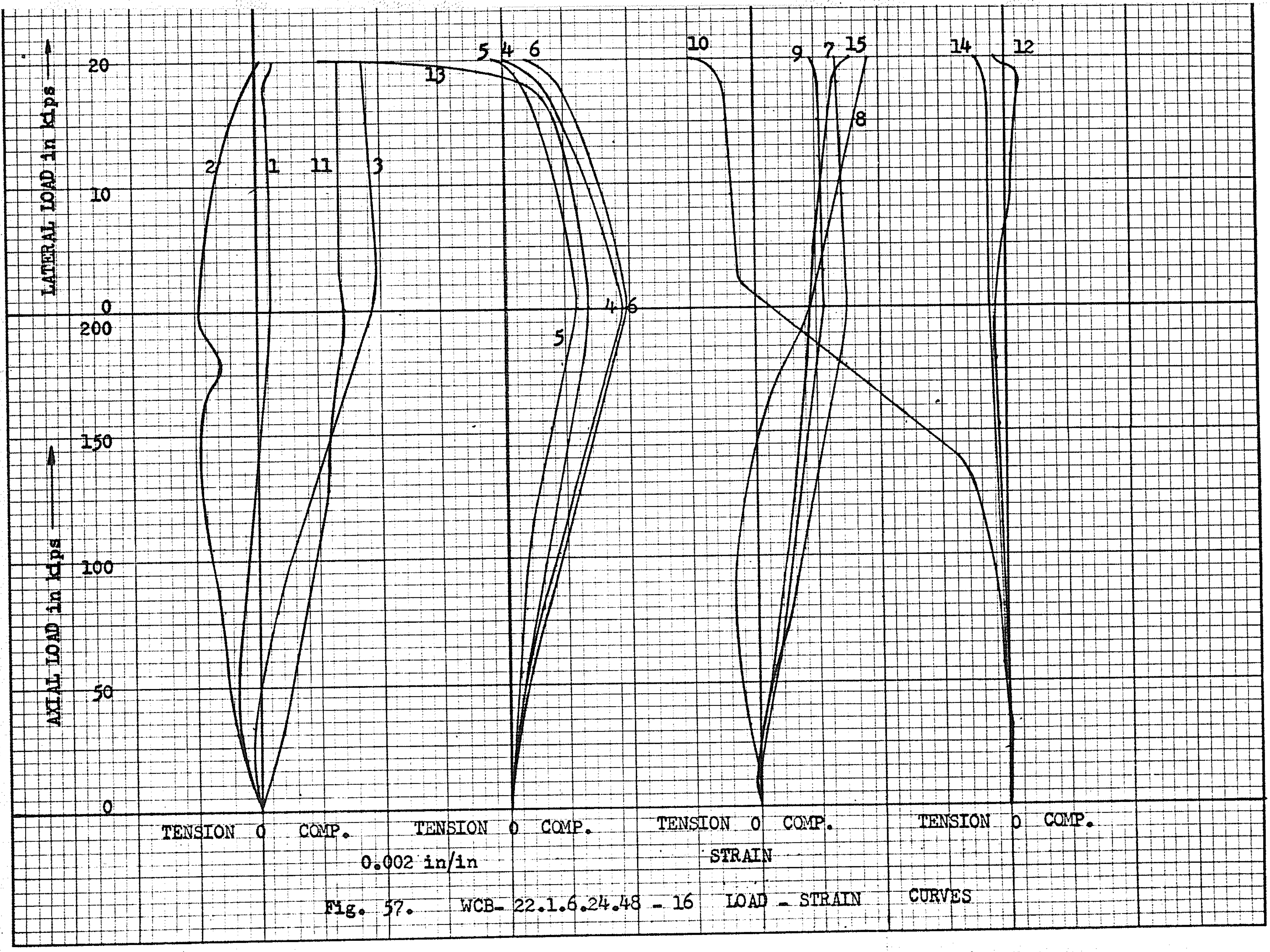

Fig. 57. WCB- 22.1.6.24.48 - 16 LOAD - STRAIN CURVES

PLATE No. 24. View of Panel WCB 22.1.6.24.48-15 after Failure.

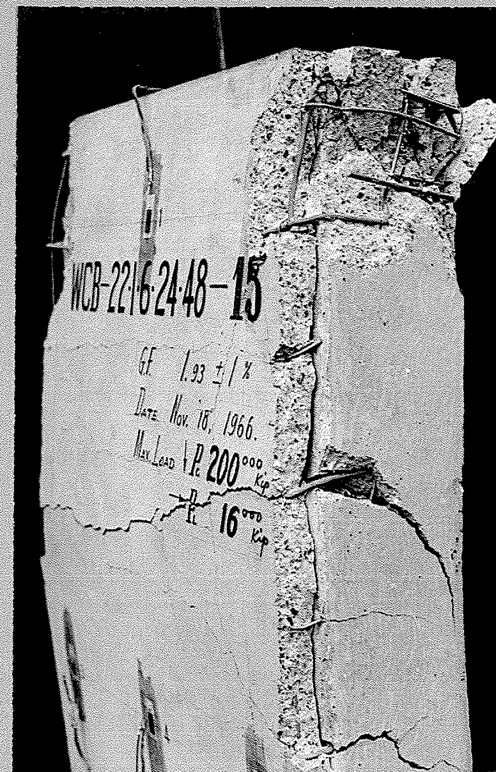

PLATE No. 24a. Enlarged View of Failure of WCB 22.1.6.24.48-15.

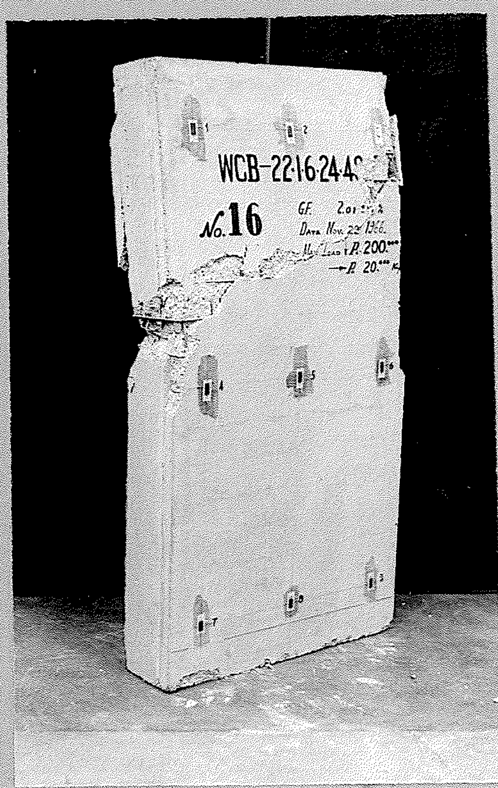

PLATE No. 25. View of Panel WCB 22.1.6.24.48-16 after Failure.

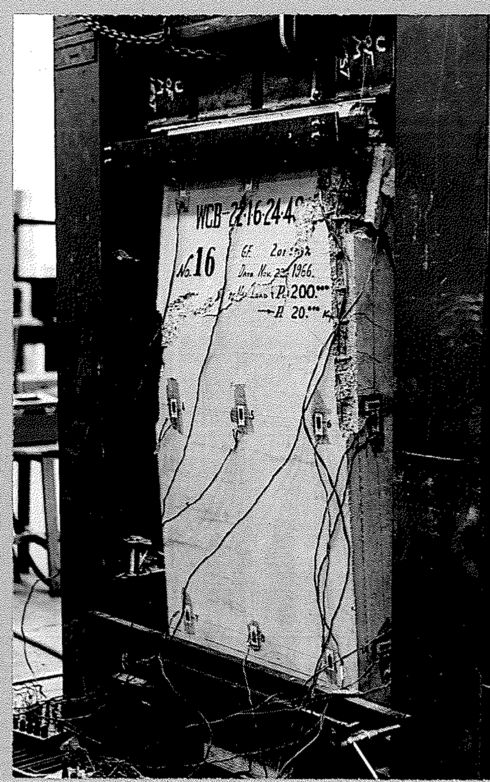

PLATE No. 25a. Panel WCB 22.1.6.24.48 - 16 in Testing Frame after Failure.

until an axial load of 105,040 lbs was applied as shown in Figure 20. For an axial load of 200 kips the average concrete compressive stress in the panel was computed as 3340 psi, and for combined axial and lateral loads of 200 and 16 kips respectively, the maximum extreme fibre compressive stress was found to be 4990 psi in the panel. The ratios of these compressive stresses of the panel to its standard concrete cylinder strength are 68 and 102% respectively.

16. SPECIMEN WCB 22.1.6.24.48-16

As shown in Plate 25, this panel failure is associated with the concrete crushing, splitting, diagonal tension cracks, and flexural cracks. It is an example of the second mode failure of the sandwich panel, described in Part 4.1. Fifteen SR-4 strain gages were attached to the panel faces, i.e., twelve vertically and three horizontally as shown in Figure 55. Load - Strain curves have been plotted for this panel as shown in Figure 57. In the upper regions of the panel, no significant vertical strains were observed but beyond an axial load of about 140 kips, a rapid increase of the horizontal tensile strain was observed (gage no. 10) under increasing load. This rapid increase of the tensile strain brought on the concrete splitting at the upper side plate. Under an increase of the lateral load, in addition to an axial load of 200 kips, the longitudinal splitting of the side plate concrete extended along the vertical edge line of the insulation core from the top towards the lower side. In the central regions of the panel, all compressive strains increased gradually under increasing load until an axial load of 200 kips was reached, and all strains decreased after lateral load was applied in addition to the axial load of 200 kips. Near failure, the rapid increase of horizontal tensile strain at the side plate (gage no. 13) is similar to the increase of the horizontal strain at the center of side plate in the specimen WCB 22.1.6.24.48-15. Yielding in reinforcement followed, and crushing of the concrete at the side plate took place after a great increase in deformation without any increase in load. In the lower regions of the panel, no considerable change of the compressive strain was observed when the lateral load was applied in addition to the axial load of 200 kips. For the axial load of 200 kips, an average concrete compressive stress of 3340 psi was found, and for combined axial and lateral loads of 200 and 20 kips respectively, the maximum extreme fibre compressive stress in the panel was computed as 5400 psi. The ratios of these compressive stresses of the panel to its standard concrete cylinder strength are 68 and 110% respectively. No apparent center deflection of the face plate of the panel was observed until an axial load of about 81 kips was reached (Figure 20).

17. SPECIMEN WCB 22.1.6.24.48-17

This panel was tested with fifteen SR-4 strain gages attached to two faces of the panel, i.e., nine gages on the face plate and six gages on the side plate as shown in Figure 58. The strain distribution on the concrete faces of the panel is shown in Figure 60. At the upper part of the panel (lower part of the panel in Plate 26), no apparent strains were observed on the face plate but on the side plate, the vertical compressive strain increased continuously under increasing axial load.

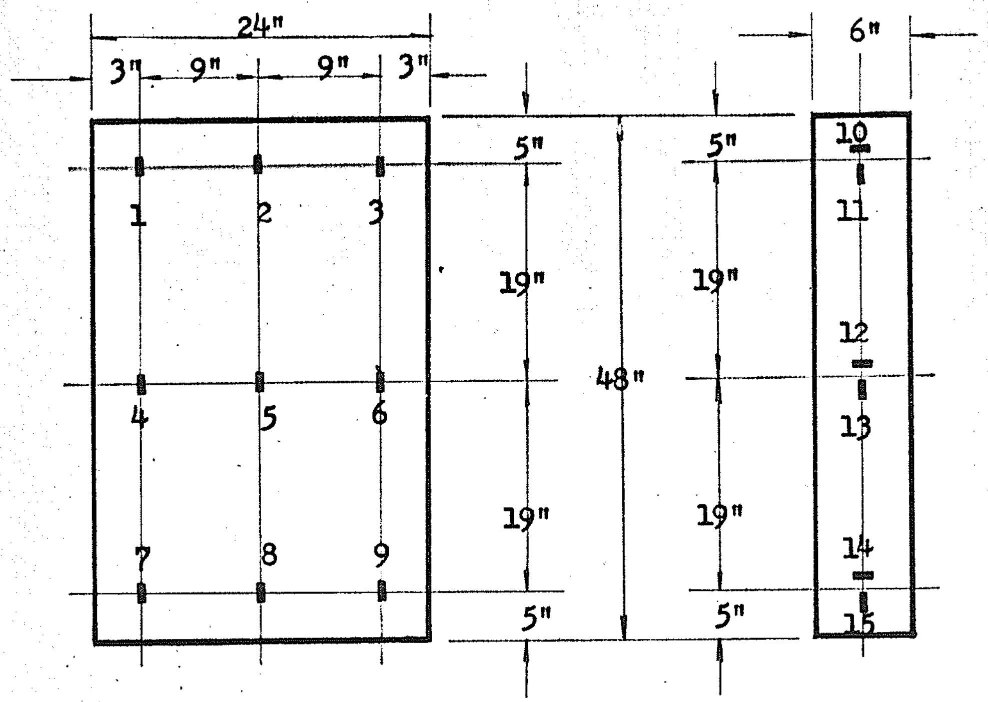

Fig. 58. STRAIN GAUGE LOCATIONS OF WCB 22.1.6.24.48- 17.

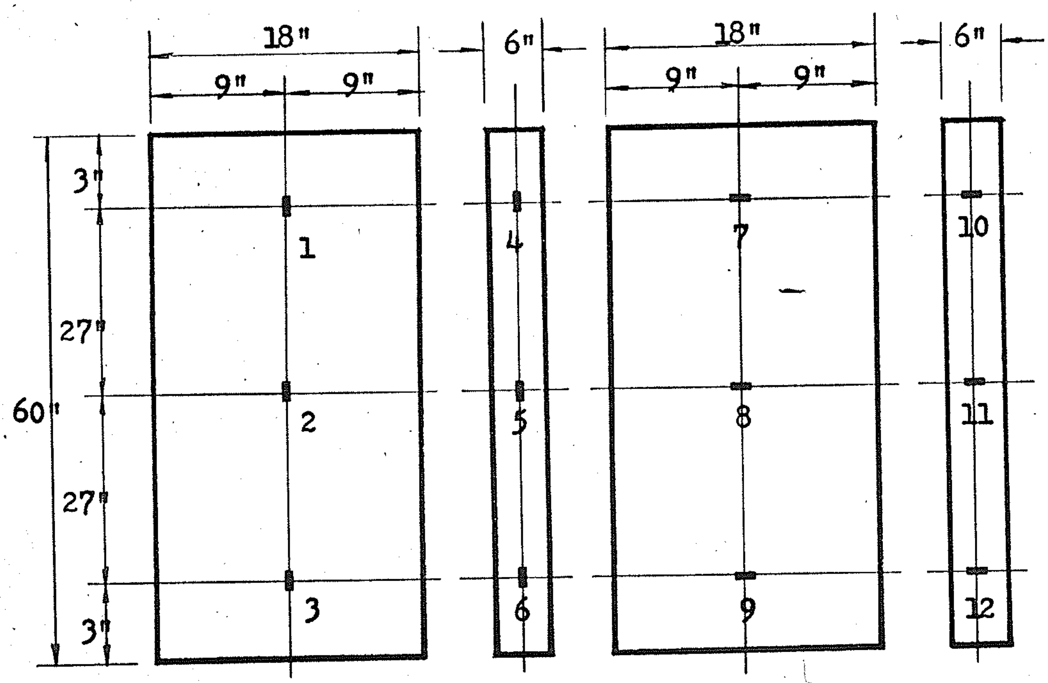

Fig. 59. STRAIN GAUGE LOCATIONS OF WCB 22.1.6.18.60- 18.

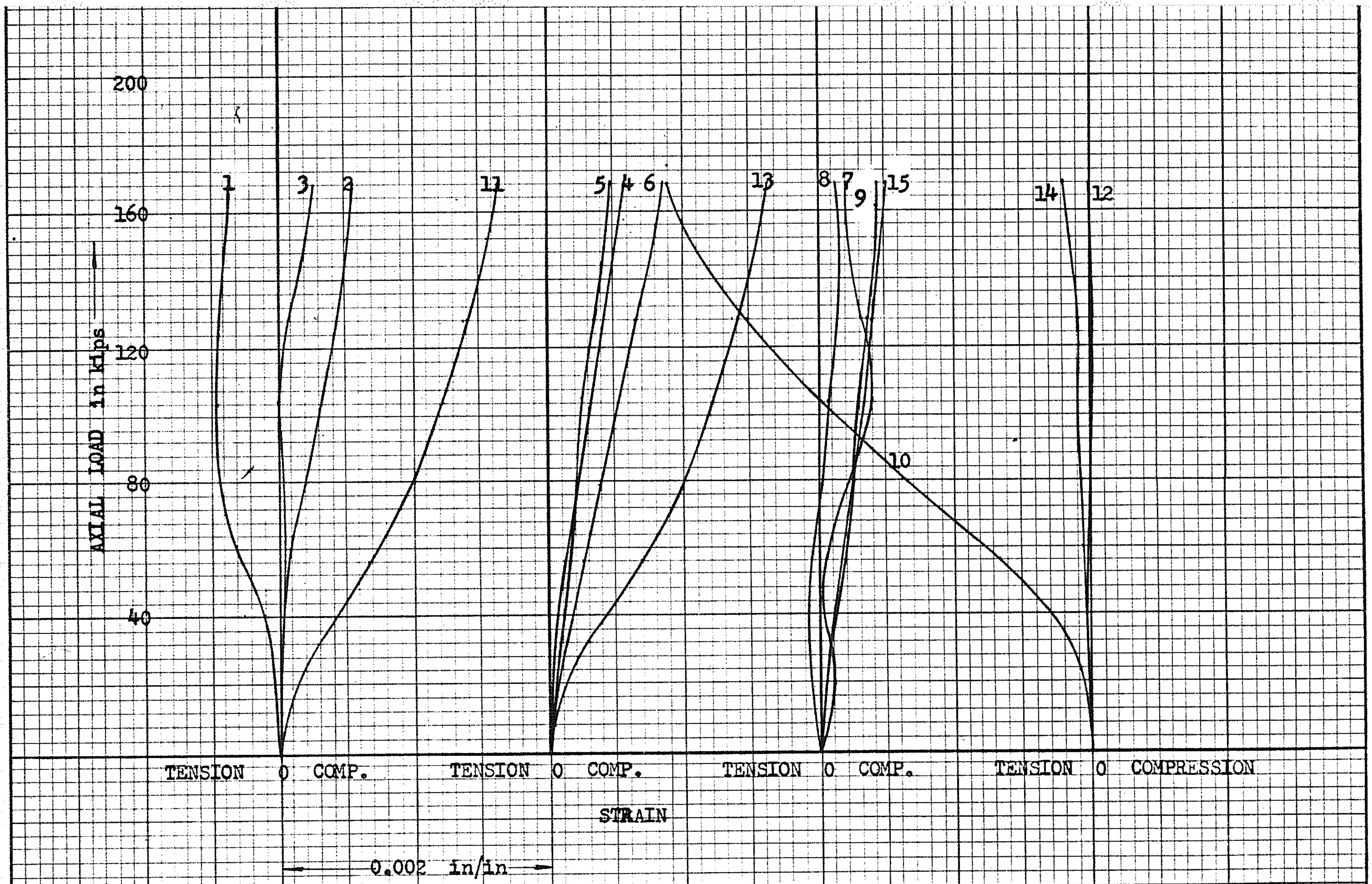

Fig. 60. WCB 22.1.6.24.48 - 17 LOAD - STRAIN CURVES

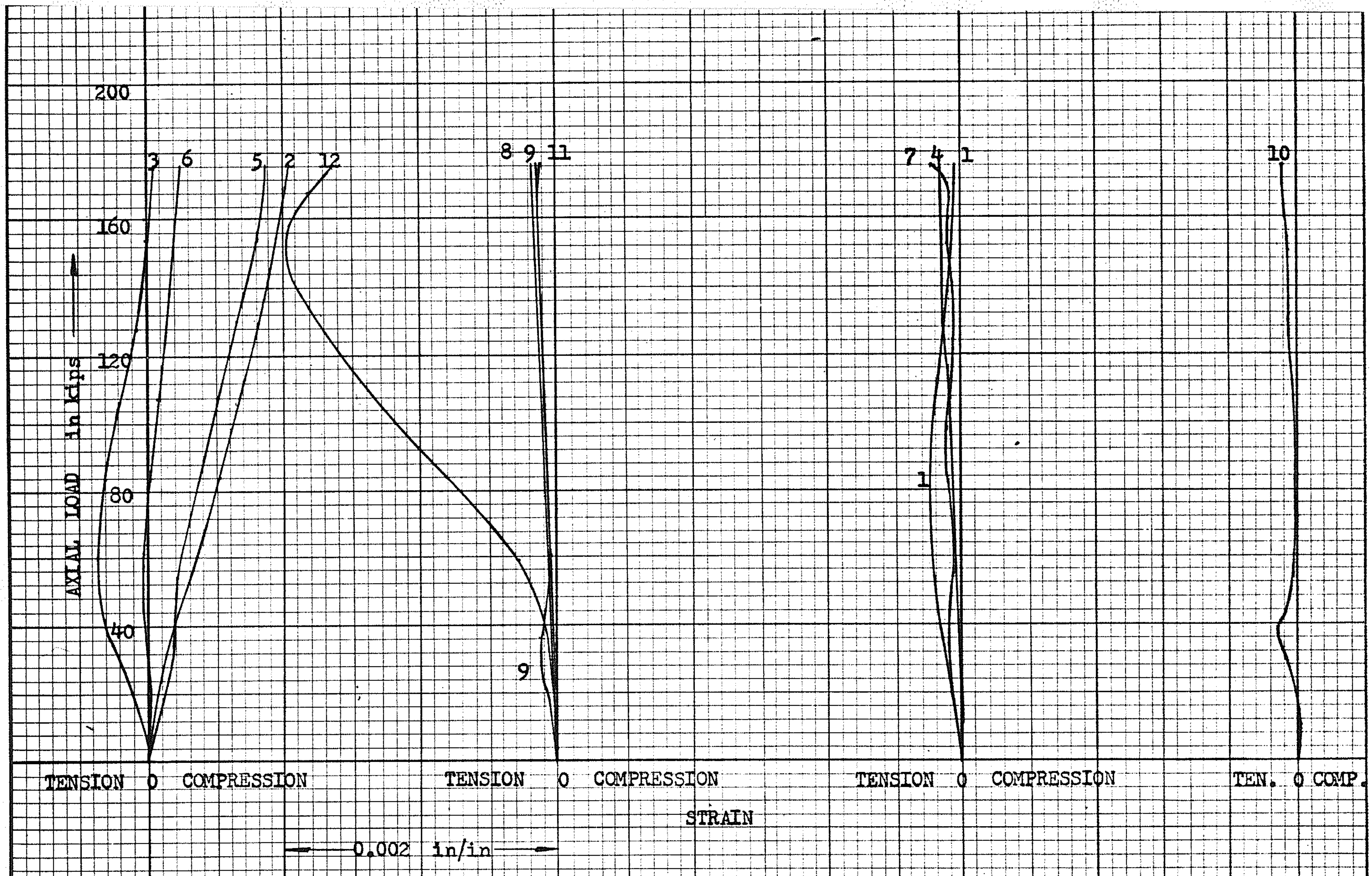

Fig. 61. WCB 22.1.6.18.60- 18 LOAD - STRAIN CURVES

PLATE No. 26. View of Panel WCB 22.1.6.24.48-17 after Failure.

PLATE No. 26a. Enlarged View of Failure of WCB 22.1.6.24.48-17.

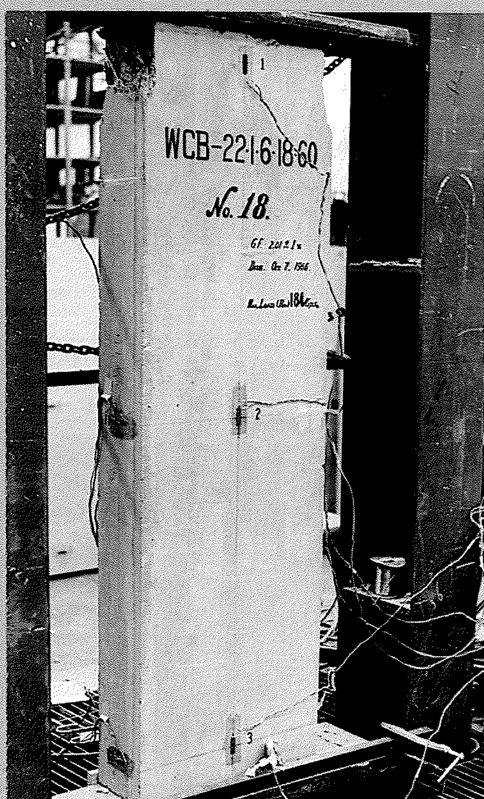

PLATE No. 27. View of Panel WCB 22.1.6.24.48-18 after Failure.

PLATE No. 27a. Enlarged View of Failure of WCB 22.1.6.18.60-18.

Especially, the horizontal tensile strain on the side plate increased very rapidly beyond a load of about 40 kips (gage no. 10). Near a load of 90 kips, longitudinal splitting appeared at the top of the side plate, and near failure, its horizontal tensile strain of 0.00311 in/in was measured. At the central part of the panel, all vertical compressive strains increased continuously under increasing load, and increasing rate of the side plate strain was about twice as much as the face plate strain. Almost no horizontal strain was observed at the central part of the side plate. At the lower part of the panel (upper part of the panel in Plate 26), no apparent strains were observed before the panel failed. At an ultimate axial load of 172 kips, longitudinal splitting at the side plate in the upper region of the panel extended rapidly, and at the same time, a great lateral movement at the bottom of the panel occurred. Then suddenly the Budd strain indicator for the lateral loading hydraulic jack indicated a lateral load of 0.05 kips, and the final failure of the panel occurred as shown in Plate 26. This mode of failure is similar to the mode of failure of the Specimen 22.1.5.24.48-13. A very small center deflection at the face plate was observed until an axial load of about 81 kips was reached as shown in Figure 20. The average concrete compressive stress of 3370 psi was found for an axial load of 172 kips, and the ratio of the average concrete stress of the panel to its standard concrete cylinder strength is 63%.

18. SPECIMEN WCB 22.1.6.18.60-18

This panel was tested with twelve SR-4 strain gages attached to the four faces of the panel, i.e., six gages horizontally and six gages vertically, as shown in Figure 59. In the lower regions of the panel, the tensile strain (gage no. 12) at the side plate increased very rapidly under increasing load until a load of 152,720 lbs was applied, and longitudinal splitting of the concrete appeared from the top towards the lower side. At the same time, a great lateral movement at the lower end of the panel occurred, and the tensile strain of 0.001982 in/in at a load of 152,720 lbs started to decrease under increasing load, as shown in Figure 61. Then the final failure was caused by crushing of the concrete in the corner regions at the upper part of the panel, as shown in Plate 27. At the center of the panel, vertical compressive strains (gage nos. 2 and 5) increased continuously under increasing load, but these strains did not become factors of considerable importance in the failure of the panel. In the other regions, no apparent strains were observed. An average concrete compressive stress of 4180 psi was found in the panel at the ultimate load of 184 kips. The ratio of an average concrete stress of the panel to its standard concrete cylinder strength is 70%. The deflection at the center of the face plate in Plate 27 increased gradually under increasing load, but no apparent deflection was observed until an axial load of about 30 kips was applied. The center deflection at the face plate was measured at 0.041 in. for a load of 81,630 lbs.

19. SPECIMEN WCB 22.1.6.18.60-19

This panel was tested with six SR-4 strain gages attached to two faces vertically, i.e., three on the face plate and three on the side

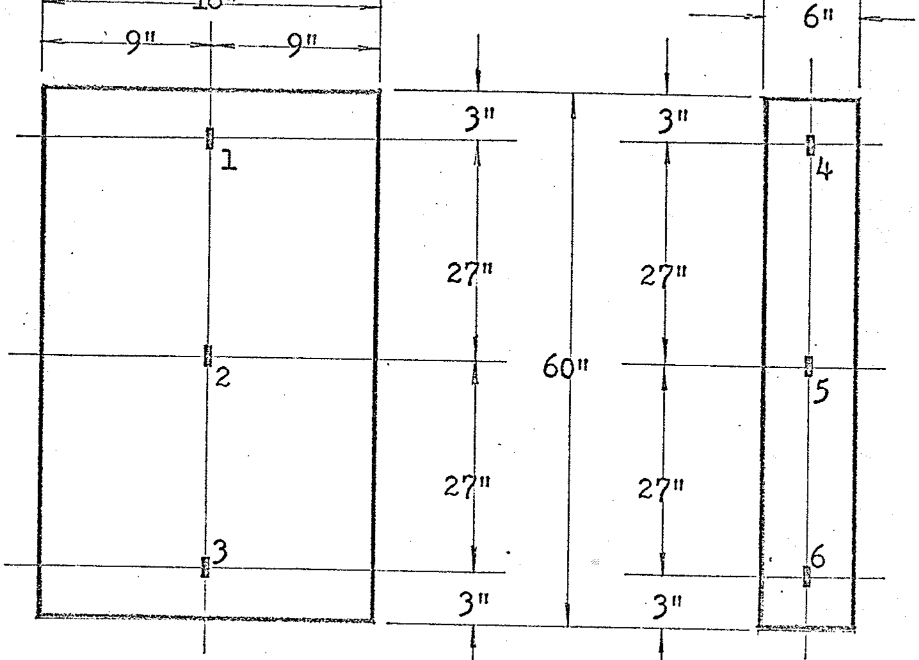

Fig. 62. STRAIN GAUGE LOCATIONS OF WCB 22.1.6.18.60- 19.

PLATE No. 28. Front View of WCB 22.1.6.18.60- 19 after Failure.

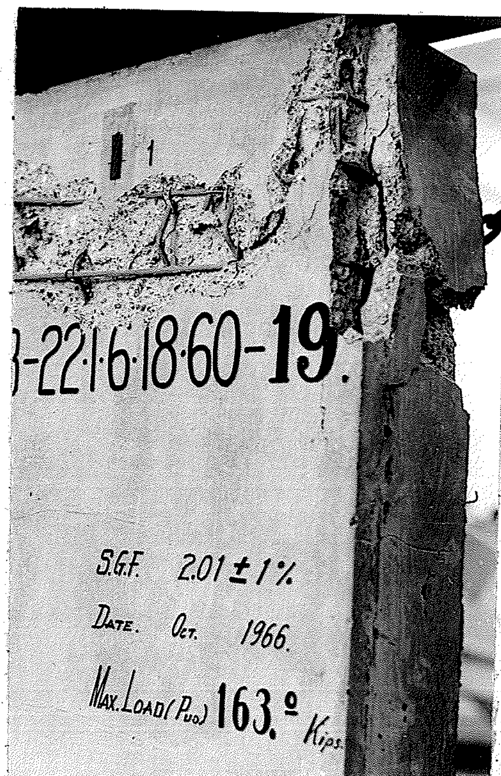

PLATE No. 28A. Side View of WCB 22.1.6.18.60- 19 after Failure.

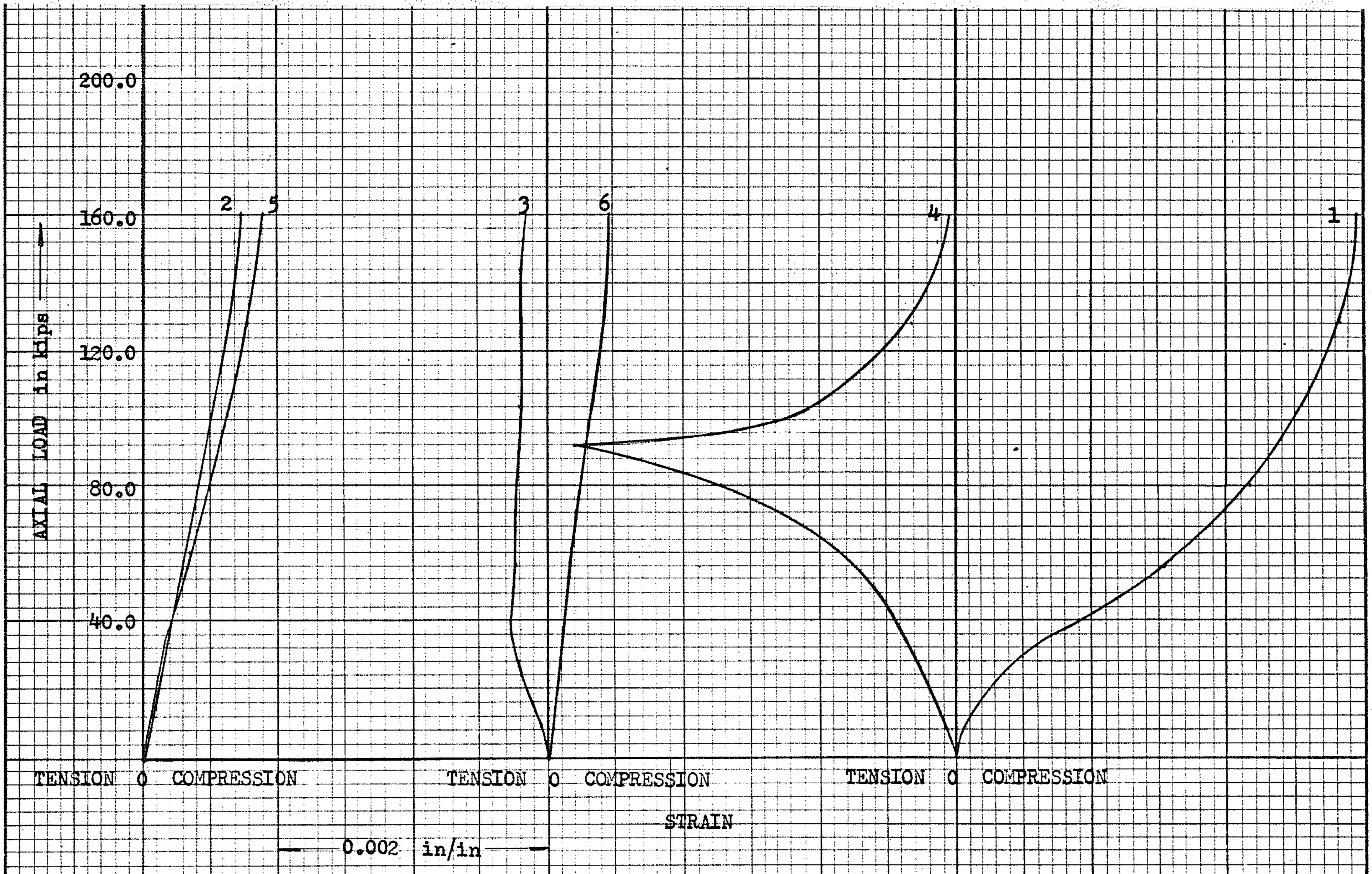

Fig. 63. WCB 22.1.6.18.48 -19 LOAD - STRAIN CURVES

plate as shown in Figure 62. In the central regions of the panel, the compressive strains (gage nos. 2 and 5) increased considerably under increasing load as shown in Figure 63. No apparent compressive and tensile strains were observed in the lower regions of the panel, Plate 28. In the upper regions of the panel, the compressive strain (gage no. 1) increased very sharply under increasing load at the face plate, and near the ultimate load, the compressive strain of 0.00296 in/in was measured. Beyond a load of 45 kips, compression cracks extending horizontally across the upper face plate developed, and longitudinal splitting of the side plate concrete appeared from the top. The tensile strain which had increased rapidly before the load reached 97,610 lbs, started decreasing sharply beyond that load due to a rapid increase of lateral movement at the lower end of the panel towards the front, and due to the widening of the longitudinal splitting of the concrete at the top of the side plate. The final failure was caused by the crushing of the concrete at the upper part of the panel after the compression steel in the face plate reached yielding. Then compression steel buckled without increase in load after failure of the concrete in compression took place. Convex deformation was observed at the face plate due to axial load, and the center deflection of 0.024 in. was measured at a load of 81,630 lbs (Figure 20). An average concrete compressive stress in the panel was computed as 3710 psi for an ultimate load of 163 kips. The ratio of an average concrete stress of the panel to its standard concrete cylinder strength is 62%.

4.3. THE PREDICTION OF LOAD CARRYING ABILITIES OF THE PANELS AND MATHEMATICAL RELATIONS.

ULTIMATE LOAD CAPACITY OF THE PANELS.

(a) SINGLE LAYER PANEL

The prediction of load carrying abilities for the single layer panel is estimated as for a wide rectangular column.

Since about 1930, a very large research project on columns was carried out at the University of Illinois.(9, 10) These tests indicated that if the concrete approached its ultimate strength before the steel reached its elastic limit, the increased deformation of the concrete near its maximum stress forced the steel stress to build up more rapidly. Thus, a column reached what might be called its yield-point only when the load became equal to approximately 85 % of the ultimate strength of the concrete (as measured by standard cylinder tests) plus the yield-point strength of the longitudinal steel.

The ultimate load for the short column, axially loaded, was discussed in the preceding section expressed as:

$$\bar{P}_o = .85 f'_c A_c + f_y A_s$$

or

$$\bar{P}_o = .85 f'_c (A_g - A_s) + f_y A_s \qquad (4.1)$$

But the 1963 ACI Code[13] states that strength reductions for length of compression members depend upon column lengths, radiuses of gyration, and terminal joint conditions. The Code allows for long column action by introducing a reduction factor which is applied to the short column capacity. It is necessary to revise the strength equation given to:

$$\bar{P}_u = R\,\bar{P}_o \tag{4.2}$$

$$\bar{P}_u = (1.13 - 0.004\,L/r)(0.85\,f'_c\,A_c + f_y\,A_{st}) \tag{4.3}$$

(b) SANDWICH PANELS

The ultimate load carrying abilities for the sandwich panels are estimated as though they are hollow rectangular tied columns as shown in Figure C-2.

By using the equations of (4.1) and (4.2), the following equation for the ultimate load of the sandwich panels, axially loaded, is obtained:

$$\bar{P}_u = (1.26 - 0.004\,\frac{t}{t'}\,\frac{L}{r})(0.85\,f'_c\,A_c + f_y\,A_{st}) \tag{4.4}$$

But some of the sandwich panels are applied the lateral load in addition to the axial load because two hundred kips. of maximum allowed axial load of the frame is not enough to fail them. For these panels, it is assumed that a section is controlled by compression because eccentricity of axial load at the end of the member, measured from the plastic centroid of the panel section, is relatively much smaller than the eccentricity of the balanced load $\bar{P}_b$ measured from the plastic centroid of panel section. For this assumption the ultimate load of panels is given:

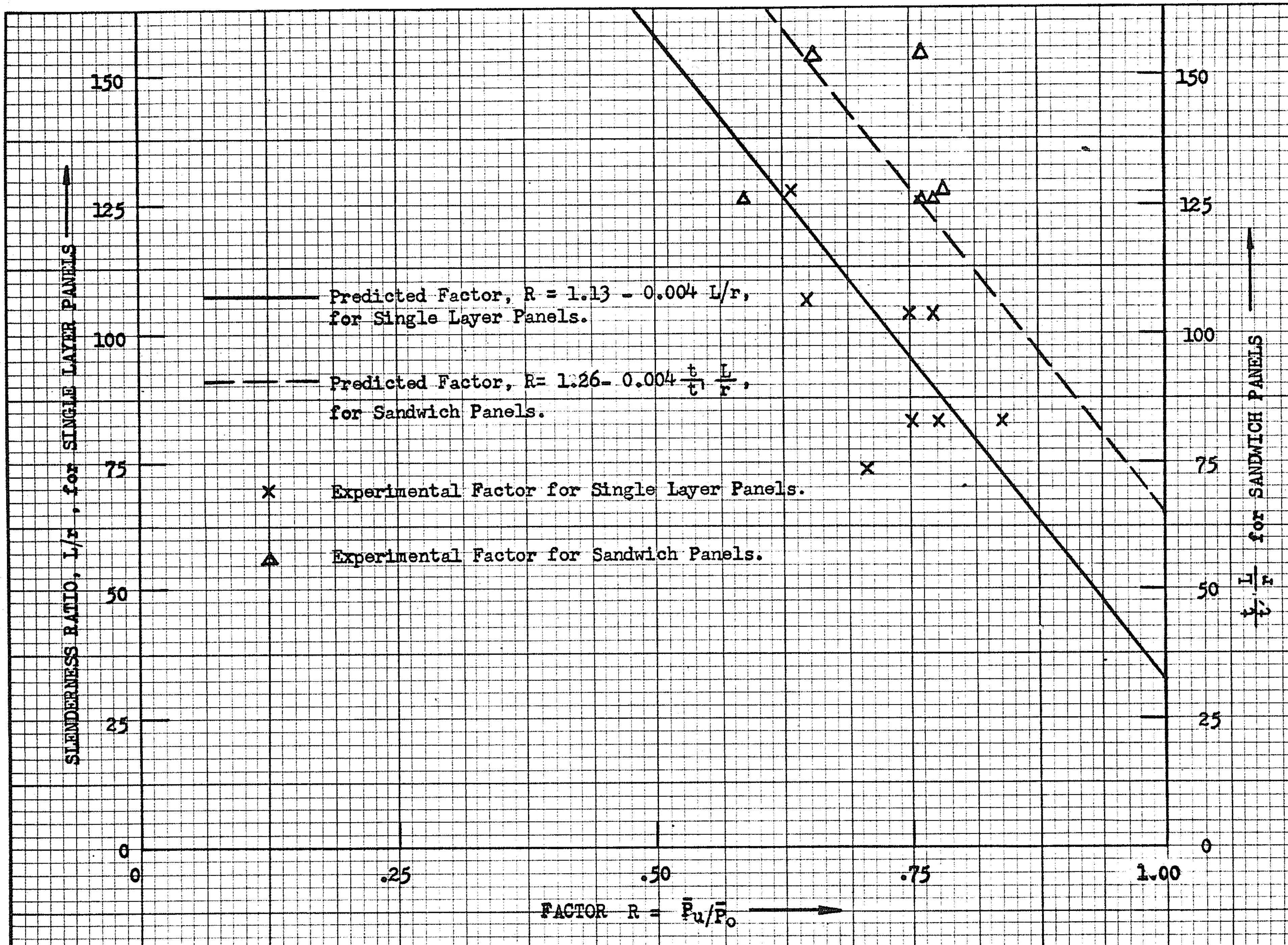

Figure 66. Factor, R, for Single Layer Panels and Sandwich Panels.

$$\bar{P}_u = \frac{\bar{P}_o}{1 + [(\bar{P}_o / \bar{P}_b) - 1]\, e/e_b} \qquad (4.5)$$

or

$$e = \frac{(\bar{P}_o/\bar{P}_u) - 1 \quad e_b}{(\bar{P}_o/\bar{P}_b) - 1} \qquad (4.6)$$

In estimating the bending of a slender sandwich panel under the action of an eccentric load, Fig. 64, the moment due to an eccentricity of load is equivalent to $\bar{P}_u \cdot e$. Then it is assumed that such an axial load with the bending moment, $\bar{P}_L . L/4$, at the middle of the panel as shown in Fig. 65, is equivalent to an eccentric load.

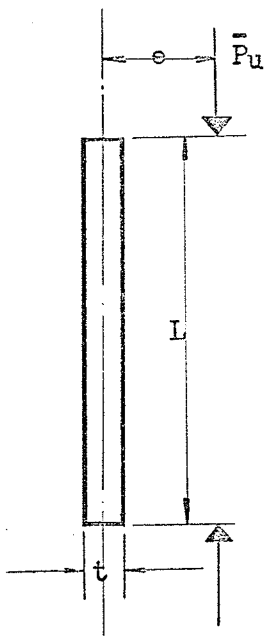

Fig. 64. Eccentric Load

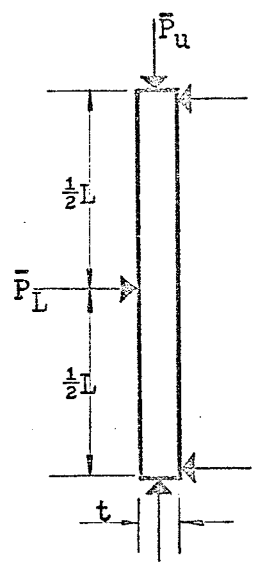

Fig. 65. Combined Axial and Lateral Loads

$\bar{P}_u$ e, as shown in Fig. 64;

so that

$$\bar{P}_u . e = \bar{P}_L . L/4 \qquad (4.7)$$

Substituting equation (4.6) in this equation, we obtain

$$\bar{P}_u \frac{(\bar{P}_o/\bar{P}_u - 1)\, e_b}{(\bar{P}_o/\bar{P}_b - 1)} = \bar{P}_L \cdot L/4 \tag{4.8}$$

or

$$\bar{P}_L \doteq \frac{4\,(\bar{P}_o/\bar{P}_u - 1)\, eb\, \bar{P}_u}{(\bar{P}_o/\bar{P}_b - 1)\, L} \tag{4.9}$$

$\bar{P}_b$ and e_b in this equation can be obtained from Appendix C-2. Phil M. Ferguson[11] states that strength reduction factor, R', for an eccentric loaded long column depends upon the ratio of $\bar{P}_u/\bar{P}_b$ and R. Then the equation (4.8) will be:

$$\bar{P}_u = R' \left[\bar{P}_o - \frac{\bar{P}_L \cdot L}{4} \frac{(\bar{P}_o/\bar{P}_b - 1)}{e_b}\right] \tag{4.10}$$

or

$$\bar{P}_u = \left[1 - \frac{\bar{P}_u}{\bar{P}_b}(1 - R)\right]\left[\bar{P}_o - \frac{\bar{P}_L \cdot L}{4} \frac{(\bar{P}_o/\bar{P}_b - 1)}{e_b}\right] \tag{4.11}$$

where $\quad R' = 1 - \frac{\bar{P}_u}{\bar{P}_b}(1 - R)$

4.4. CONCLUSIONS

The following conclusions are based on the result of this investigation:

This study shows that very high average concrete compressive strength in the sandwich panels was found. The two concrete side plates containing a styrofoam insulation core between have been shown to be an important factor for obtaining greater values of stiffness and resisting shear strength in the sandwich panel. Therefore, precast concrete sandwich panels may be considered better for the purposes of resisting heat transfer and bearing load than ordinary dense concrete panels for one story buildings.

The concrete face plate thickness of one inch may be realistic in practice if proper shear connectors or concrete ribs are used longitudinally between two face plates.

Axially loaded sandwich panels resist very high bending stress. However, when initially lateral load is applied on the sandwich panels they can not carry much of the axial load due to lateral deformation of the panels.

The most important findings have been summarized in Section 4.1.

The behaviour of single layer and sandwich reinforced concrete panels for bearing load can be predicted approximately as though they were wide and hollow rectangular columns. The prediction of the ultimate strength of the panels appears possible only by means of empirical relationships. The expressions of reduction factor, R, for ultimate axial loads on the panels suggested in Section 4.3. have been revised a number of times during the investigations.

The author believes that this study has produced interesting results concerning a basic concept in precast concrete buildings, and that further study and experimentation would yield profitable improvements.

Further research work which could be undertaken to assess for concrete sandwich panel construction would be as follows:

a. Axial and eccentric load carrying abilities of full scale panels in combination with lateral load

b. Comparison of structure behaviour on secondary stress effects of reinforced and prestressed concrete sandwich panels

c. Panel behaviour under periods of freezing and thawing of the exterior panel face and various moisture conditions

d. Heat transfer characteristic under freezing and thawing cycles

e. Fire retarding characteristic of thin walled concrete sandwich panels with various commercial insulations.

PART FIVE

APPENDICES

APPENDIX A STRAIN/LOAD READING

WCB-11-1-12-24-1 LOAD (lbs) - STRAIN(micro in/in)

Axial Load	Gauge 1	Gauge 2	Gauge 3	Gauge 4	Gauge 5	Gauge 6	Gauge 7	Gauge 8	Gauge 9	Gauge 10
0	0	0	0	0	0	0	0	0	0	0
2000	-87	-42	-53	-34	-10	-26	+4	+4	-26	-48
4000	-164	-82	-115	-76	-27	-66	+6	-12	-58	-103
6000	-232	-125	-175	-122	-57	-110	-11	-26	-81	-137
8000	-295	-169	-234	-169	-94	-157	-39	-46	-110	-174
10000	-346	-206	-285	-216	-129	-202	-65	-72	-139	-212
12000	-394	-245	-330	-252	-158	-241	-85	-102	-170	-246
14000	-434	-276	-370	-286	-186	-278	-119	-136	-210	-288
16000	-472	-318	-412	-320	-214	-316	-130	-176	-252	-332
18000	-510	-338	-446	-354	-244	-354	-150	-222	-299	-380
20000	-542	-367	-478	-384	-266	-386	-170	-268	-345	-420
22000	-570	-392	-505	-410	-288	-416	-192	-318	-396	-474
24000	-597	-415	-530	-434	-319	-446	-219	-371	-450	-528
26000	-620	-436	-550	-456	-327	-472	-227	-427	-510	-584
28000	-638	-452	-564	-476	-344	-496	-240	-486	-574	-644
30000	-652	-470	-574	-490	-352	-516	-252	-556	-646	-712
32000	-658	-484	-572	-492	-358	-536	-262	-628	-730	-788
34000	-656	-488	-556	-484	-346	-544	-264	-720	-832	-874
36000	-646	-492	-534	-466	-328	-544	-264	-820	-940	-964
38000	-624	-484	-486	-430	-290	-538	-254	-934	-1078	-1076
40000	-588	-468	-436	-380	-240	-508	-232	-1070	-1242	-1198
42000	-532	-432	-308	-292	-144	-464	-204	-1240	-1462	-1344
44000	-458	-382	-156	-160	0	-402	-154	-1450	-1752	-1514
46000	-320	-260	+244	+204	+400	-256	-40	-1786	-2448	-1800

WCB-11-1-12-30-2 LOAD(lbs) - STRAIN(micro in/in)

Axial Load	Gauge 1	Gauge 2	Gauge 3	Gauge 4	Gauge 5	Gauge 6	Gauge 7	Gauge 8	Gauge 9	Gauge 10	Gauge 11	Gauge 12
0	0	0	0	0	0	0	0	0	0	0	0	0
2000	-39	-54	-78	12	-15	-36	31	36	6	-2	-36	-75
4000	-96	-113	-153	12	-27	-72	73	88	40	-2	-90	-171
6000	-156	-168	-216	12	-37	-96	119	127	78	-2	-147	-278
8000	-220	-228	-276	12	-46	-118	180	176	119	-18	-212	-390
10000	-278	-276	-328	14	-53	-131	241	212	155	-20	-282	-560
12000	-338	-319	-374	16	-55	-140	289	268	183	-40	-360	-627
14000	-391	-356	-415	22	-56	-145	322	312	208	-64	-434	-725
16000	-440	-392	-448	26	-56	-148	337	346	232	-97	-513	-820
18000	-479	-474	-474	34	-54	-148	346	370	245	-134	-603	-916
20000	-514	-444	-498	48	-48	-144	344	382	254	-180	-696	-1012
22000	-548	-464	-512	64	-36	-132	344	394	260	-232	-806	-1104
24000	-572	-482	-522	78	-20	-100	334	394	260	-292	-924	-1196
26000	-594	-496	-532	104	2	-92	320	396	260	-352	-1042	-1276
28000	-604	-504	-532	144	36	-60	300	392	254	-428	-1184	-1360
30000	-608	-504	-520	220	86	-4	272	382	244	-516	-1364	-1416
32000	-502	-420	-438	522	272	190	232	394	210	-704	-1752	-1546
34000	-472	-400	-406	814	456	416	168	344	168	-824	-2160	-1618
35000	-470	-400	-406	992	632	644	128	308	136	-872	-2440	-1630

WCB-11-1-12-36-3 LOAD(lbs) - STRAIN(micro in/in)

Axial Load	Gauge 1	Gauge 2	Gauge 3	Gauge 4	Gauge 5	Gauge 6	Gauge 7	Gauge 8	Gauge 9	Gauge 10	Gauge 11	Gauge 12
0	0	0	0	0	0	0	0	0	0	0	0	0
2000	10	-3	-19	-12	-16	-27	-27	-24	-11	-52	-39	52
4000	20	-22	-23	-29	-36	-60	-56	-52	-26	-101	-87	47
6000	18	-50	-42	-48	-56	-92	-82	-76	-42	-146	-130	28
8000	8	-80	-64	-64	-74	-122	-112	-104	-60	-198	-169	2
10000	-14	-111	-81	-82	-94	-155	-145	-139	-82	-256	-217	-34
12000	-36	-143	-100	-98	-111	-184	-168	-164	-107	-308	-267	-74
14000	-64	-178	-120	-118	-130	-214	-196	-200	-140	-362	-317	-112
16000	-98	-216	-142	-134	-148	-246	-228	-234	-178	-416	-370	-154
18000	-135	-258	-162	-153	-165	-278	-258	-273	-220	-473	-426	-201
20000	-174	-297	-184	-167	-180	-308	-288	-313	-269	-530	-486	-250
22000	-218	-334	-202	-177	-194	-334	-318	-354	-320	-596	-550	-304
24000	-260	-368	-214	-181	-198	-356	-345	-394	-378	-668	-624	-361
26000	-298	-396	-220	-176	-196	-372	-366	-434	-439	-754	-706	-422
28000	-336	-408	-208	-154	-176	-372	-378	-466	-508	-856	-814	-488
30000	-378	-420	-192	-116	-144	-364	-384	-508	-588	-978	-950	-564
32000	-412	-420	-154	-44	-78	-328	-372	-540	-680	-1140	-1140	-660
34000	-436	-376	-56	104	60	-248	-334	-562	-790	-1372	-1424	-780
35000	-448	-336	22	286	196	172	-298	-574	-872	-1542	-1624	-834

LOAD(lbs) - STRAIN(micro in/in)

	WCB-11-2-13-48-4		WCB-12-2-13-48-5		WCB-12-2-13-48-6	
Axial Load	Gauge 1	Gauge 2	Gauge 1	Gauge 2	Gauge 1	Gauge 2
0	0	0	0	0	0	0
9720	-67	20	-38	-34	-48	-20
21900	-211	42	-120	-108	-108	-52
29300	-312	47	-188	-180	-162	-84
41300	-471	49	-310	-334	-248	-132
49070	-599	52	-410	-408	-332	-171
61100	-791	62	-580	-476	-443	-223
68800	-926	72	-682	-508	-542	-248
81630	-1238	126	-860	-540	-782	-294
89610	-1582	196	-1480	-520	-1230	-294
97610	-2280	454	-2930	-210	-2183	-186

WCB-12-2-18-60-7 LOAD(lbs) - STRAIN(micro in/in)

Axial Load	Gauge 1	Gauge 2	Gauge 3	Gauge 4	Gauge 5	Gauge 6	Gauge 7	Gauge 8	Gauge 9	Gauge 10	Gauge 11	Gauge 12	Gauge 13	Gauge 14
0	0	0	0	0	0	0	0	0	0	0	0	0	0	0
9720	-2	-7	-10	-14	-16	-10	-16	-16	-26	-18	-4	-4	-3	2
17430	-10	-54	-69	-90	-110	-90	-113	-136	-154	-130	-23	-14	-5	43
25750	-16	-96	-127	-170	-205	-172	-216	-261	-292	-250	-40	-26	-8	80
33570	-20	-132	-182	-245	-294	-254	-311	-373	-420	-360	-60	-40	-15	106
41300	-31	-181	-250	-331	-395	-350	-420	-499	-556	-478	-91	-64	-28	122
49070	-15	-227	-312	-411	-484	-439	-516	-610	-674	-578	-122	-89	-46	122
57000	-13	-274	-377	-493	-584	-533	-623	-712	-801	-684	-169	-120	-73	114
64690	-16	-317	-433	-564	-669	-612	-710	-826	-913	-769	-212	-146	-92	108
72940	-24	-378	-508	-659	-789	-730	-832	-958	-1068	-875	-272	-174	-112	108
81630	-44	-452	-604	-784	-940	-876	-986	-1120	-1222	-992	-336	-196	-118	106
89610	-60	-522	-684	-884	-1068	-1000	-1112	-1252	-1354	-1080	-406	-214	-130	94
97610	-78	-638	-808	-1048	-1280	-1214	-1328	-1464	-1540	-1198	-488	-204	-96	124
105040	-102	-736	-958	-1256	-1556	-1484	-1588	-1708	-1796	-1288	-560	-168	-28	156
113120	-184	-944	-1205	-1624	-2140	-2030	-2110	-2140	-2120	-1336	-608	-24	212	216

WCB-12-2-18-60-8 LOAD(lbs) - STRAIN(micro in/in)

Axial Load	Gauge 1	Gauge 2	Gauge 3	Gauge 4	Gauge 5	Gauge 6	Gauge 7	Gauge 8	Gauge 9	Gauge 10	Gauge 11	Gauge 12	Gauge 13
0	0	0	0	0	0	0	0	0	0	0	0	0	0
9720	-2	0	-4	-4	-18	-8	-10	-6	-8	-7	-6	-17	-2
17430	-2	-1	-20	-25	-40	-47	-67	-66	-76	-74	-48	-64	-6
25750	-3	-2	-45	-60	-88	-97	-134	-136	-156	-150	-66	-110	-15
33570	-6	-6	-91	-108	-146	-156	-208	-219	-239	-224	-82	-137	-33
41300	-10	-14	-138	-152	-197	-205	-269	-268	-306	-288	-103	-166	-60
49070	-14	-42	-196	-203	-256	-264	-334	-330	-376	-354	-123	-202	-97
57000	-30	-72	-260	-257	-316	-324	-401	-396	-444	-416	-148	-242	-142
64690	-44	-98	-316	-304	-370	-374	-455	-448	-506	-468	-175	-272	-190
72940	-64	-130	-382	-356	-427	-432	-516	-508	-569	-525	-208	-300	-245
81630	-86	-164	-456	-414	-492	-494	-586	-574	-645	-592	-245	-329	-299
89610	-106	-204	-530	-471	-557	-544	-652	-652	-726	-662	-282	-361	-354
97610	-124	-232	-592	-520	-638	-604	-718	-718	-798	-728	-320	-404	-400
105040	-138	-258	-652	-570	-676	-664	-792	-786	-876	-794	-360	-432	-444
113120	-150	-292	-728	-628	-746	-734	-868	-862	-952	-864	-408	-460	-492
121200	-168	-332	-812	-692	-824	-820	-952	-948	-1020	-936	-456	-488	-540
128820	-208	-410	-916	-758	-900	-902	-1036	-1036	-1100	-1010	-528	-500	-596
133200	-224	-446	-972	-796	-944	-960	-1084	-1096	-1148	-1052	-584	-532	-620

WCB-22-1-5-18-48-9 LOAD(lbs) - STRAIN(micro in/in)

Axial Load	Gauge 1	Gauge 2	Gauge 3	Gauge 4	Gauge 5	Gauge 6	Gauge 7	Gauge 8	Gauge 9	Gauge 10	Gauge 11	Gauge 12	Gauge 13	Gauge 14	Gauge 15	Gauge 16
0	0	0	0	0	0	0	0	0	0	0	0	0	0	0	0	0
9720	3	-2	1	0	0	-4	1	-5	-4	-1	0	2	0	0	1	0
17430	22	-40	9	-28	3	-20	4	-20	-20	-13	2	29	-50	-32	6	-13
25750	56	-98	22	-74	14	-60	13	-64	-44	-31	4	64	-229	-76	14	-34
33570	79	-152	35	-97	19	-98	18	-114	-60	-51	6	94	-378	-116	18	1
41300	87	-207	45	-132	24	-139	24	-184	-81	-74	8	123	-540	-162	24	5
49070	96	-263	58	-159	41	-190	28	-258	-102	-104	10	120	-682	-212	30	23
57000	110	-318	74	-212	65	-238	35	-312	-126	-131	12	100	-812	-261	34	40
64690	124	-376	92	-262	88	-292	44	-364	-152	-160	16	86	-1036	-312	44	50
72940	158	-428	104	-348	108	-336	48	-424	-180	-196	22	74	-1176	-360	48	74
81630	192	-484	116	-410	126	-394	52	-488	-210	-236	28	64	-1300	-420	52	96
89610	288	-540	136	-464	144	-448	56	-544	-235	-280	36	56	-1420	-480	60	136
97610	384	-592	148	-504	158	-496	60	-604	-272	-316	44	50	-1500	-530	66	164
105040	476	-640	164	-536	176	-540	62	-640	-295	-360	52	44	-1568	-580	72	220
113120	548	-684	182	-584	190	-588	64	-660	-325	-404	60	38	-1634	-636	80	276
121200	638	-736	196	-628	200	-640	64	-684	-350	-448	72	30	-1700	-696	88	308
128820	726	-784	216	-686	218	-692	68	-710	-374	-508	86	18	-1768	-748	96	336
136490	944	-834	236	-752	242	-744	68	-726	-398	-560	96	4	-1834	-808	106	370
144200	1350	-1340	264	-864	264	-808	58	-752	-420	-612	128	-8	-1960	-872	112	408
152720	1472	-1984	300	-944	268	-892	56	-800	-448	-700	116	-8	-2080	-984	132	768
160970	1620	-1064	360	-1100	268	-952	36	-760	-460	-756	152	-72	-2100	-920	112	1800

WCB-22-1-5-18-48-10 LOAD(lbs) - STRAIN(micro in/in)

Axial Load	Gauge 1	Gauge 2	Gauge 3	Gauge 4	Gauge 5	Gauge 6	Gauge 7	Gauge 8	Gauge 9	Gauge 10	Gauge 11	Gauge 12
0	0	0	0	0	0	0	0	0	0	0	0	0
9720	2	-4	2	-2	-2	-3	26	-1	-10	6	1	0
17430	24	-18	16	-3	-26	-31	74	11	-48	16	8	18
25750	23	-22	66	-16	-56	-58	126	24	-90	28	16	32
33570	40	-36	126	-18	-82	-79	184	-37	-118	49	20	48
41300	86	-55	184	-34	-120	-116	255	52	-149	82	24	77
49070	135	-76	218	-112	-154	-147	322	70	-149	110	28	104
57000	170	-102	247	-162	-192	-163	369	88	-155	133	30	122
64690	254	-134	310	-236	-235	-160	399	106	-175	152	34	142
72940	320	-160	385	-282	-276	-132	516	122	-236	148	38	150
81630	402	-198	492	-362	-326	-120	540	150	-282	184	40	162
89610	490	-228	578	-408	-364	-118	561	168	-301	226	46	176
97610	626	-260	693	-448	-406	-114	596	189	-326	294	46	184
105040	782	-298	812	-484	-451	-100	624	209	-351	504	47	196
113120	932	-336	904	-517	-490	-93	650	234	-363	684	46	209
121200	1168	-372	1056	-548	-548	-92	690	282	-370	796	46	220
128820	1548	-412	1156	-572	-596	-88	712	314	-378	902	46	220
136490	1764	-452	1316	-604	-642	-56	736	334	-390	1004	52	244
144200	2020	-492	1470	-612	-688	-16	756	348	-416	1004	64	256
152720	2380	-532	1620	-652	-736	64	800	376	-436	932	56	276
160970	2640	-556	1840	-696	-824	108	816	400	-460	864	68	288
168380	2830	-564	1880	-724	-848	112	838	424	-470	860	79	296
176500	3010	-600	1930	-752	-864	124	856	448	-472	820	88	304

WCB-22-1-5-18-48-11   LOAD(lbs) - STRAIN(micro in/in)

Axial Load	Gauge 1	Gauge 2	Gauge 3	Gauge 4	Gauge 5	Gauge 6	Gauge 7	Gauge 8	Gauge 9	Gauge 10	Gauge 11	Gauge 12
0	0	0	0	0	0	0	0	0	0	0	0	0
9720	1	1	34	13	4	14	1	-19	38	-32	-16	-20
17430	2	2	273	33	12	111	2	-58	127	-147	-50	-84
25750	12	4	1198	40	18	628	36	-92	176	-258	-90	-180
33570	76	8	1254	52	20	812	60	-128	188	-348	-128	-230
41300	202	8	1412	64	22	996	92	-172	200	-498	-170	-276
49070	332	10	1692	70	24	1104	94	-220	208	-592	-220	-296
57000	544	16	2070	76	24	1128	116	-264	216	-656	-268	-288
64690	704	16	2280	80	24	1168	204	-308	216	-724	-304	-288
72940	792	24	2510	80	24	1360	272	-368	216	-784	-360	-248
81630	880	32	2720	80	24	1610	400	-416	180	-848	-412	-248
89610	952	36	2896	88	24	2166	752	-480	144	-904	-472	-248
97610	982	40	3030	104	24	2490	808	-528	88	-956	-524	-248
105040	1020	40	3210	104	24	2730	848	-584	44	-1014	-568	-248
113120	1020	44	3310	112	32	2890	856	-648	12	-1032	-624	-248
121200	1044	48	3440	112	44	2890	848	-704	-32	-1080	-680	-248
128820	1048	58	3440	124	40	3810	828	-736	-68	-1120	-712	-232
136490	1080	70	3430	140	40	4100	820	-790	-120	-1140	-740	-220
144200	1090	50	3140	160	40	3130	800	-780	-140	-1150	-750	-140

WCB-22-1-5-24-48-12 LOAD(lbs) - STRAIN(micro in/in)

Axial Load	Gauge 1	Gauge 2	Gauge 3	Gauge 4	Gauge 5	Gauge 6	Gauge 7	Gauge 8	Gauge 9	Gauge 10	Gauge 11	Gauge 12
0	0	0	0	0	0	0	0	0	0	0	0	0
9720	4	4	10	-5	-12	-10	4	-18	8	0	4	-2
17430	10	10	43	-45	-38	-16	36	-29	32	10	16	-10
25750	40	10	125	-120	-67	-19	45	-49	60	38	28	-21
33570	52	13	104	-182	-98	-29	46	-72	89	72	36	-24
41300	80	22	76	-208	-130	-42	46	-198	96	118	40	-29
49030	73	36	60	-216	-162	-44	68	-126	99	196	42	-26
57000	68	52	50	-210	-200	-49	91	-156	84	410	42	-21
64690	71	68	52	-190	-234	-54	118	-190	70	674	46	-16
72940	69	82	52	-186	-273	-58	147	-231	49	962	51	-8
81630	72	98	60	-168	-304	-64	170	-262	20	1176	88	2
89610	64	120	56	-148	-338	-70	196	-304	154	1240	96	16
97610	64	140	62	-144	-380	-80	214	-332	596	1524	104	12
105040	68	156	62	-128	-412	-96	220	-372	556	2080	104	8
113120	64	172	68	-124	-440	-112	224	-400	512	2390	108	8
121200	64	204	64	-112	-476	-124	224	-448	440	2710	104	12
128820	72	224	56	-88	-512	-144	216	-488	360	2910	120	16
136490	64	256	48	-80	-544	-188	220	-536	312	3370	104	20
144200	60	256	64	-80	-604	-188	216	-576	248	3590	108	24
152720	72	268	52	-72	-616	-212	208	-640	180	3910	112	24
160970	90	280	60	-60	-660	-240	220	-630	100	4260	140	20
168380	60	260	40	-40	-680	-260	220	-720	50	4580	140	10
176500	80	270	60	-40	-690	-300	240	-730	-40	4730	100	0
184920	100	240	20	-40	-720	-230	240	-740	-100	4980	100	-20
193960	120	280	60	0	-740	-270	260	-830	-240	5570	190	-40

WCB-22-1-5-24-48-13 LOAD(lbs) - STRAIN(micro in/in)

Axial Load	Gauge 1	Gauge 2	Gauge 3	Gauge 4	Gauge 5	Gauge 6	Gauge 7	Gauge 8	Gauge 9	Gauge 10	Gauge 11	Gauge 12	Gauge 13	Gauge 14
0	0	0	0	0	0	0	0	0	0	0	0	0	0	0
9720	1	2	2	-1	-5	-1	6	0	-11	18	-18	8	-5	-6
17430	6	3	4	-6	-24	-25	19	2	-44	42	-85	24	-27	-36
25750	10	5	0	-14	-43	-43	23	-5	-72	62	-145	39	-45	-59
33570	18	8	-6	-24	-65	-66	26	-3	-106	98	-222	55	-68	-104
41300	21	12	4	-36	-85	-92	18	-20	-151	169	-300	70	-92	-155
49070	30	50	16	-50	-110	-122	-14	-94	-207	222	-384	84	-118	-208
57000	36	68	18	-72	-136	-146	-33	-135	-246	265	-468	96	-140	-256
64690	42	95	4	-94	-166	-180	-56	-184	-284	332	-580	108	-168	-304
72940	49	121	-16	-114	-197	-208	-82	-234	-320	400	-694	123	-194	-350
81630	60	152	-44	-144	-233	-248	-104	-290	-363	478	-814	137	-222	-400
89610	60	189	-56	-170	-272	-288	-130	-344	-404	530	-918	150	-251	-445
97610	60	234	-68	-202	-300	-320	-158	-398	-444	632	-998	162	-274	-488
105040	56	228	-80	-236	-342	-364	-200	-460	-492	758	-1084	168	-304	-538
113120	42	240	-96	-266	-376	-404	-224	-508	-526	888	-1148	176	-328	-578
121200	30	288	-112	-306	-422	-444	-262	-570	-568	1074	-1216	180	-364	-624
128820	24	318	-120	-340	-468	-488	-306	-636	-606	1341	-1282	176	-396	-672
136490	36	344	-106	-368	-520	-548	-320	-696	-648	1656	-1304	178	-408	-708
140000	60	372	-106	-300	-534	-746	-392	-800	-678	2123	-1038	154	-396	-740

WCB-22-1-5-24-48-14 LOAD(lbs) - STRAIN(micro in/in)

Axial Load	Gauge 1	Gauge 2	Gauge 3	Gauge 4	Gauge 5	Gauge 6	Gauge 7	Gauge 8	Gauge 9	Gauge 10	Gauge 11
0	0	0	0	0	0	0	0	0	0	0	0
9720	-11	-7	-4	-4	-8	-12	-3	-4	-20	-12	-14
17430	-24	+6	-10	-19	-36	-42	0	-6	-68	-75	-51
25750	-36	18	-8	-38	-63	-65	-15	-4	-93	-144	-76
33570	-44	47	-16	-62	-100	-101	-33	0	-137	-216	-133
41300	-50	99	-24	-89	-140	-136	-56	-2	-181	-299	-180
49070	-60	177	-35	-166	-188	-165	-76	-7	-224	-386	-220
57000	-89	252	-68	-150	-232	-211	-102	-19	-262	-484	-254
64690	-110	343	-116	-190	-280	-254	-128	-30	-306	-594	-286
72940	-132	412	-152	-232	-320	-306	-150	-50	-345	-672	-321
81630	-156	440	-183	-268	-370	-346	-169	-73	-380	-746	-356
89610	-184	448	-218	-318	-423	-392	-195	-118	-431	-805	-392
97610	-213	444	-234	-360	-474	-424	-216	-139	-470	-852	-418
105040	-252	431	-262	-408	-522	-466	-240	-178	-516	-902	-448
113120	-272	426	-279	-430	-550	-486	-252	-198	-539	-930	-462
121200	-348	368	-300	-504	-620	-540	-280	-256	-600	-1006	-504
128820	-422	310	-322	-548	-672	-580	-304	-296	-638	-1062	-534
136490	-488	252	-352	-600	-730	-638	-336	-334	-686	-1120	-560
144200	-548	200	-380	-652	-786	-658	-364	-374	-726	-1184	-592
152720	-612	148	-412	-706	-844	-704	-396	-414	-770	-1360	-622
160970	-674	94	-444	-766	-904	-748	-432	-462	-836	-1348	-652
168380	-736	52	-472	-820	-956	-782	-464	-514	-856	-1436	-684
176500	-800	12	-498	-878	-1016	-838	-496	-556	-888	-1512	-704
184920	-864	-26	-522	-944	-1080	-852	-520	-616	-936	-1604	-726
193960	-922	-54	-550	-1004	-1130	-880	-562	-668	-960	-1688	-738
200000	-944	-62	-558	-1028	-1148	-892	-572	-688	-970	-1736	-742

Lateral Load	Gauge 1	Gauge 2	Gauge 3	Gauge 4	Gauge 5	Gauge 6	Gauge 7	Gauge 8	Gauge 9	Gauge 10	Gauge 11
500	-956	-62	-548	-1020	-1148	-878	-576	-712	-982	-1822	-744
1000	-966	-68	-544	-996	-1130	-854	-572	-720	-980	-1844	-748
2000	-964	-80	-544	-952	-1116	-814	-574	-732	-984	-1844	-756
3000	-970	-88	-544	-912	-1060	-774	-580	-748	-984	-1852	-770
4000	-988	-108	-556	-874	-1032	-742	-588	-772	-988	-1880	-804

WCB-22-1-6-24-48-15 LOAD(lbs) - STRAIN(micro in/in)

Axial Load	Gauge 1	Gauge 2	Gauge 3	Gauge 4	Gauge 5	Gauge 6	Gauge 7	Gauge 8	Gauge 9	Gauge 10
0	0	0	0	0	0	0	0	0	0	0
9720	4	6	-4	-14	-10	4	4	-22	-22	-44
17430	58	27	-8	-38	-45	15	13	-126	-54	-82
25750	146	43	-12	-64	-74	32	32	-221	-88	-116
33570	244	61	-20	-91	-118	64	50	-289	-124	-154
41300	314	53	-37	-122	-149	100	78	-360	-156	-185
49070	362	36	-66	-154	-188	87	100	-441	-193	-221
57000	394	15	-98	-190	-224	64	110	-518	-228	-254
64690	422	-8	-131	-228	-268	40	114	-574	-266	-290
72940	440	-35	-178	-258	-304	8	84	-626	-301	-322
81630	462	-64	-228	-299	-348	-29	64	-684	-339	-372
89610	482	-92	-272	-339	-390	-85	6	-738	-378	-396
97610	429	-126	-314	-353	-402	-128	-38	-785	-419	-442
105040	252	-234	-356	-381	-427	-166	-72	-836	-456	-482
113120	211	-269	-394	-412	-458	-204	-118	-884	-489	-516
121200	174	-318	-431	-441	-489	-247	-153	-930	-524	-556
128820	121	-344	-474	-478	-522	-286	-208	-984	-566	-584
136490	86	-398	-512	-508	-554	-316	-254	-1016	-600	-678
144200	50	-412	-554	-546	-592	-354	-300	-1050	-636	-664
152720	4	-456	-614	-588	-632	-396	-358	-1088	-674	-714
160970	-32	-492	-652	-620	-662	-428	-406	-1128	-712	-744
168380	-74	-540	-704	-664	-708	-470	-466	-1180	-752	-786
176500	-116	-584	-754	-700	-740	-508	-522	-1220	-792	-806
184920	-164	-616	-812	-744	-788	-548	-592	-1268	-828	-848
193960	-208	-674	-866	-786	-828	-588	-666	-1320	-866	-884
200000	-240	-708	-898	-812	-852	-624	-720	-1358	-890	-918

Lateral Load	Gauge 1	Gauge 2	Gauge 3	Gauge 4	Gauge 5	Gauge 6	Gauge 7	Gauge 8	Gauge 9	Gauge 10
3000	-282	-700	-828	-772	-816	-622	-804	-1374	-810	-834
6000	-316	-674	-736	-704	-744	-600	-868	-1404	-734	-760
9000	-368	-672	-644	-640	-676	-592	-960	-1520	-664	-704
12000	-408	-638	-472	-562	-566	-576	-996	-1556	-374	-420
15000	-484	-648	-208	-460	-408	-570	-1076	-1682	932	820

WCB-22-1-6-24-48-16 LOAD(lbs) - STRAIN(micro in/in)

Axial Load	Gauge 1	Gauge 2	Gauge 3	Gauge 4	Gauge 5	Gauge 6	Gauge 7	Gauge 8	Gauge 9	Gauge 10	Gauge 11	Gauge 12	Gauge 13	Gauge 14	Gauge 15
0	0	0	0	0	0	0	0	0	0	0	0	0	0	0	0
9720	2	4	6	-4	-10	-6	6	10	10	0	-12	10	-8	-2	-2
17430	36	63	29	-22	-29	-30	24	34	11	-3	-65	10	-30	-6	-16
25750	134	161	74	-47	-48	-54	16	54	7	-6	-129	11	-56	-6	-32
33570	160	197	60	-71	-66	-78	-11	78	-34	-18	-192	15	-84	-1	-53
41300	156	208	34	-100	-84	-112	-39	105	-58	-6	-228	18	-118	2	-73
49070	152	216	-6	-130	-102	-156	-79	130	-103	18	-261	22	-134	7	-102
57000	148	240	-42	-168	-120	-197	-126	132	-137	34	-296	23	-164	14	-126
64690	140	257	-78	-208	-134	-236	-174	144	-169	51	-324	23	-193	22	-152
72940	128	260	-122	-252	-156	-280	-224	164	-292	70	-355	23	-222	28	-178
81630	113	277	-160	-298	-160	-326	-274	169	-226	88	-394	26	-252	32	-198
89610	99	296	-204	-346	-168	-372	-313	162	-251	113	-426	26	-284	38	-216
97610	84	324	-246	-390	-179	-416	-354	155	-274	134	-451	26	-314	44	-233
105040	70	347	-294	-427	-199	-456	-386	144	-293	155	-476	28	-342	49	-250
113120	55	376	-347	-470	-219	-498	-420	126	-314	186	-498	28	-374	56	-268
121200	40	404	-400	-510	-239	-542	-453	102	-334	224	-516	32	-404	64	-282
128820	26	428	-448	-552	-266	-583	-482	73	-350	264	-540	36	-431	69	-301
136490	9	453	-498	-594	-302	-625	-515	44	-372	398	-552	40	-460	74	-320
144200	-4	468	-546	-632	-330	-664	-544	8	-396	573	-570	48	-490	81	-336
152720	-20	484	-606	-678	-370	-712	-576	-38	-416	786	-591	48	-522	86	-356
160970	-36	486	-664	-725	-407	-761	-601	-79	-437	916	-622	53	-553	95	-374
168380	-52	488	-724	-770	-434	-814	-632	-118	-460	1072	-652	62	-584	98	-388
176500	-70	290	-794	-822	-478	-862	-666	-212	-500	1278	-680	72	-638	110	-412
184920	-90	286	-852	-872	-524	-912	-696	-280	-528	1516	-698	84	-650	112	-412
193960	-112	474	-916	-928	-570	-964	-720	-360	-558	1736	-720	92	-678	120	-446
200000	-128	468	-958	-960	-600	-996	-738	-438	-576	1882	-722	96	-696	120	-456

Lateral Load	Gauge 1	Gauge 2	Gauge 3	Gauge 4	Gauge 5	Gauge 6	Gauge 7	Gauge 8	Gauge 9	Gauge 10	Gauge 11	Gauge 12	Gauge 13	Gauge 14	Gauge 15
3000	-124	432	-965	-888	-560	-936	-728	-520	-568	2110	-696	56	-664	120	-472
6000	-128	400	-952	-792	-504	-864	-712	-592	-548	2140	-688	12	-624	120	-496
9000	-128	352	-936	-708	-448	-792	-712	-680	-544	2170	-684	-40	-572	144	-532
12000	-112	272	-928	-600	-376	-692	-688	-748	-528	2190	-696	-40	-520	148	-560
15000	-100	212	-896	-480	-288	-596	-672	-808	-520	2210	-672	-72	-432	148	-600
18000	-88	144	-876	-308	-184	-460	-688	-880	-524	2220	-696	-124	-164	144	-656
20000	-144	-40	-872	-8	96	-192	-664	-908	-480	2470	-696	96	1370	204	-784

WCB-22-1-6-24-48-17 LOAD(lbs) - STRAIN(micro in/in)

Axial Load	Gauge 1	Gauge 2	Gauge 3	Gauge 4	Gauge 5	Gauge 6	Gauge 7	Gauge 8	Gauge 9	Gauge 10	Gauge 11	Gauge 12	Gauge 13	Gauge 14	Gauge 15
0	0	0	0	0	0	0	0	0	0	0	0	0	0	0	0
9720	-4	16	-3	-8	-18	-10	-36	8	-6	4	-10	0	-3	2	0
17430	-7	26	-9	-18	-29	-41	-102	28	-12	30	-89	0	-28	2	-32
25750	-10	58	-14	-26	-50	-86	-68	63	-47	86	-182	7	-56	10	-70
33570	-26	86	-23	-38	-72	-122	-70	88	-93	183	-298	12	-84	26	-102
41300	-45	148	-22	-55	-92	-170	-21	88	-138	333	-433	8	-120	36	-139
49070	-68	217	-19	-77	-114	-214	-28	78	-168	578	-560	0	-156	42	-158
57000	-94	279	-25	-104	-136	-252	-32	64	-190	658	-680	2	-186	46	-182
64690	-118	372	-19	-131	-160	-292	-80	48	-207	916	-782	0	-218	50	-208
72940	-164	426	-24	-170	-196	-340	-164	16	-228	1184	-920	0	-256	60	-240
81630	-204	454	-28	-208	-222	-392	-212	-12	-244	1388	-1000	0	-288	70	-268
89610	-244	448	-16	-242	-222	-434	-436	-36	-264	1568	-1070	0	-318	74	-296
97610	-280	452	-10	-274	-236	-480	-412	-56	-276	1750	-1138	-2	-350	80	-320
105040	-312	448	4	-312	-256	-520	-400	-72	-296	1980	-1216	0	-492	100	-328
113120	-352	436	-16	-344	-292	-560	-372	-96	-316	2150	-1264	-4	-412	104	-356
121200	-376	444	-76	-372	-312	-616	-344	-104	-332	2350	-1330	-8	-452	104	-376
128820	-420	436	-84	-408	-336	-648	-312	-140	-368	2500	-1384	-4	-480	96	-392
136490	-448	424	-120	-440	-372	-724	-280	-168	-392	2650	-1456	-8	-504	112	-416
144200	-480	412	-164	-476	-404	-752	-248	-176	-416	2790	-1520	0	-540	120	-432
152720	-508	392	-208	-520	-440	-800	-212	-184	-432	2950	-1576	0	-576	132	-460
160970	-528	392	-224	-528	-452	-816	-200	-184	-440	2970	-1596	0	-592	144	-472
168380	-568	376	-272	-588	-488	-864	-200	-136	-432	3110	-1640	0	-636	192	-504

WCB-22-1-6-18-60-18   LOAD(lbs) - STRAIN(micro in/in)

Axial Load	Gauge 1	Gauge 2	Gauge 3	Gauge 4	Gauge 5	Gauge 6	Gauge 7	Gauge 8	Gauge 9	Gauge 10	Gauge 11	Gauge 12
0	0	0	0	0	0	0	0	0	0	0	0	0
9720	2	2	0	1	1	2	4	0	4	-28	2	2
17430	56	-54	51	-6	-30	-23	24	8	50	6	10	18
25750	80	-119	183	-11	-61	-12	108	13	90	59	16	42
33570	145	-168	260	-19	-199	16	112	17	126	108	20	63
41300	200	-236	297	7	-141	25	92	24	168	144	27	118
49070	228	-295	330	30	-181	22	89	29	57	40	32	178
57000	240	-352	360	43	-223	16	96	34	26	10	36	284
64690	230	-403	378	48	-266	14	100	43	24	12	43	404
72940	216	-458	380	52	-311	6	106	55	31	12	50	556
81630	204	-522	306	42	-368	-19	102	66	35	10	60	802
89610	200	-565	272	44	-413	-31	102	76	52	36	66	972
97610	212	-612	240	54	-456	-50	110	88	64	36	76	1224
105040	204	-652	208	60	-500	-66	92	96	70	20	80	1480
113120	204	-708	166	84	-556	-92	88	108	76	54	88	1622
121200	164	-758	124	108	-610	-112	84	120	88	54	100	1712
128820	152	-802	90	120	-656	-128	88	132	94	72	108	1824
136490	104	-852	52	152	-704	-146	96	140	104	60	112	1942
144200	92	-900	44	186	-758	-172	108	148	112	88	124	1978
152720	84	-960	8	188	-804	-200	104	168	140	72	144	1982
160970	64	-984	-12	184	-876	-216	80	172	144	88	148	1954
168380	60	-1008	-32	152	-856	-216	88	184	160	104	144	1820
176500	56	-1032	-48	184	-892	-240	224	184	152	100	120	1632

WCB-22-1-6-18-60-19   LOAD(lbs) - STRAIN(micro in/in)

Axial Load	Gauge 1	Gauge 2	Gauge 3	Gauge 4	Gauge 5	Gauge 6
0	0	0	0	0	0	0
9720	-36	-40	14	13	-45	-34
17430	-76	-92	64	66	-88	-68
25750	-230	-120	150	190	-140	-80
33570	-560	-180	210	370	-170	-100
41300	-960	-220	300	490	-220	-120
49070	-1290	-250	220	640	-280	-150
57000	-1540	-300	220	770	-340	-160
64690	-1780	-330	230	920	-390	-180
72940	-2000	-360	220	1120	-460	-200
81630	-2170	-410	220	1720	-500	-240
89610	-2310	-450	210	2350	-560	-270
97610	-2430	-480	200	2800	-610	-290
105049	-2560	-520	200	1060	-660	-320
113120	-2600	-560	200	710	-690	-340
121200	-2770	-610	190	420	-740	-390
128820	-2830	-660	180	310	-790	-420
136490	-2860	-670	180	260	-820	-430
144200	-2900	-690	180	180	-850	-460
152720	-2920	-700	160	120	-870	-470
160970	-2960	-730	160	40	-900	-480

APPENDIX B DEFLECTION/LOAD READING

LATERAL DEFLECTIONS OF CENTERS DUE TO AXIAL LOAD IN INCHES

Axial Load (lbs)	WCB 1	WCB 2	WCB 3	WCB 4	WCB 5	WCB 6	WCB 7	WCB 8	WCB 9	WCB 10	WCB 11	WCB 12	WCB 13	WCB 14	WCB 15	WCB 16	WCB 17	WCB 18	WCB 19
0	.0	.0	.0	.0	.0	.0	.0	.0	.0	.0	.0	.0	.0	.0	.0	.0	.0	.0	.0
1000	.01	.01	.01																
5000	.04	.05	.04																
10000	.06	.09	.09	.001	.000	.000	.001	.000	.000	.000	.000	.000	.000	.001	.001	.001	.000	.000	.001
15000	.08	.12	.16	.007	.005	.009	.012	.001	.005	.000	.006	.001	.002	.003	.003	.002	.002	.002	.007
20000	.11	.16	.24																
25000	.15	.25		.021	.018	.014	.021	.004	.004	.001	.010	.001	.003	.005	.006	.002	.003	.009	.016
30000	.23																		
33570				.032	.029	.020	.033	.019	.010	.002	.012	.004	.004	.005	.002	.003	.004	.016	.015
41300				.043	.037	.024	.049	.024	.011	.002	.013	.006	.004	.004	.001	.006	.003	.020	.016
49070				.067	.054	.036	.058	.035	.013	.003	.014	.005	.004	.001	.002	.003	.001	.022	.016
57000				.082	.069	.042	.064	.039	.013	.012	.014	.004	.005	.002	.001	.003	.002	.025	.014
64690				.102	.094	.061	.068	.044	.017	.018	.011	.005	.006	.003	.000	.004	.001	.026	.016
72940						.084	.090	.050	.020	.020	.009	.006	.006	.004	.001	.006	.004	.032	.020
81630						.102	.114		.021	.021	.008	.006	.007	.006	.001	.007	.008	.041	.024
89610							.133		.022	.023	.005	.006	.012	.008	.002				
97610							.266			.026	.004	.006	.024	.010	.004				
105040										.027	.004	.008	.032	.012	.005				
113120										.028	.003	.008	.038						
121200										.029	.001	.007	.053						
Remark											Side Panel								

APPENDIX C SOME RELEVANT FORMULA

C- 1. THE ULTIMATE LOAD CAPACITY OF BALANCED RECTANGULAR MEMBER

Since W. Ritter presented the theory of parabolic stress distribution in 1899, many studies of inelastic concrete stress distribution in flexural members based on the parabolic stress distribution have been done.

The author assumes that the stress-strain relation for the flexural analysis of the balanced member due to flexural load may be expressed as shown in Figure C-1, and that stress distribution pattern at failure in compression is m degree parabola {Figure C-1, (b)}. Then for a rectangular member of depth d and width b:

$$y = k\, f_c^m \tag{C.1}$$

$$\bar{C}_b/b = \int_o^c f_c\, dy \tag{C.2}$$

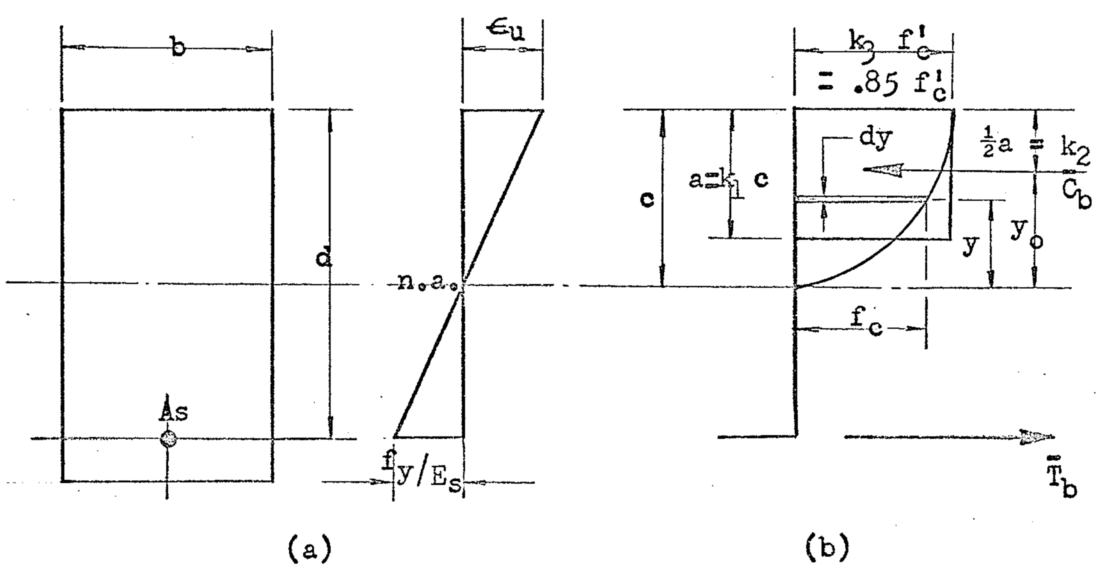

Figure C-1. Balanced Member. (a) Strains. (b) Stresses and Forces.

From equations (C.1) and (C.2),

$$\bar{C}_b = m\ b\ c\ f_c'/(1+m) \qquad (C.3)$$

$$y_o = (1+m)c/(1+2m)$$

If it is assumed that width of rectangular stress block is $k_3\ f_c'$ $= .85\ f_c'$, the resultant compression for balanced rectangular member may be obtained as follows:

$$\bar{C}_b = .85\ f_c'\ 2(c - y_o)b$$

Substitute equation (C.3) into this expression,

$$m\ c\ f_c'/(1+m) = .85 \times 2\ f_c'\ c(1 - \frac{1+m}{1+2m})$$

Hence,

$$m = 2.333 \qquad (C.4)$$

Since

$$\int_o^c f_c\ dy = k_1\ c\ k_3\ f_c'$$

$$m\ c\ f_c'/(1+m) = c\ f_c'\ k_1\ k_3$$

$$k_1 = 0.824 \qquad (C.5)$$

where an accepted value for $k_3 = 0.85$

$$a = k_1 c = 0.824 c$$

Therefore

$$k_1 k_3 = 0.824 \times 0.85 \doteq 0.7$$

Since

$$k_2 = k_1 /2$$

$$k_2 = 0.412 \qquad (C.6)$$

These values, $k_1 k_3$ and k_2, are plotted on Figure C-2. Einvind Hognestad[12] presented a study of the ultimate strength of columns in 1957. Figure C-2 shows values of $k_1 k_3$ and k_2 of Hognestad's, ACI Code-1963, and the author's findings from the assumption of m^{th} parabola for concrete stress distribution.

According to ACI Code Art. 1503 g-1963, the fraction factor k_1 shall be taken as .85 for strengths up to 4000 psi and shall be reduced continuously at a rate of .05 for each 1000 psi of strength in excess 4000 psi.

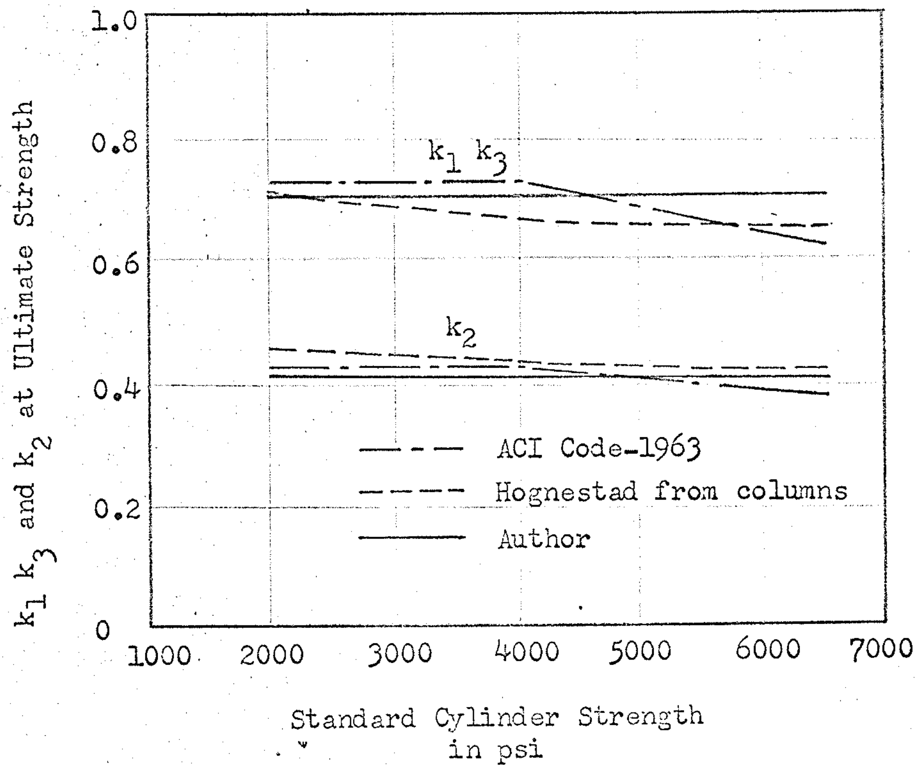

Figure C-2. Values of $k_1\ k_3$ and k_2 for Reinforced Concrete Member.

From equation (C.5) the following equations may be derived:

$$jd = d - \tfrac{1}{2}a \tag{C.7}$$

$$\bar{C}_b = \left[\epsilon_u\, d / (\epsilon_u + f_y/E_s)\right] \times .7\, f'_c\, b \tag{C.8}$$

Since $\bar{T}_b = \bar{C}_b$,

$$\bar{M}_b = .7\, f'_c\, j\, c\, b\, d \tag{C.9}$$

where

$$c = \left[\epsilon_u / (\epsilon_u + f_y/E_s)\right] \times d$$

C-2. THE ULTIMATE LOAD CAPACITY AND ITS ECCENTRICITY FOR BALANCED SANDWICH PANEL

As shown in Figure C-3, the balanced load and its eccentricity for sandwich panels are calculated as for hollow rectangular tied columns:

$$c = \epsilon_u d/(\epsilon_u + f_y/E_s)$$

$$\epsilon_{s1} = f_y/E_s$$

$$\epsilon_{s2} = \epsilon_{s1}(d_2 + \tfrac{1}{2}t - c)/(d - c)$$

$$\epsilon'_{s1} = \epsilon_u(c - d')/c$$

$$\epsilon'_{s2} = \epsilon u(c - \tfrac{1}{2}t + d_2)/c$$

$$\bar{C}_{s1} = A'_{s1}(f_y\ \epsilon'_{s1}/\epsilon_{s1} - .85\ f'_c) \qquad (C.10)$$

$$\bar{C}_{s2} = A'_{s2}(f_y\ \epsilon'_{s2}/\epsilon_{s1} - .85\ f'_c) \qquad (C.11)$$

These values take account of concrete displaced by steel, then

$$\bar{T}_{s1} = A_{s1}\ f_y \qquad (C.12)$$

$$\bar{T}_{s2} = A_{s2}\ E_s\ \epsilon_{s2} \qquad (C.13)$$

From C- 1 may be obtained :

$$\bar{C}_c = .85\ f'_c(a\ b - a\ b_1 + 2b_1\ d') \qquad (C.14)$$

where

$$a = .824\ c$$

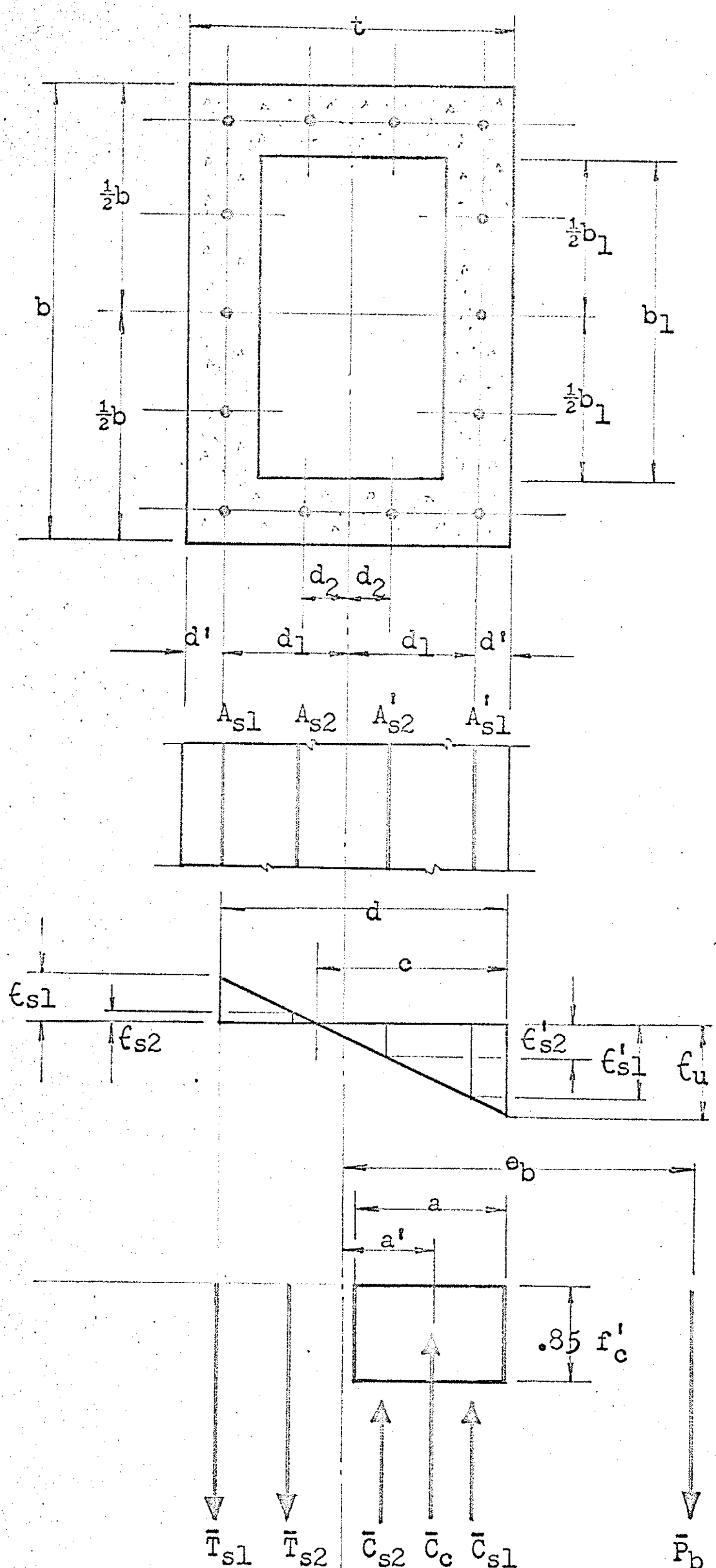

Figure C-2. Balanced Sandwich Panel Loads.

$$a' = \tfrac{1}{2}t - \frac{4\, b_1\, d'^2 + (b - b_1)a^2}{4\, b_1\, d' + 2a(b - b_1)} \qquad (C.15)$$

when $\epsilon'_{s1} \leq \epsilon_{s1}$,

$\epsilon'_{s2} \leq \epsilon_{s1}$,

and $\epsilon_{s2} \leq \epsilon_{s1}$.

All internal forces in the sandwich panel, $\bar{C}_c$, $\bar{C}_{s1}$, $\bar{C}_{s2}$, $\bar{T}_{s1}$, and $\bar{T}_{s2}$, are in equilibrium with $\bar{P}_b$ as shown in Figure C-3, then

$$\bar{P}_b = \bar{C}_c + \bar{C}_{s1} + \bar{C}_{s2} - \bar{T}_{s1} - \bar{T}_{s2} \qquad (C.16)$$

$$e_b = \frac{\bar{C}_c\, a' + (\bar{C}_{s1} + \bar{T}_{s1})d_1 + (\bar{C}_{s2} + \bar{T}_{s2})d_2}{\bar{P}_b} \qquad (C.17)$$

APPENDIX D NOTATION

Some of the letter symbols have been defined in this thesis when they are introduced. The common symbols used are listed here for easy reference:

A = area

A_c = net area of concrete

A_g = gross area of concrete

A_s = area of longitudinal reinforcement

a = k_1 c = depth of equivalent rectangular stress block

b = panel width

C = compressive force

C_c = internal force in compression concrete

C_s = internal force in compression reinforcement

c = distance from extreme compression fiber to centroid of tension reinforcement

E_c = modulus of elasticity for concrete

E_f = Young's modulus

E_r = reduced modulus of elasticity

E_s = modulus of elasticity for steel

E_t = tangent modulus of elasticity

e = eccentricity of the resultant load on a panel, measured from the gravity axis

e_b = maximum permissible eccentricity of $\bar{P}_b$

f_c = concrete stress

f_s = stress in tension reinforcement

f_y = yield-point stress for steel

f_{cu} = average ultimate concrete compressive stress due to axial load

f'_c = compressive strength of standard concrete cylinder

f'_{cu} = maximum ultimate concrete stress in extreme fiber due to combined axial and lateral loads

G = shear modulus of elasticity

I = moment of inertia of concrete panel section

jd = arm between $\bar{T}$ and $\bar{C}$ internal forces

k = numerical factor

k_1 = ratio of average stress to maximum stress in flexural member

k_2 = ratio of depth to resultant of compressive stress and depth to neutral axis

k_3 = ratio of maximum compressive stress to cylinder strength

L = panel length

n = ratio of modulus of elasticity of steel to that of concrete

P_o = axial load capacity of actual member

P_u = axial load capacity of panel

$\bar{P}_b$ = ultimate load of eccentrically loaded panel at simultaneous crushing of concrete and yielding of tension reinforcement

$\bar{P}_L$ = ultimate load of laterally loaded panel in addition to axial load

$\bar{P}_o$ = ultimate load of axially loaded panel when eccentricity is zero

$\bar{P}_u$ = ultimate load of axially loaded panel

p = A_s/A_g

R = reduction factor

r = radius of gyration

T = tensile force

T_s = internal force in tension reinforcement

t = over-all depth of panel section

t_c = thickness of insulation core

t' = face plate thickness of sandwich panel

w = weight of concrete

ϵ_u = ultimate strain in concrete

ϵ_s = strain in reinforcement

B I B L I O G R A P H Y

1. Collins, F. Thomas; "Precast Concrete Sandwich Panels for Tilt-up Construction," ACI Journal, Oct. 1954, Proc. Vol.

2. Anderson, L. O. and Wood, L. W.: "Performance of Sandwich Panels in FPL Experimental Unit," U S Forest Service Research Paper FPL 12, May 1964.

3. Plavtema, F. F.: "Sandwich Construction, the Bending and Buckling of Sandwich Beams, Plates and Shells," John Wiley and Sons, Ins., 1966.

4. Roberts, S. B.: "Sandwich Walls Precast for Pulp Mill," Eng. News -Record, Feb. 1951.

5. Grennan, P. M.: "Precast Sandwich Wall makes Costs Tumble," Eng. News-Record, Jan. 1952.

6. Amirikian, A.: "Promising Future predicted for Precast Thin-Shell Construction," ASCE Civil Eng., Mag. Vol. 23, Aug. 1963.

7. Leabu, V. F.: "Problems and Performance of Precast Concrete Wall Panels," ACI Journal, Oct. 1959, Proc. Vol. 56.

8. Pfeifer, D. W. and Hanson, J. A.: "Precast Concrete Wall Panels, Flexural Stiffness of Sandwich Panels," Port. Cem. Ass. Dev. Dept. Bull. D 99, 1965.

9. Richart, F. E. and Brown, R. L.: "An Investigation of Reinforced Concrete Columns," Univ. of Ill. Eng. Exp. Sta. Bull. No. 267, 1934.

10. Hognestad, E.: "A Study of Combined Bending and Axial Load in Reinforced Concrete Members," Univ. of Ill. Eng. Exp. Sta. Bull. No. 399, 1951.

11. Ferguson, Phil M.: "Reinforced Concrete Fundamentals," second edition, John Wiley & Sons, Inc., 1965, pp. 436.

12. Hognestad, E.: "Confirmation of Inelastic Stress Distribution in Concrete," Proceedings ASCE, Vol. 83, Paper No. 1189, March 1957, pp. 2 - 8.

13. ACI Standard 318-63: "Building Code Requirements for Reinforced Concrete," American Concrete Institute, June 1963.